LEVELS IN ^{153}Eu AND ^{155}Eu POPULATED BY THE BETA DECAY AND (^{3}He,d) REACTIONS

LEVELS IN ^{153}Eu AND ^{155}Eu POPULATED BY THE BETA DECAY AND (^{3}He,d) REACTIONS

by

JAMES UNGRIN, M.SC.

A Thesis

Submitted to the Faculty of Graduate Studies

in Partial Fulfilment of the Requirements

for the Degree

Doctor of Philosophy

McMaster University

October, 1968

DOCTOR OF PHILOIOPHY (1968) McMASTER UNIVERSITY
(Physics) Hamilton, Ontario.

TITLE: Levels in ^{153}Eu and ^{155}Eu Populated by the Beta Decay and (^{3}He,d) Reactions

AUTHOR: James Ungrin, B.Sc. (Hons.) (Manitoba)
M.Sc. (Manitoba)

SUPERVISOR: Professor M. W. Johns

NUMBER OF PAGES: xi, 156

SCOPE AND CONTENTS:

Thirty-one excited levels in ^{153}Eu and thirty-four in ^{155}Eu have been located by means of the (^{3}He,d) and beta decay reactions. The energies, intensities, and decay scheme classifications of forty-four gamma rays in ^{153}Eu and fifty-two in ^{155}Eu have been measured by means of singles and coincidence experiments using NaI and Ge(Li) detectors. Angular distribution studies of the reaction deuterons have been made and a number of levels have been assigned unique ℓ values. An interpretation of the level schemes in terms of the Nilsson model has been attempted.

ACKNOWLEDGEMENTS

In examining documents of this type in the past this author has noticed a rather short and generally obscure section labeled Acknowledgements. Not until the present work was almost complete did he recognize the significance of such a section and the enormous amount of generous aid given to him during his stay at McMaster. Sincere and very appreciative thanks must go first to the author's supervisory committee consisting of Dr. M. W. Johns, the author's director of research, from whom much has been gained not only as a physicist but also as a person, Dr. D. G. Burke without whose direct and generous help in arranging for accelerator time at the University of Rochester and in discussing the results of these experiments, a large portion of the present work could not have been done, and Dr. R. H. Tomlinson. A portion of the present work was carried out together with Dr. Z. Sujkowski of Warsaw during his stay at McMaster and his contribution to this work and friendship is also gratefully recognized.

The help of the reactor staff in obtaining a large number of active samples at various ridiculous hours of the morning, of the computer centre in running many "bugged" programs, of Dr. W. P. Alford and the accelerator staff at the University of Rochester in making available beam time and in discussing results, of Dr. G. T. Ewan of the Chalk River National

Laboratory in making several Ge(Li) detectors available during the course of the present studies, and of Dr. G. R. Satchler for the D.W.B.A. calculations, all are gratefully acknowledged.

The author would like to express his very sincere thank-you to the entire Physics community at McMaster and particularly to the Beta Spectroscopy group of which he was a part. The tolerance of fellow graduate students, faculty and staff to his brands of humour and music (?) and their generous aid and friendship both professionally and otherwise is gratefully recognized and will long be remembered.

The ability of Mrs. H. Kennelly of converting a large number of almost randomly placed words intended to pass for sentences, into a reasonably ordered document is acknowledged not only with gratitude but also with some amazement.

The financial assistance of the National Research Council in the form of research grants and studentships is also gratefully acknowledged.

TABLE OF CONTENTS

LIST OF TABLES

LIST OF FIGURES

CHAPTER I

INTRODUCTION

1.1 Nuclear Level Studies

The area of physics generally classed as "low energy nuclear spectroscopy" has, since the discovery of natural radioactivity, provided much information about the low-lying excited states of ensembles of nucleons. Since the recognition early in this century of a new short range force which was much stronger than the well known gravitational (about 10^{40} times) or electromagnetic forces (about 10^{3} times), much effort has been directed in an attempt to understand this force in the search for a more complete description of nature. The nuclear force has proven, however, to be so complex that no exact description of it yet exists some 30 or 40 years after it was first proposed. The work of the nuclear spectroscopist has been, during this period, and still continues to be, to try to obtain a more complete list of the various measurable nuclear properties which will shed some further light on the interaction mechanism involved.

The quantum mechanical wave function describing an assembly of nucleons is characterized by a set of eigenvalues. Among this set are three important and measurable quantities; the energy of the assembly and its quantum mechanical spin

and parity. Due to the nuclear interaction the total mass of a nucleus is somewhat less than the sum of the non-interacting nucleon masses of which it is made. For a given system there will exist some configuration which will maximize this difference. Any other arrangement may be considered as an unstable or excited state of the assembly and a rearrangement of the system to the one of minimum mass (maximum binding energy) will result. Various processes which may include the rejection of one or more nucleons (ie α decay) or even as drastic an event as a breakup of the nucleons into two major pieces (fission) may occur in reaching this final stable equilibrium. These processes which may differ in half-life from a matter of 10^{-20} sec. to 10^{15} years have been observed by experimenters and much of the data acquired in nuclear spectroscopy studies has been obtained through measurements of the emissions resulting from a nucleon rearrangement.

Nucleon emission will generally take place from a nucleus whenever the energy required for such emission is available. However, when the energy difference between the excited and equilibrium states forbids this, two other modes of decay,namely lepton and boson emission,occur. In a system of A nucleons consisting of Z protons and N neutrons leptonic or beta decay can occur through the change of a neutron into a proton or a proton into a neutron with the accompanying emission of one or two leptons. Neutron rich isotopes decay

through the change of a neutron into a proton and the emission of an electron and anti-neutrino from the nucleus. For the case of proton rich isotopes two generally competing processes occur. In the first a proton is changed into a neutron with the corresponding ejection of a positron and a neutrino, while in the second process, known as electron capture, the transmutation takes place via the capture of an orbital electron with the emission of only one lepton, the neutrino. For both of the directions of decay an increase in binding energy results and the emitted leptons are found to carry away an energy equal to the energy difference between the initial and final states. A measurement of the beta "end-point" energy which corresponds to the electron (or positron) carrying away all the available energy determines the energy difference between the two nuclear configurations involved. An absolute determination of energy can generally only be obtained through a direct measure of the total nuclear mass.

In addition to the relative energies of various nucleon configurations some information about the spins and parities of the states connected by the beta decay process may be obtained. It is known that the beta decay process most favourably connects states whose parities are the same and whose spins differ by zero or one unit of angular momentum. Such transitions are said to be "allowed". If the states concerned have opposite parities and spins differing by zero, one

or two units of angular momentum, the transition rates are greatly reduced (several orders of magnitude). Such transitions are said to be "first forbidden". Transition rates decrease rapidly with increasing spin changes so that it is very difficult to observe transitions in which spin changes of more than two occur. Decay rates also increase rapidly with increasing decay energy. By appropriate mathematical manipulation, one can obtain from the measured rate, an energy-independent comparative measure of the transition rates called the ft value. This can often be used to distinguish between various possible spin and parity choices.

The configuration in which a nucleus is left after beta decay or nucleon emission often is still not the most stable one available and further rearrangement is often found to take place with the accompanying emission of electromagnetic radiation or of an orbital electron. Transitions from one excited state to another, or to the final equilibrium or "ground state" of the system are found to take place through the emission of electromagnetic quanta known as gamma rays or monoenergetic conversion electrons. The emitted gamma radiation removes from the nucleus an energy equal to the energy difference of the two nuclear states and in addition carries away one or more units (denoted λ) of angular momentum. The radiation, of multipolarity λ, is classed as magnetic ($M\lambda$) or electric ($E\lambda$) and parity changes in the nucleus

for these two types of transitions are governed by the respective rules $\Delta\pi = (-1)^{\lambda+1}$ and $\Delta\pi = (-1)^{\lambda}$. Transition probabilities vary as $[(2\lambda+1)!!]^{-2}E^{2\lambda+1}$ where E is the energy difference between the initial and final state. It is obvious then that transitions of lower multipolarity are favoured and that, as in the case of the beta decay processes, only transitions between states which differ by 1 or 2 units of angular momenta are likely to occur with appreciable intensity. In the conversion electron process decay energy is transferred to an atomic electron through the interaction of the nuclear electromagnetic field with it. The electron is then ejected from the atom with an energy equal to the difference between the two nuclear states involved minus the electron binding energy. Ejection from various atomic orbitals may take place and the relative rates depend on the nuclear states connected by this decay process. Determinations of the photon and electron energies and of the multipolarities of the transitions through angular correlation measurements or through observations of the relative gamma and conversion electron rates have been used extensively to establish nuclear level positions as well as spins and parities.

In addition to the beta and gamma decay mechanisms some of the naturally occurring radioactive isotopes have been observed to decay with the emission of several nucleons. Alpha decay which consists of the emission of a tightly bound group

of two protons and two neutrons was one of the earliest observed transmutation processes. While both neutron and proton emission have been observed, their occurrence is somewhat rare. As in the above discussion energy differences and level natures can be determined by an examination of the emitted particle spectra.

Nuclear level properties are seen then to be observable as the result of an examination of the emissions from nuclei as they proceed to their stable configuration from some excited state. A rather limited number of nuclei exist in nature, however, which are in these unstable configurations. Most naturally occurring isotopes have been able to reach an equilibrium state in the time since their creation. In order to obtain information about a wider range of nuclei, a considerable number of artificial methods of nuclear excitation have been developed. Many new proton and neutron rich isotopes have been produced through the bombardment and subsequent capture of neutrons, protons, α particles etc. by stable nuclei. These methods have allowed the range of beta, gamma, and alpha decay investigations to be extended to almost all regions of the periodic table.

In addition to the capture and decay processes, the reaction mechanisms involved in the capture by or the transfer of nucleons to a nucleus have proven to yield valuable nuclear information. The "stripping" and "pick-up" reactions where

one or possibly two nucleons are exchanged between a target nucleus and an accelerated projectile which has been directed at it have been used for this purpose. During the transfer of a particle to the nucleus as in a (^{3}He,d) stripping reaction, the "stripped" particle, in this case a proton, carries to the target a certain amount of energy and angular momentum. An energy measurement of the detectable final outgoing projectile, the deuteron, will yield information as to the energy position of the resultant assembly of nucleons. Furthermore by observations of the preferred directions of deuteron exit from the reaction assembly information of spin and parity are obtainable. Some direct information about the nuclear force mechanism may also be found.

In all the above processes some restrictions exist in the population of the various available energy levels to which an excited state may decay. As we have seen, observations of either beta or gamma decay place limitations on the differences in spin and parity of the two states involved. Similar though less restrictive, limitations apply to particle reactions. However, by studying the rates of population and decay of the levels in a nucleus by several different processes, one is generally able to obtain a more complete description of its level structure.

1.2 The Shell Model and Spherical Nuclei

Since the nuclear force between two nucleons has not been completely solved, attempts to theoretically predict the properties of a system of one or two hundred particles would seem to be without much hope of success. However,many problems in physics have been brought to near or complete solution by the ordered classification of experimental data into some scheme or model from which predictions of additional properties can be more confidently made. As the amount of information on nuclear structure increased during the 1930's and 1940's certain systematic trends were noted. In particular, nuclear spins and parities showed a definite pattern in close analogy to the case for atomic electrons. Nuclei containing even numbers of neutrons and protons were all found to have 0 ground state spin and positive parity indicating a pairing off of nucleons in a similar manner to the case for atomic electrons. Marked increases in the binding energies of nuclei containing certain "magic" numbers of neutrons or protons were noted along with drastic changes in the neutron capture cross-sections and energy level densities for nuclei near these mass values. An interpretation of these facts on the basis of a "shell" model similar to the one used effectively in atomic spectroscopy seemed probable.

Various attempts were made to solve the problem of a many body nucleus in terms of an average central potential

of the square well or harmonic oscillator type. However, only very limited agreement with experiment was achieved for most of these early attempts. Mayer (1948) in 1948, and also independently Haxel, Jensen, and Suess (1949), introduced to the existing models the concept of a non-central interaction between the orbital angular momentum $\underline{\ell}$ of a nucleon in a nucleus, and its intrinsic spin $\underline{s}$. By suitably adjusting the strength of this $\underline{\ell} \cdot \underline{s}$ force they were able to arrive at an ordering of the nuclear ground state spins which agreed quite satisfactorily with most experimental data for nuclei of mass less than 150 or near the Pb region of the nuclide chart. The model also accounted for the "magic" numbers and could explain many low-lying excited states, particularly in odd mass nuclei.

In addition to the above mentioned 0+ ground state spin and parity of even-even nuclei, a second unusual property of these nuclei has been widely recognized. No even-even nucleus is known to exhibit levels below about 1 MeV of energy which are of an intrinsic nature. An "energy gap" exists in the excitation spectrum. The independent particle field used in the shell model calculations does not account for this fact and it would appear then that there exists some residual interaction which must be accounted for in addition to the average field. The nucleon motions are in some way correlated and the entire nucleus should be treated as a many-body system of interacting Fermions which move in a self-consistent field. The

existance of an energy gap in semiconductors had been recognized for some time and Bardeen, Cooper, and Schrieffer (1957) developed an explanation by treating the electrons involved in the system as quasi-bound pairs of correlated particles. The application of a similar treatment to a system of nucleons was introduced by Belyaev (1959) and also by Bohr, Mottleson, and Pines (1958). In their treatments a pairing interaction is considered to exist between nucleons in conjugate orbitals (j,m) and (j,-m) (denoted below as ν and $\bar{\nu}$). No pairing is assumed to exist between neutrons and protons. The nuclear Fermi surface is postulated to be diffuse and even for a nucleus in its ground state, pairs of nucleons are assumed to exist in levels above the level which the no-pairing model would define as the ground state. Likewise, levels below this ground level are assumed to be partially empty. Using the formalism of second quantization, the ground state of a nucleon system is given by

$$\Phi = \prod_{\nu} (U_\nu + V_\nu A_\nu^+ A_{\bar{\nu}}^+) \mid O\rangle$$

where U^2 and V^2 meet the condition that $U^2 + V^2 = 1$ and respectively denote the probability that a particular energy state ν will be empty or occupied by a pair. Furthermore to conserve the correct number of nucleons, a second condition, $2 \sum_\nu V_\nu^2 = N$, is required. $\mid O\rangle$ denotes the particle vacuum and A_ν^+ is the particle creation operator which produces a particle

in state ν. Particles occur only in pairs and any level is either empty (with probability U^2) or occupied by a conjugate pair (with probability V^2). The probability of occupation, V^2, can be expressed as

$$V^2 = \frac{1}{2}\left(1 - \frac{\varepsilon_\nu - \lambda}{E_\nu}\right)$$

where

$$E = \sqrt{(\varepsilon_\nu - \lambda)^2 + \Delta^2}$$

and

$$\Delta = G\Sigma_\nu U_\nu V_\nu .$$

The quantity λ is the "chemical potential" and corresponds to the energy of the maximum occupied level of the system with no pairing while ε_ν is the energy position of the level ν in this no-pairing system. G, which is the pairing interaction strength, has the form E/A where E is of the order of 25 MeV for protons and 20 MeV for neutrons and A is the atomic mass number. The quantity Δ defined above has the physical interpretation of being equal to one-half of the experimentally observed energy gap.

The above discussion has been centred mainly on the equilibrium or ground states of nuclei. Excited states of odd mass nuclei in the "shell model" region have often been explainable in terms of the odd nucleon being excited to a higher energy level. In the even-even nuclei, a qualitative one and

two phonon vibrational description of the low-lying levels has been current for a number of years. The introduction of the quasi-particle concept has given new meaning to these qualitative ideas.

A quasi-particle is essentially a linear combination of a particle and a hole. For odd mass nuclei the extra nucleon may be treated as a particle or as a hole in the pair that occupies a particular level. The single particle or intrinsic states of the level spectrum of such a nucleus are said then to be "one quasi-particle states. In even-even nuclei intrinsic states are formed through the breakup of a pair along with the elevation of one of the nucleons to a higher energy orbital. These states are known as two quasi-particle states. Coherent superpositions of two and four quasi-particle states have been used to explain many of the "vibrational" levels which exist in "spherical" nuclei. On the other hand, Sakai (1967), in an extensive survey of the levels of even mass nuclei,has recently classified many of these levels as rotational bands. Even the levels in the doubly magic ^{16}O and ^{40}Ca nuclei have been grouped into rotational bands built on quasi-beta- and quasi-gamma-vibrational levels. A pair break-up in an odd mass nucleus leads to three quasi-particle states of the type recently observed in ^{177m}Lu (Alexander et al 1964).

Although a large portion of the existing experimental data can be explained by the shell model with its various extensions, there are several regions of "deformed nuclei" that

require a somewhat different model.

1.3 Deformed Nuclei and the Nilsson Model

There exist three main regions of the nuclide chart for which the shell model fails not only in a detailed description of the excited states but also in its predictions of ground state spins and parities. These regions with $A \sim 20$, $150<A<190$, and $A>220$, are characterized by several features. Nuclei in these mass regions are generally midway between the magic numbers of neutrons or protons, and are found to have large electric quadrupole moments, and to exhibit highly enhanced E2 transition rates. Furthermore rotational spectra of the type observed for asymmetric molecules in atomic spectroscopy have been observed. These experimentally observed features lead to attempts to consider nuclei in certain regions as having a permanent non-spherical shape. This shape can be explained in terms of the quadrupole interaction between nucleons. Pairing forces tend to produce a stable spherical shape while the quadrupole force favours deformation. Permanent deformation will arise as for instance at $N \approx 92$ when the quadrupole force exceeds the pairing interaction.

Of special interest are the single particle levels that would arise in a permanently deformed nucleus. The fundamental solution of their nature was proposed by Nilsson (1955) for the case of axially-symmetric deformed nuclei. Extensions of the

calculations for the case of a more general case have been made by Newton (1960). Both works deal essentially with the solution of the single particle wave equation

$$(H_o + H_\varepsilon + c\bar{\lambda}\cdot\bar{s} + D\lambda^2)\ \psi_\alpha = E_\alpha\ \psi_\alpha$$

using a deformed oscillator potential defined by $H_o + H_\varepsilon$. λ plays a role essentially identical to ℓ and C and D are adjusted in strength to yield the shell model levels at zero nuclear deformation. The overall effect of the deformed potential is to perturb the (2j+1)-fold degeneracy of a spherical model state of spin j. For instance a state having spin 9/2 in the "shell model" requires 10 nucleons to fill it; in the Nilsson model, this state is resolved into 5 distinct levels with spins from 1/2 to 9/2 each of which contain two nucleons. The energies of the resolved levels are quite sensitive to their spin value and to the nuclear deformation. Nilsson used in his solution a basic set of states of the type $|N\ell\Lambda\Sigma\rangle$ where N is the oscillator quantum shell and Λ and Σ are the projections of the orbital angular momentum ℓ, and the spin s, on the symmetry axis. A state ψ_Ω is expanded to the form

$$\psi_\Omega = \Sigma\ A_{\ell\Lambda}\ |N\ell\Lambda\Sigma\rangle\ .$$

In a deformed potential the single particle spin j is not a good quantum number, but its projection on the symmetry axis, denoted by Ω, $(\Omega=\Lambda+\Sigma)$ is a constant of the motion. The states ψ_Ω are most often expressed in terms of the quantum numbers

$\Omega\pi[Nn_3\Lambda]$ and are expanded in terms of shell model states of good quantum number j , ie $\psi_\Omega = \sum_j C_{j\Omega}\,\psi_{j\Omega}$, where the $C_{j\Omega}$ and $A_{\ell\Lambda}$ coefficients are related by $C_{j\Omega} = \sum_{\ell\Lambda} (\ell\tfrac{1}{2}\Lambda\Sigma|j\Omega)A_{\ell\Lambda\Omega}$. n_3 is the projection of N on the 3 or symmetry axis.

The expansion of a state such as the $\frac{1}{2}$+[411] will contain five terms corresponding to the $\frac{1}{2}$ projections of the $g_{9/2}$, $g_{7/2}$, $d_{5/2}$, $d_{3/2}$ and $s_{1/2}$ shell model states which appear in the N=4 oscillator shell. Nilsson in his original calculations based his expansions only in terms of levels in the same shell. Recent calculations (Soloviev 1967) have predicted a 1 or 2% contribution to the expansion from the next available shell, ie for the above case, the N=6 shell. The expansion coefficients $C_{j\Omega}$ which can be calculated for a given nuclear deformation can be experimentally extracted from pickup and stripping reaction cross sections and will be further discussed in a later section.

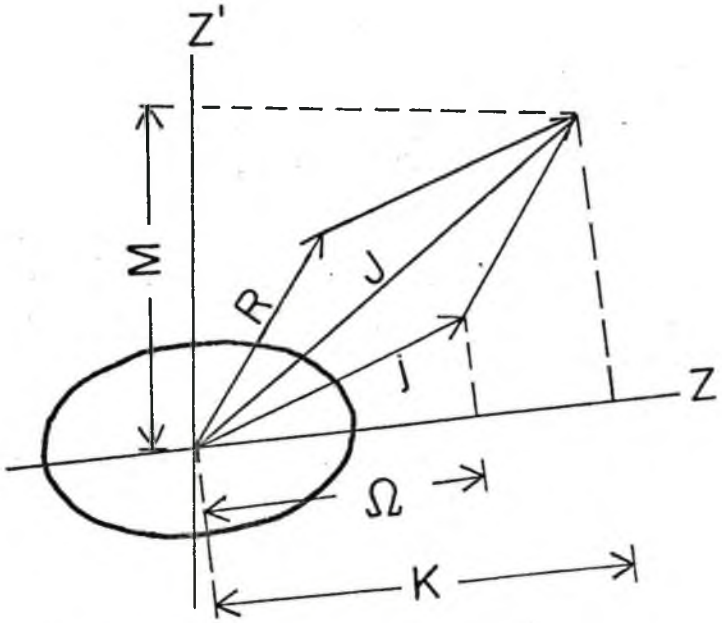

Figure I

Figure 1 shows schematically the various quantum numbers involved in the discussions of the excited level structure. J is a good quantum number at all times and represents the total spin while j and R represent the particle and core contributions, respectively. The projections on the arbitrary Z axis and on the symmetry axes are clear.

Excitations of nuclei in the deformed regions can be of several types. There are single particle or "one quasi-particle" levels, vibrational levels, and rotational bands built on either the intrinsic or vibrational states. Vibrational levels can be explained, as for the case of spherical nuclei, as arising from two quasi-particle excitations. Many two quasi-particle configurations may contribute to an observed vibrational level and extensive detailed calculations of the composition of many levels have been carried out by various workers, notably Bes et al (1966) and Marshalek and Rasmussen (1963).

It can be shown that the rotational bands for axially symmetric nuclei show the form

$$E_{JK} = \varepsilon_K + \frac{\hbar^2}{2I}\left[J(J+1) - 2K^2 + \delta_{K,1/2} A(-1)^{J+\frac{1}{2}}(J+1/2)\right]$$

where A is the decoupling parameter and is given by

$$A = \sum_j (-1)^{J+1/2}(J+1/2)\, C^2_{j1/2}.$$

The quantity I is the moment of inertia perpendicular to the symmetry axis and is a quantity much more characteristic of the band than of the nucleus in which it occurs. The above expression fits most bands to about 5% in energy. More sophisticated expansions in terms of the square or cube of the quantity in the square brackets have been used to explain such quantities as "centrifugal stretching" and band mixing.

1.4 Stripping Reactions in the Collective Region

Much information about nuclear models and forces has been obtained through studies involving direct reactions. In most general terms, a direct reaction is one in which the outgoing particle leaves the target nucleus in a time comparable to that required for the incoming projectile to travel across the nucleus. This is typically of the order of 10^{-21} sec. Of particular interest in recent years have been the single particle transfer class of direct reactions, specifically the so-called "stripping" and "pick-up" reactions. In both of these reactions a projectile consisting of one or more nucleons (at least two for stripping) is directed at a target nucleus and during the collision at the nuclear surface of the target, a single neutron or proton is transferred between the two groups of nucleons. In "stripping" a particle is transferred to the nucleus while in "pick-up" a nucleon is removed. In either case an outgoing particle exists which carries away a large amount of information both about the nuclear structure of the product nucleus and about the nuclear

interaction involved. As in the case of lepton and photon decay processes, certain restrictions on the possible states which will be populated exist, and several different stripping and pick-up experiments leading to states in the system of interest may be required to obtain a complete picture of the level scheme.

Exact details of the interaction involved between the target and incoming particle require a complete knowledge of the nuclear force. However, because of the complexity of the problem, several approximation methods have been derived which reasonably explain a large portion of the existing data. Details of the distorted wave Born approximation (D.W.B.A.) have been developed by various workers starting from the original stripping theory of Butler (1951).

Satchler (1958), following the work of French et al (1960), shows that the differential cross section for a stripping reaction of the (^{3}He,d)or(d,p) form can be written

$$\frac{d\sigma}{d\Omega} = \frac{2I_f+1}{2I_i+1} \sum_{\ell} S_{\ell} \, \phi_{\ell}(\theta).$$

I_f and I_i are the final and initial target spins while $\phi_{\ell}(\theta)$ is the single particle reaction cross section for angular momentum transfer $\ell\hbar$ at an angle θ. Details concerning Q value, target and projectile masses, Coulomb corrections, etc are all included in the $\phi_{\ell}(\theta)$ term which is obtained from the optical model by means of a D.W.B.A. calculation.

The remaining term in the expression, S_ℓ, contains the nuclear structure information. The summation exists as a result of the fact that the differential cross-section depends only on the orbital angular momentum, ℓ, of the captured nucleon and for the case of an odd mass or odd-odd target several possible ℓ values may combine to yield the same final j. A simple summation is possible because the different possible total spin values $j = \ell \pm \frac{1}{2}$ do not interfere.

For nuclei in the collective regions where the Nilsson wave functions discussed earlier apply, the spectroscopic factor, S_ℓ, can be expanded as

$$S_\ell = \sum_j \theta_{j\ell}^2$$

where

$$\theta_{j\ell} = g \sqrt{\frac{2I_1+1}{2I_f+1}} \langle I_i, J, \pm K_i, \mp \Delta K | I_f K_f \rangle C_{j\ell} \langle \phi_i | \phi_f \rangle .$$

The $C_{j\ell}$ values are the previously discussed coefficients used in the expansion of the Nilsson wave functions in terms of shell model states, while $\langle \phi_i | \phi_f \rangle$ is the overlap integral of the initial and final nuclear states (apart from the transferred nucleon) and, except for cases where drastic changes in nuclear deformation are expected, is taken to be equal to unity. g is a normalization factor arising from the symmetry requirements of the rotational matrices and equal to $\sqrt{2}$ for K_i or $K_f = 0$ and equal to one otherwise.

For the special case of an even-even nucleus only one possible ℓ value can be used in populating a state of given

spin and parity. Using the normalization properties of the Clebsch-Gordon coefficients and reducing the summation to a single ℓ value, the differential cross-section expression becomes

$$\frac{d\sigma}{d\Omega} = 2C_{j\ell}^{2}\ \phi_{\ell}.$$

The "strength" of the reaction is thus spread to several members of the rotational band built on a particular Nilsson orbital . Since a given single particle Nilsson wave function is in fact characterized by the expansion coefficients, $C_{j\ell}$, the relative cross sections of the different rotational members will form a distinctive pattern. It may be noted also that since the $C_{j\ell}$'s for a given state arising from an oscillator shell with quantum number N are limited to j values of $N+\frac{1}{2}$ or less, only a limited number of members of a rotational band will be populated by the reaction.

No allowance has been made in the above discussion for pairing and for the diffuse nature of the Fermi surface. For a stripping reaction where a nucleon is transferred to an unoccupied orbital, the above equation should be altered to

$$\frac{d\sigma}{d\Omega} = 2\ C_{j\ell}^{2}\ \phi_{\ell}U^{2}\ .$$

U^2 is the quantity previously discussed in the pairing theory extensions of the nuclear models and denotes the probability of the orbital being unoccupied by a pair.

The above expressions will be used in the analysis of the (^{3}He,d) stripping experiments described in the present work to compare experimental results with the theoretical predictions and to determine the nature of newly established nuclear levels.

CHAPTER II

INSTRUMENTATION AND TECHNIQUE

2.1 Gamma Ray Studies

A major portion of the information presently known about nuclei has been obtained through studies of the gamma rays emitted by nuclei as they proceed to their ground states. Many of the known excited state energies, spins, parities and lifetimes have been established through studies of the energies and intensities of transitions seen in "singles" spectra, or through determinations of their polarization, multipolarities, and time or angular correlations derived through "coincidence" measurements. Numerous advances have been made in both the instrumentation required for these studies and in the various techniques employed.

2.1.1 Detectors and Detection Processes

The earliest instruments used for the detection of gamma radiation were the proportional and Geiger counters which required the gamma quantum to transfer its energy to an electron in the counter volume in order to have an event detected. The energetic electron then produced numerous ion pairs in the gas volume which were collected to produce a detectable voltage pulse. Practically no energy resolution can be achieved with Geiger counters, and while proportional counters do in fact provide excellent resolution, their efficiency is extremely

low. These factors together with the long recovery times involved have led to their almost disappearance from present spectroscopic instrumentation.

The development of high resolution ($\frac{\Delta p}{p} \leq 0.5\%$) beta spectrometers in the period 1945-1950 provided for the first time a method of determining accurately the energies and intensities of transitions up to about 1 MeV in energy. In these studies thin samples of high-Z materials such as U or Th were placed in front of the radiating sample, and the monoenergetic "external conversion" photo-electrons knocked out of the material by the gamma rays were then analyzed by the beta spectrometer. Since the electron binding energies are well known, these studies, together with the related internal conversion studies, were able to determine energies below about 1 MeV to $\pm$ 0.5 keV. Unfortunately, the large source strengths and long half-lives required as well as the restriction to lower energies because of rapidly decreasing photo-electron efficiencies restricted the range of isotopes that could be investigated. Similar restrictions applied to the diffraction crystal spectrometers developed during this period but which still provide the most accurate measurements of gamma rays below about 500 keV.

Most reliable experimental studies of gamma ray energies and intensities determined directly began with the introduction of the scintillation spectrometer to nuclear spectroscopy in 1949. The scintillation counter operation is based on the

production of light in a crystal following the interaction of radiation with it. The light is then converted to an electrical signal through the use of a photomultiplier tube which linearly amplifies the resultant pulse to a detectable and usable size. The interaction of the radiation with the detection crystal involves the three well known photoelectric, Compton, and pair production processes of which the photoelectric is generally most useful. Details of the dependence of the various processes on the energy of the quanta, on the crystal size and geometry, and of their relative contributions to a gamma ray spectrum have been extensively investigated (Siegbahn 1966).

Two important features absent in the previously used ionization chambers are found in the scintillation counter. The scintillation detector is able to provide an accurate energy determination of the gamma ray as well as being much more efficient due to its increased density. An additional very significant improvement exists also in the short recovery time of the detector which allows one to use higher count rates and to investigate very short half-lives. However, in the very inefficient conversion of the light to an electrical signal, large statistical fluctuations are introduced in the number of photoelectrons produced at the photocathode resulting in a Gaussian pulse height distribution for a mono-energetic incoming transition. This results in typical peak widths of 7-8% for the photopeak of a 700 keV transition. With the realization of the

extreme complexity of the gamma ray spectra of most nuclei continuous searches have been made for more efficient radiation detectors which might remove or significantly reduce these peak widths.

The development of the solid state Ge(Li) detector (Freck and Wakefield (1962), Tavendale and Ewan (1963)) introduced changes in nuclear spectroscopy comparable to those brought about by the scintillation counter some 13 years earlier. This type of detector, whose method of detection is similar to that of the gas ionization counters, is able to provide an improvement over the scintillation counter of greater than one order of magnitude in the resolution for a 1 MeV gamma ray. The Ge(Li) detector consists of a single crystal of high purity p-doped germanium which is changed to "intrinsic" germanium by drifting Li ions into the crystal under the action of an electric field. Complete details of the various fabrication methods are available in the literature (Camp 1967).

Germanium detectors, which must be operated at liquid nitrogen temperatures for optimum performance, act essentially as ionization chambers. A quantum of gamma radiation interacts with an electron in the intrinsic region of the detector via one of the three previously mentioned processes and transfers its energy wholely or partly to it. The electron is then slowed down in the crystal volume through the production of "electron-hole" ion pairs each of which require 2.85 eV of energy to be formed.

An applied voltage is used to sweep these ions from the crystal and to produce a voltage pulse which is directly proportional in size to the energy of the incoming quantum. Neglecting random thermal noise and factors such as "leakage" currents and detector "capacitance", a 662 keV gamma ray stopped in the crystal should produce about 2.3×10^5 ion pairs with a statistical fluctuation of 4.8×10^2 pairs. This would lead to a possible resolution of ~ 1.3 keV at this energy. Fano (1947) has shown, however, that since the total energy of the quantum is given up to the crystal, the treatment of the ionization of each pair as an independent event is incorrect. The resultant distribution is then not purely Gaussian, but is reduced in width by a "Fano factor", F. Original estimates placed the value of this factor at about 0.5, but more recent calculations yield estimates as low as 0.1. In either case the theoretical limit of energy resolution for a 662 keV gamma transition is of the order of 0.5 keV or less. Detectors have been used in the present investigation which yielded a resolution of 1.5 keV at this energy.

Some price is paid, however, for the large increase in energy resolution afforded by the Ge(Li) detector. Present fabrication techniques limit their active volumes to about 50 cc as compared to the ~ 1000 cc volumes available for NaI scintillation counters. This sizeable volume decrease which results in reduced detection efficiency, combined with the large

fabrication costs,have prevented the Ge(Li) detector from completely replacing the scintillation counter.

2.1.2 Coincidence Studies

The information gained through the measurement of the energies and intensities of the gamma rays emitted by the decay of a nucleus is normally insufficient to form a unique nuclear level scheme. For certain cases, where several gamma rays whose energies have been very accurately determined cascade to the ground state via intermediate levels, a reasonably reliable scheme may be constructed by adding the energies of these cascading pairs to arrive at probable level energies. For most decays, however, confirmation of these cascades by means of coincidence measurements is required. Additional information may also be gained by these studies. For instance, weak transitions which may be obscured in singles spectra by the large Compton distributions of higher energy transitions are often greatly enhanced, and may in fact only be observed in coincidence data. Conversely certain transitions known from singles spectra and which are "ground state" transitions from levels which are not fed by gamma rays may be identified as such by their absence in coincidence spectra.

In a coincidence measurement, two detectors "look at" a common source of radiation. Electronic circuits are then used to select from the events detected by the two detectors, those

events which are related in time, or time and energy. In the present coincidence experiments the energies of gamma rays which were detected in the two counters within a time period 2τ(~100 nsec) of each other were recorded. The time 2τ is known as the resolving time of the circuit. Various types of angular correlation and time delayed coincidence experiments have been developed which in addition to relating pairs of cascading gamma rays yield information as to the spins and lifetimes of the intermediate states. The coincidence measurements in the present studies have been used only to establish level positions.

The experimental equipment used in the present work is shown schematically in Figure 2. Gamma ray detection was achieved through the use of a hybrid system of a NaI scintillation counter together with a solid state Ge(Li) detector. The NaI detector was used because of its high efficiency while the Ge(Li) detector was employed to provide the high resolution necessary to resolve the individual transitions observable in the complex decay spectrum. Sources were placed in the central hole of a shaped anti-Compton shield placed between the detectors which "looked at" the source in a 180° geometry. Because of several very intense low energy transitions in the nuclei investigated it was found necessary to use a lead and cadmium absorber in front of the efficient NaI counter to keep from overloading the pulse handling equipment.

COINCIDENCE ARRANGEMENT

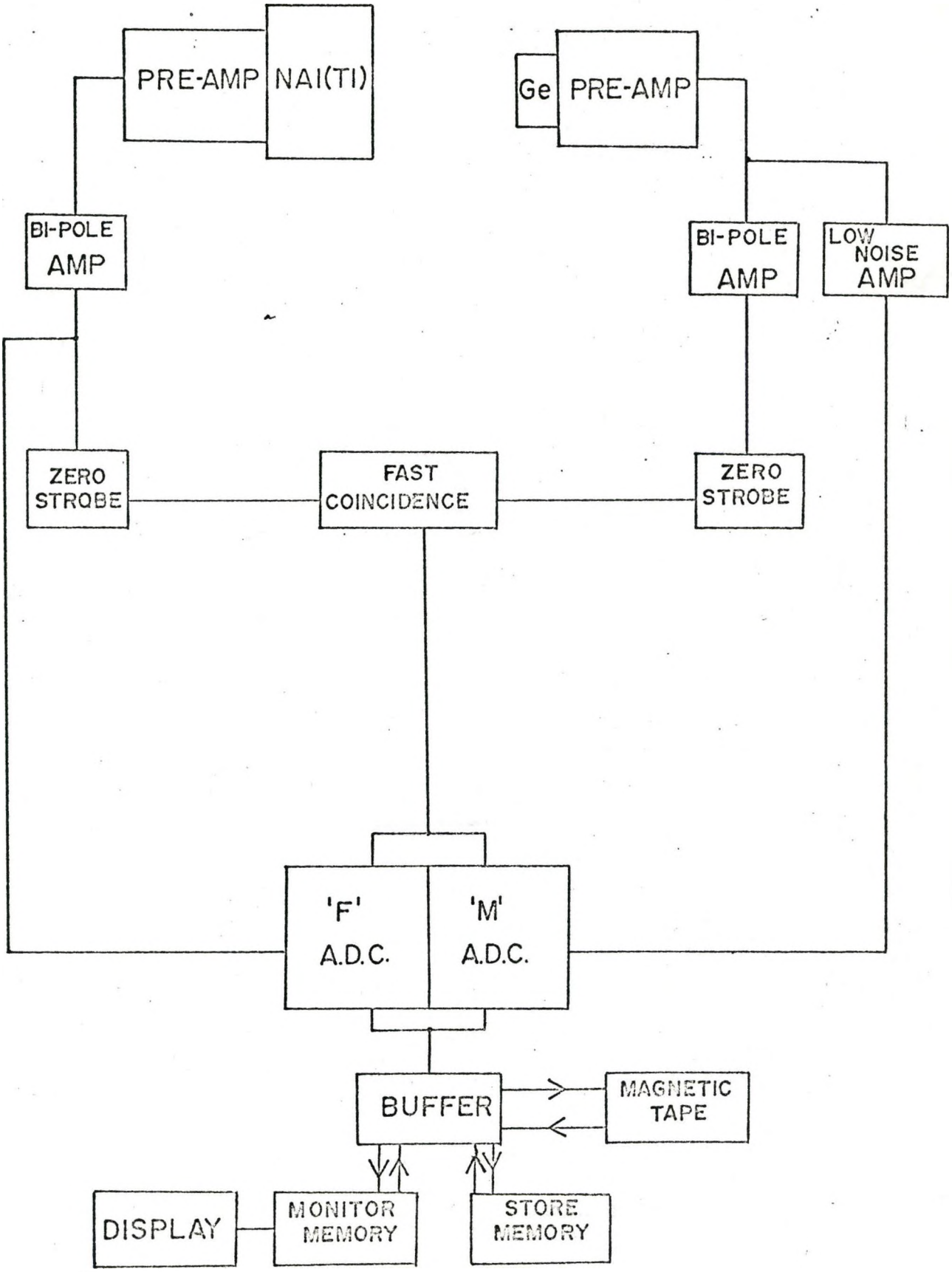

FIGURE 2

In order to record all the possible gamma-gamma coincidence events at one time, a two parameter Nuclear Data analyzer was used to accept the pulses from the two detectors. Coincident linear pulses from low noise amplifiers were fed into two 4096 channel Nuclear Data 161F analogue-to-digital converters, shown schematically in Figure 2. The converters were gated by a fast coincidence circuit operated at a ~ 100 nanosecond resolving time (2τ) using the "cross-over pickoff" technique. Since only 4096 channels were available in the memory of the analyzer, a buffer and magnetic tape system was used to "address record" the coincidence events. The energies of coincident gamma rays observed in the two detectors were converted to digital "addresses" by the ADC's which analyzed the corresponding linear pulses. These X(NaI) and Y(Ge(Li)) "addresses", which were recorded on magnetic tape for later "sorting" by a computer, defined in effect a three dimensional surface where the number of events per digital location are measured along the Z direction. A slice or section of this space perpendicular to the Ge(Li) or Y axis and passing through a channel or group of channels on that axis, yields a NaI spectrum in coincidence with the selected Ge(Li) energy range. A section of the surface in the opposite direction will likewise yield the Ge(Li) spectrum in coincidence with a chosen NaI energy range.

From the point of time economy it was found preferable to store a number of events in the analyzer memory and then to

write them on magnetic tape in blocks rather than to record individual events directly. Each location of the analyzer memory was composed of 18 magnetic bits (capacity 262,144 counts) and by combining the 8 most significant information bits from the NaI converter with the 10 most significant from the Ge(Li) converter, 18 bit words suitable for storage in these locations were formed. This choice of 8 bits and 10 bits defined a 256 × 1024 (ie $2^8 \times 2^{10}$) channel matrix which was found convenient for the present studies. (By choosing other combinations of bits, different sized matrices could of course be formed. Likewise by writing individual events on tape, or using two memory locations per coincidence event, a matrix of up to 4096 × 4096 channels could be defined.)

One half (2048 channels) of the analyzer memory was used to sequentially store the address recorded events which were then "dumped" on magnetic tape in 2050 word blocks which included a two word identification tag. At a tape density of 200 linear bits per inch it was possible to record about 1.6×10^6 coincidence events on one 300 ft. reel of magnetic tape. The arrangement of the events recorded on such a tape into a final ordered matrix required about 100 minutes of computing time on the University's 7040 computer. The events "sorted" in this manner were then written on a second tape for eventual typing and analysis of the matrix.

The second 2048 channels of the analyzer memory were used

to monitor the "projections" of all the coincidence events unto either the NaI or Ge(Li) axes of the matrix. These projections were found to be very valuable in checking the progress of the experiment as well as in choosing "gates" during the analysis of the coincidence data. By properly choosing these "gates" which then yielded the gamma ray spectra coincident with the energy range defined by them, and by subtracting from these chosen spectra, the spectra associated with gates containing the same number of channels adjacent to the peak gate, it is possible to obtain "difference" spectra which are a good approximation to the spectrum of gamma rays in coincidence with a single gamma ray. Both difference and direct spectra were found useful in the present study, but because of the nature of the spectrum most of the information was extracted from Ge(Li) spectra defined by NaI gates.

2.1.3 Analysis of Gamma Ray Spectra

The determination of the energies, intensities, and level scheme positions of the transitions observed in a complex gamma ray study is complicated by several factors. Detector efficiencies and resolution are among the more important factors involved. Because of the broad photopeak and Compton distribution responses of NaI detectors, strong transitions often completely mask weaker transitions. Investigations taking advantage of the improved resolution by Ge(Li) detectors have often doubled or tripled the number of transitions observed in a decay study.

The decrease in efficiency brought about by the reduced volume of these detectors, however, may be so great in some cases, that it is impossible to obtain meaningful statistics during the decay time of the sample. Therefore, a combination of detectors as for instance in the form of a Ge(Li)-NaI coincidence arrangement, may often be needed. Recent improvements in electronic circuitry resulting in decreased resolving times and larger capacity pulse height analyzers have produced large improvements in the coincidence techniques required to place both newly observed and previously established transitions in a level scheme. However, additional factors such as accidental summing, back-scattered peaks, chance coincidences, and Compton contributions to gates as well as the ever present problems of chemical and isotopic impurity continue to create traps for the unwary. It is easy to misinterpret the results of experiments and arrive at erroneous conclusions.

In the investigation of singles gamma ray spectra from which energies and intensities are extractable, the linearity and efficiency of the detection system are among the two most important factors to be considered. Most gamma ray detectors presently employed produce output voltage pulses whose size is proportional to the photon energy, although for the case of NaI a deviation from linearity is known to exist below 100 keV (Siegbahn (1966)). The large widths of scintillation photo-peaks do, however, give rise to several energy determination

problems. Often several unresolved transitions are included in one peak and the only indication of this may be a slight broadening of the peak width. Furthermore, because it is difficult to determine its position to better than 5% of its width it is generally difficult to determine the gamma ray energy corresponding to a single peak better than $\pm$ 2 keV. Because of these problems, Ge(Li) counters with their much narrower peaks, have almost completely replaced NaI(Tl) counters for energy determinations.

The Ge(Li) counter is known to produce pulse heights which are a very linear function of energy over a wide range (Siegbahn (1966)). Using a typical detector of about 2.0 keV resolution (F.W.H.M.) at 500 keV and a 4000 channel ADC to cover an energy range of 1 MeV, the peak width is of the order of 8 channels. It is possible, for most strong peaks, to determine a peak position to ~ $\pm$ 0.15 channels or to $\pm$ 0.04 keV, having, therefore, a relative error of 6 parts in 10^5 at 500 keV. This is somewhat beyond the linearity of most ADC's and careful determinations of the deviations from linearity need to be performed using many known transitions or a precision pulser. In the present work, using a Nuclear Data 161F ADC, a non-linearity of the order of 2 channels in a channel range of 3400 was found. The energies of strong transitions were determined with errors of 0.10 to 0.15 keV.

Of equal importance to the energy determination is the

determination of gamma ray intensities. These are usually relative intensities, although it is possible to determine the absolute intensities in quanta per decay, if the absolute detection efficiencies and source strength are known. A determination of the intensities of the detected radiation can be made from the peak areas in a measured spectrum if the detection efficiency is known. Many efficiency calculations and tabulations have been made for NaI detectors of various sizes and for various geometries and crystal mountings (Heath (1957) , Chinaglia and Malvano (1966)). However, because of the various methods of drifting and the rather uncertain relation between efficiency and detector volume, no similar reliable calculations exist for Ge(Li) detectors and efficiency calibration must therefore generally be achieved by using some known standard for comparison. For the present studies photopeak efficiencies were determined with standard sources by comparing the peak areas produced by the Ge(Li) detectors with those produced in an equal time by a 7.5 cm × 7.5 cm NaI detector of known efficiency when the sources were placed in a standard geometry. The values obtained in this way were checked by examining the spectrum of 12 year ^{152}Eu and using the relative gamma ray intensities as determined by Dzhelepov et al (1966).

The method of obtaining both difference and direct spectra from the coincidence matrix has already been outlined.

Spurious peaks may appear in these spectra due to improperly subtracted Compton contributions of higher energy transitions to the gates as well as from chance coincidences. For a source strength N and a resolving time 2τ it can be shown readily that the true-to-chance ratio is given by $R = \frac{1}{2\tau N_o}$. Steps must generally be taken to maximize this ratio; however, in cases where appreciable chance events do exist, they must be subtracted. In analyzing the properly corrected spectra, system linearity and detection efficiencies, as in the case of singles spectra, must be considered. Often certain gamma rays may be seen only in coincidence spectra and their intensities must be derived from these data. The efficiency factor needed to extract this information, however, is not the same as that of the singles spectra. It involves instead the product of the efficiencies of the two detectors used, a knowledge of the branching ratios of gamma rays from the levels involved, and a knowledge of the coincidence efficiency of the electronic circuit, which may depend on energy. It is often sufficient to know the energy dependence of the detector efficiencies since the results can usually be normalized to some well-known cascade in the decay scheme.

2.2 Charged Particle Detection

The impact of semi-conductor detectors on the study of gamma rays has already been discussed. Such detectors are also widely used for particle detection and have revolutionized the

the possiblities for coincidence measurements in reaction studies. However, for charged particles of energy 10 MeV or less , magnetic spectrometers still provide the best energy resolution. The tandem Van de Graaff accelerator can provide a beam with an energy stability of the order of one part in 10,000 and various magnetic spectrographs have been designed and built in an attempt to take maximum advantage of this stability.

The spectrograph used in the present work was of the "Enge Split-pole" type and was built for the University of Rochester tandem MP accelerator laboratory by AB Scandatronics of Sweden. Detailed descriptions of the design and magneto-optics of this type of instrument have been given in several publications (Enge (1958),(1964)) and only a general description will be given here. Figure 3 taken from an article by Spencer and Enge (1967), shows a schematic top view of the spectrograph. It may be immediately noted that this type of spectrograph is somewhat unique in that it consists of two separate pole pieces enclosed by one current coil. The field developed in the gap is used to provide second order double focussing. Vertical focussing, whose main purpose is to increase the collecting power of the instrument, is achieved in the fringing field areas, particularly at the entrance to the first gap. Two-dimensional focussing is achieved over an energy range $\frac{E_{max}}{E_{min}} \sim 8$ and the spectrograph can accept

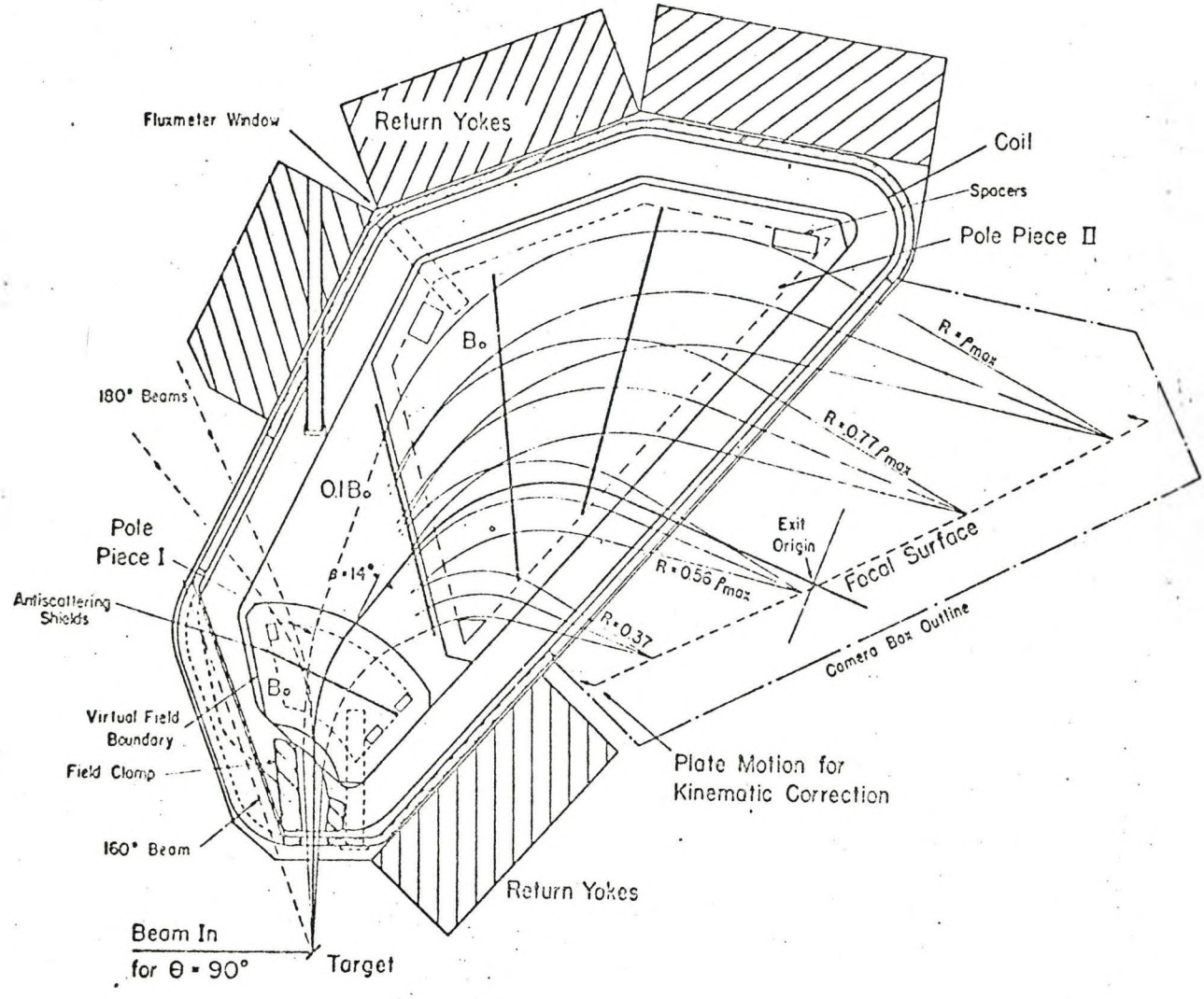

Top View of Spectrograph

Figure 3

particles from the target for reaction angles up to 160°.

Particles leaving the target at some chosen angle θ within a solid angle $d\theta$, which is of the order of 2 or 3 milli-steradians, enter the spectrograph through a collimating aperture. The particles are then deflected due to the interaction of the magnetic field with the charged particles, and are focussed in a plane labelled as the focal surface in the diagram. Because the strength of the electromagnetic interaction between a fixed magnetic field and a moving charged particle is dependent on the velocity and hence the energy of the ion, identical particles of different energies are focussed at different positions on the focal plane. Typical particle paths (larger ρ for higher energies) are indicated in the diagram. The magnetic field strength is measured by means of a proton N.M.R. probe, and the entire target chamber and spectograph assembly are evacuated to a pressure of about 10^{-7} torr.

To first order, a particle of mass M(proton=1), charge Z, and energy E(MeV) will have its focus position defined by the equation

$$H\rho = \frac{144}{Z} \sqrt{ME}$$

where H is in kilogauss and is 4.2578 times the proton resonance in megahertz, and ρ is the "radius of curvature". If a particle is detected at a position s (cms) along the focal surface then ρ is given by

$$\rho = a_o + a_1 s + a_2 s^2 + \ldots \quad \text{cms}$$

where $a_o = 92.94114,$

$a_1 = -0.40703,$

and $a_2 = 0.36026 \times 10^{-4}$.

A measurement of magnetic field strength and focal surface position will then yield the particle energy which,combining the above expressions, may be written as:

$$E = \frac{1}{M} \left(\frac{ZH}{144} [a_o + a_1 s + a_2 s^2]\right)^2$$

Allowances for relativistic velocities and nuclear target recoil are required to obtain a more exact expression. Corrections in the position of the focal surface must also be made after allowance for this "kinematic" shift and are listed in the literature (Spencer and Enge (1967)).

Particles which have been magnetically analyzed and focussed by the spectrograph are recorded in nuclear emulsions mounted in the camera box and placed in the focal plane. The emulsions used in the present work were 25 micron thick NTB nuclear emulsions mounted on 1.5 mm thick glass backings and manufactured by the Eastman Kodak Co. The plates measured 25 cms in length by 2.5 cms in width and six exposures were made with each camera loading. Following the developing (8 minutes in D-19 developer at 18°C) and fixing (30 minutes in sodium thiosulphate at 18°C) of the emulsions, the plates were scanned in 1/4 mm wide strips across the plate width under a 400 power travelling microscope, and the numbers of particle tracks per

strip were recorded. In the present work the energy dispersion was about 250 keV per cm. Because in general several reactions with different Q values may result for one combination of incoming beam and target, several reaction products, ie deuterons, alphas or tritons, may be focussed at the same position in the focal plane. These particles will have different ionizing powers and will generally leave different density tracks in emulsions; however, it is generally advantageous to use absorbers over the emulsions whenever possible to remove these background events.

A second possible method of particle detection can be achieved through the use of a position-sensitive semi-conductor detector. The momentum measure of the spectrograph and the energy measurement of the detector can be used to distinguish between possible reaction products. However, at the present time no economical detectors which cover an appreciable portion of the energy range are available. The advantages of having a spectrum produced at the time of the experiment and the possible study of coincidences between the magnetically analyzed particles and gamma rays from the de-exciting nucleus should be realized in the near future as larger detectors are developed.

2.3 Source and Target Preparations

2.3.1 Gamma Sources:

Sources of 22.4 min ^{155}Sm and 47 hr ^{153}Sm were obtained by irradiating isotopically enriched Sm_2O_3 (99.3% ^{154}Sm, 99.2% ^{152}Sm) in the McMaster reactor at a flux of about 2×10^{13} n/cm^2/sec. Samples were sealed in quartz vials for irradiation and were then transferred either to tape backings or into gelatine capsules for counting. For the case of ^{155}Sm, sample masses of from 0.1 to 1.0 mg and irradiation times of 1 to 15 minutes were used yielding samples of from 10 to 100 μCuries of activity. New material was used for each irradiation, and although no chemical purification was carried out, the only impurity activity found was trace amounts of 9.3 hr ^{152m}Eu. Counting of the samples was generally begun 5 to 10 minutes after irradiation. Similar conditions were used in examining the low energy portion of the ^{153}Sm decay, except that samples were allowed to decay for at least one half-life before counting was begun to allow the ^{155}Sm and ^{152m}Eu impurity activities to decay. However, in order to investigate the extremely weak transitions above 200 keV in the ^{153}Sm decay, irradiation times of up to 20 hrs with corresponding source strengths of the order of 20 mCuries were required. As in the case of ^{155}Sm, no chemical purification was carried out, and in addition to trace amounts of ^{152m}Eu, some transitions associated with the decay of 40.2 hr ^{140}La were observed.

2.3.2 Accelerator Targets

Several important features are required of targets which are to be used in reaction experiments, particularly for experiments in which the desired information is obtained largely or solely through the study of outgoing charged particles. Deuterons, protons, alphas, etc. interact strongly with matter via their Coulomb fields and lose appreciable energy in doing so. Furthermore, this energy loss is a function of the path length in the material, so that depending on the origin of the ion in the target, a range of energy losses will occur. Since both the tandem Van de Graaff accelerator and the analyzing spectrographs are able to maintain an energy stability of several parts in 10,000, spreads in particle energy due to target thickness effects must be kept to this order of size. Placed against this requirement, however, is the need to have a thickness large enough to produce an appreciable number of events in a reasonable time and which will stand up for several hours to bombardment by a current of several microamperes of 20 to 30 MeV ions. Chemical and isotopic purity, as for almost all nuclear spectroscopic studies,is also required.

The Sm targets used in the present work were prepared by reducing isotopically enriched Sm_2O_3 to a metal using the La reduction technique (Westgaard (1966)) and by evaporating the metal during this process nto carbon backings by electron bombardment. Since La metal oxidizes fairly rapidly, fresh

samples of fine filings were obtained from a piece of high purity La before each evaporation. It was also found necessary to dry the Sm_2O_3 in a Pyrex crucible over a flame before evaporation. The La (12 mgs) and Sm_2O_3 (10 mgs) were, after thorough mixing, placed in a Ta crucible for outgassing. The crucible which was 12 mm long was made of 5 mm diameter tantalum rod with a 3 mm diameter hole drilled into it. The depth of the hole was 10 mm and a tapered tantalum top with a 1.2 mm central aperature was used to cap the assembly. The rate of reduction and evaporation was found to depend quite critically on the size of this aperture.

The crucible containing the La and Sm_2O_3 mixture was mounted vertically in an evaporating boat made of thin tantalum sheet and was placed in a vacuum chamber. After evacuation to a pressure of about 10^{-7} torr a current of several amperes was passed through the boat. The current was gradually increased so that after about 10 minutes the temperature of the assembly was about 800°C. During this time period the pressure in the chamber was found to initially rise quite rapidly due to outgassing and then to again decrease. Without this outgassing sequence it was found that the crucible often "burped" during the later evaporation expelling a large portion of the La-Sm_2O_3 mixture.

The target backings used in the present work were 50 $\mu g/cm^2$ carbon foils evaporated along with a $BaCl_2$ substrate

onto standard 2.5 cm width microscope slides and were manufactured by the Yissum Research Development Co. of Israel.

Since the magnetic spectrograph acts essentially as a lens system, the particle tracks of a particular energy recorded on the nuclear emulsion should cover an area which is an approximate reproduction of the beam spot area on the target. It is possible, however, during the course of a several hour exposure for the beam position to wander a fraction of a mm causing a smearing of the "object" position and a corresponding decrease in the resolution of the "image". In order to reduce this effect, "line" targets of about 0.5 mm in width were produced by masking all but a 0.5 mm wide strip of the carbon with tantalum sheet.

The crucible, after the above "preheating" procedure, was mounted in the target pan of a Varian electron gun in a vacuum chamber. Three slides of carbon backings, two masked and one unmasked, were mounted vertically above the crucible at a distance of about 9 cms. The chamber was evacuated to a pressure of ~ 10^{-8} torr and the crucible was slowly heated by electron bombardment (5 keV) until it reached a temperature of 1280°C. Reduction of the Sm_2O_3 and evaporation of the metal by the

$$Sm_2O_3 + \rightleftarrows 2Sm\uparrow + La_2O_3$$

process was found to occur appreciably at this temperature and was accompanied by the appearance of a faint blue glow

above the crucible top. A conversion and evaporation rate of about 1 mg/min and 8μg/cm^2/min onto the backings was found to occur at this temperature. Evaporation was generally continued for about 10 minutes producing target thicknesses of 60-90 μg/cm^2. Various temperatures were tried in an attempt to optimize conversion rates while also keeping the La impurity in the evaporated targets to a minimum. A neutron activation analysis of Sm metal samples produced at 1280°C showed a La content of less than 1 part in 1000, and no trace of La impurity peaks was found in the particle spectra.

Targets to be used for the stripping reactions were finally produced by floating the Sm and carbon foils on distilled water and then mounting these foils on 2.5 cm square polished aluminum frames which had a 1.0 cm diameter central hole. No deterioration was found in targets which were then kept in dessicators for periods of several weeks before usage. Each target was generally able to sustain two microampere currents of 28 MeV ^{3}He ions for 8 or 10 hours.

CHAPTER III

THE DECAY OF ^{155}Sm

3.1 Introduction

The level structures and decay properties of nuclei near the edge of the rare earth region of deformation (A ~ 150-155) have been of considerable interest since the introduction of the deformed nucleus models of Bohr and Mottelson (1953) and Nilsson (1955). The decay of ^{152}Eu to levels in both $^{152}Gd(\beta-)$ and $^{152}Sm(\beta+)$ illustrates well the transition properties of these nuclei. A majority of the excited levels of 90 neutron ^{152}Sm have been well explained in terms of the ground state rotational, and the β and γ vibrational bands predicted by the deformed models. However, no similar suitable explanation appears to work properly for the levels of the 88 neutron isobar ^{152}Gd.

The energy levels of the odd proton $^{155}_{63}Eu$ nuclide which are fed by the beta decay of ^{155}Sm have been studied by various workers using both magnetic and scintillation spectrometers (Schmid and Burson (1959), Sund et al (1960), Kracik et al (1963), Funke et al (1965A)). These studies established the strongly fed low-lying levels. Considerable doubt existed, however, as to the position of weakly populated higher-lying levels and as to the existence and placement of most gamma transitions above

Z=63	Eu 153 stable	Eu 154 16y	Eu 155 1.8y	Eu 156 15d
Sm 151 90y	Sm 152 stable	Sm 153 47h	Sm 154 stable	Sm 155 22.3 m

Figure 4 Reduced Nuclide Chart

200 keV. The present investigation was begun in the hope of resolving the existing conflicts and also in order to extend the known data through the use of Ge(Li) detectors in singles and coincidence experiments. Details of the experiments carried out and of the interpretation of the data obtained are presented in this chapter along with a comparison with the results of other workers published during the course of the present study. A reduced portion of the nuclide chart relevant to the present studies is shown in Fig. 4.

3.2 Half-Life Measurement

The half-life of ^{155}Sm was measured by following the decay of the prominent 245 keV gamma ray for 10 half-lives with a Ge(Li) detector. Spectra were recorded sequentially for one or two live-time minutes and stored in the Nuclear Data 160M memory unit which had been divided into sixteen 256-channel sections. Figure 5 shows a semi-logarithmic plot of the integrated peak area as observed for some 215 minutes. A half-life value of 22.4 ± 0.3 minutes was obtained by a weighted non-linear least squares fit to the data using the method of maximum likelihood. This value is to be compared to the value of 22 minutes accepted by the Nuclear Data Sheets(1963).

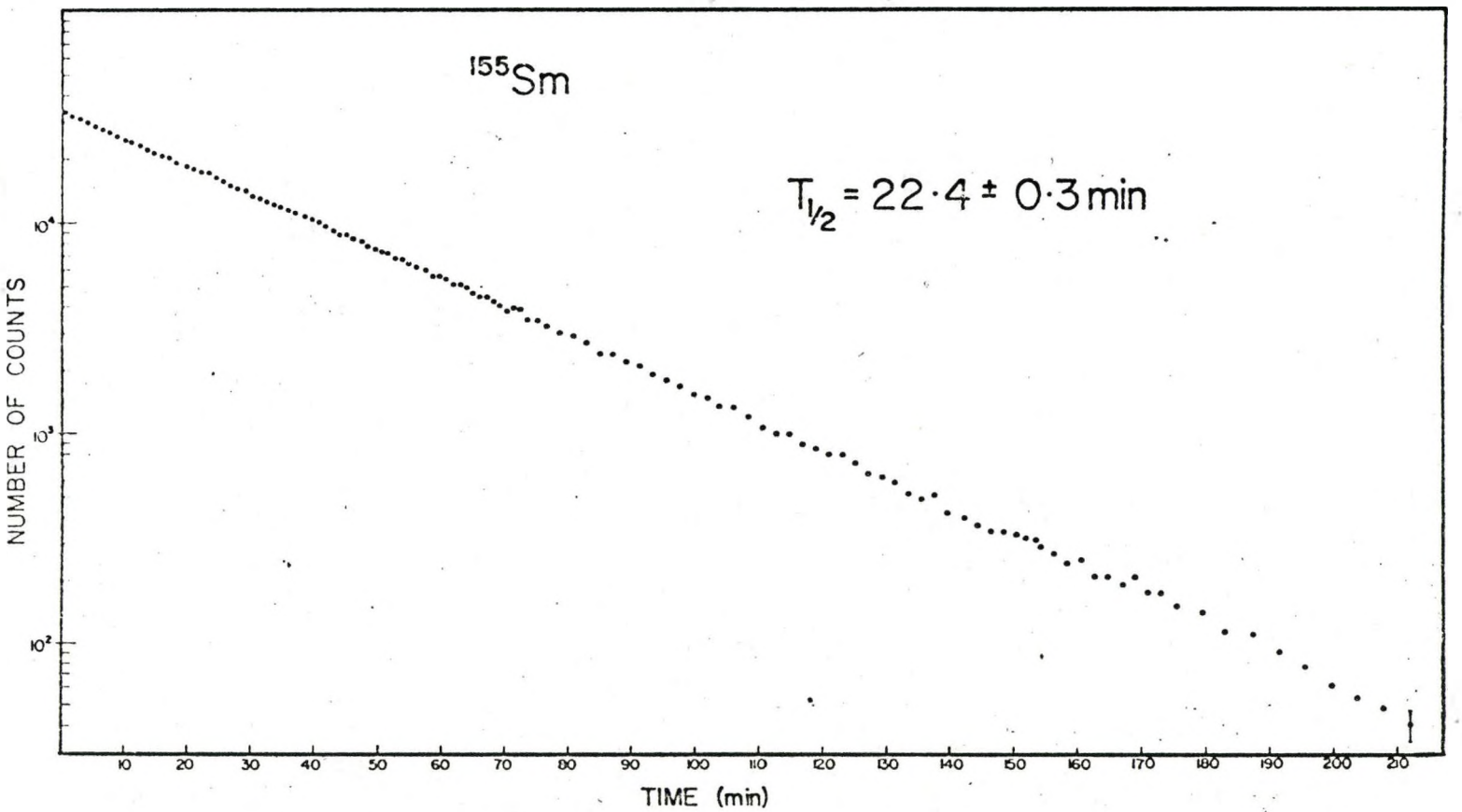

Figure 5 ^{155}Sm Half-Life

3.3 Ge(Li) and Si(Li) Singles Gamma Ray Results

The Ge(Li) gamma ray spectra were taken using two different detectors. A 6 cm^3 active volume "wrap around" detector was used for the preliminary runs, but its maximum resolution of about 6 keV was inadequate to resolve several doublets. Later experiments used a 1.5 cm^2 × 4 mm thick Nuclear Diodes planar detector which when coupled to a cooled F-E-T TC130 preamplifier yielded an optimum resolution of 1.8 keV at 400 keV. Multiple sources (up to 30 per run) were used in accumulating the spectra and energy calibration was achieved through the use of a composite gamma ray source consisting of ^{155}Sm and several well known standards. The standards used included ^{241}Am, ^{57}Co, ^{141}Ce, ^{203}Hg, ^{137}Cs, ^{54}Mn, ^{65}Zn, ^{60}Co, and ^{207}Bi. Corrections for system non-linearity as earlier discussed were also applied.

Figure 6 shows a spectrum accumulated during about 20 hours of counting time using the planar detector. The dominance of the 104.3 keV gamma ray in this decay is quite obvious. Quanta below about 70 keV are quite highly absorbed because of a dead layer of ~ 0.8 mm Ge on the detector surface. A graded 1.5 mm thick Pb + 0.8 mm thick Cd absorber was used between the source and detector in the investigation of the higher energy portion of the spectrum. This amount of absorber reduced the number of 104 keV quanta reaching the detector by about 2 orders of magnitude and Figure 7 shows a spectrum obtained in this manner.

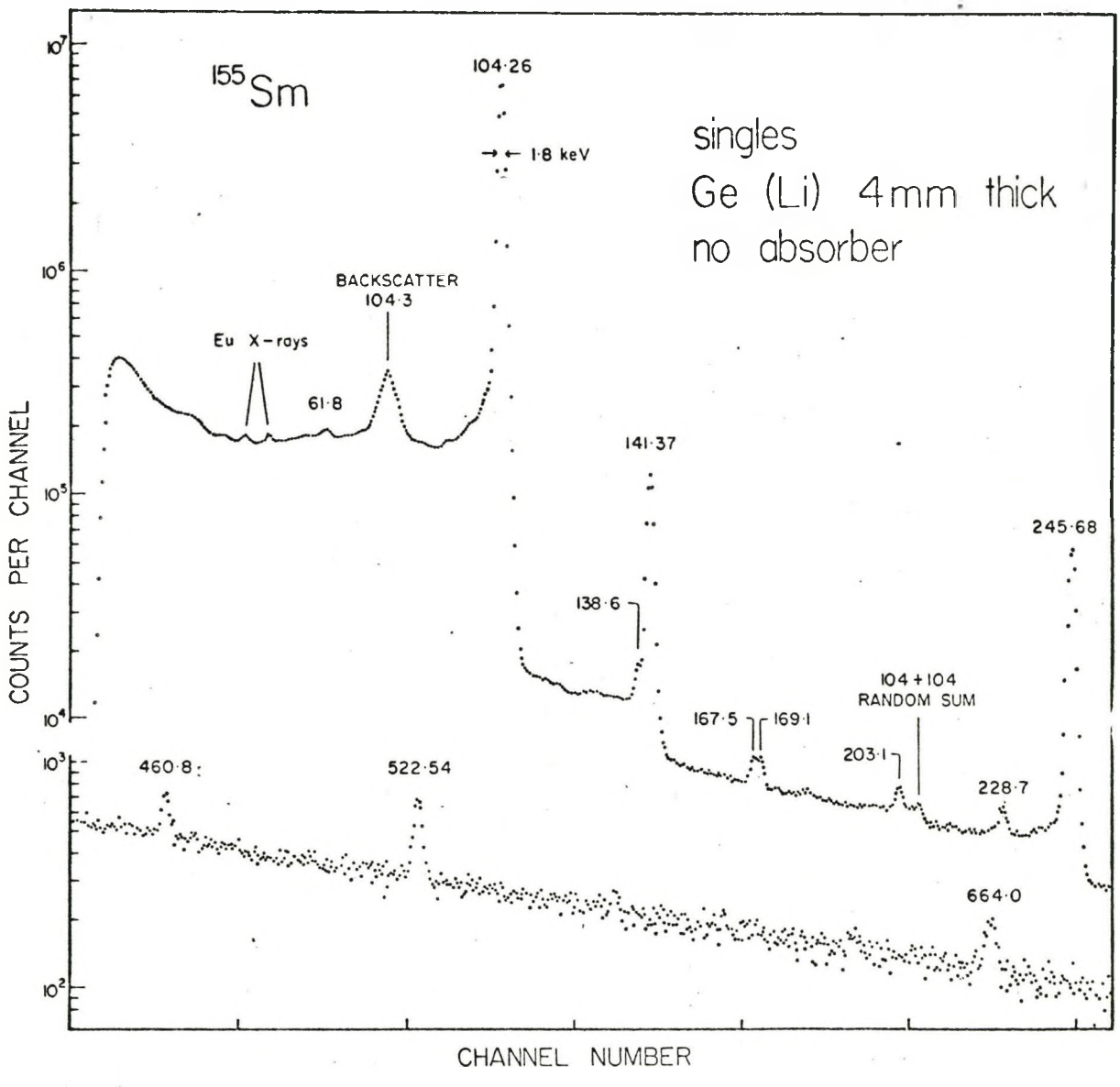

Figure 6 ^{155}Sm Low Energy Ge(Li) Spectrum

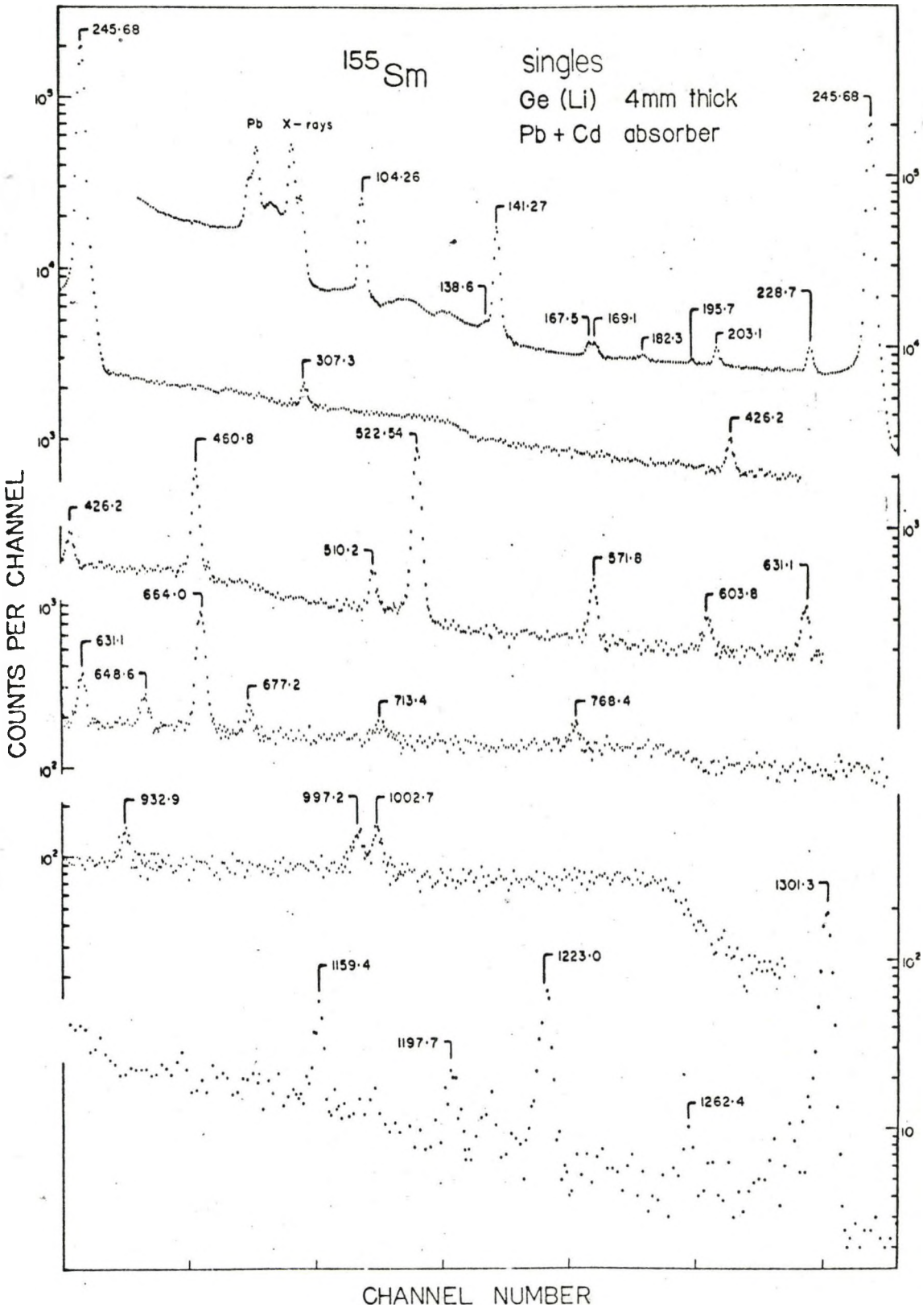

Figure 7 ^{155}Sm Ge(Li) Spectrum with Absorber

A Si(Li) detector was used to investigate the highly absorbed low energy region of the gamma ray spectrum. The detector was 1 mm thick by 1.5 cm^2 and, when operated at liquid nitrogen temperatures and coupled to a cooled F-E-T pre-amplifier, gave a 3.0 keV resolution at 100 keV. The gamma ray spectrum obtained is shown in Figure 8. The Eu X-ray and 61.9 keV peaks are seen much more prominently than in the Ge(Li) spectra. Peaks are also resolved at 26.6 and 78.6 keV, near the Compton edge and backscattered peak of the 104 keV transition, respectively. The upper insert of the diagram shows the analysis used in decomposing the 0-30 keV region in order to determine the 26 keV transition energy and intensity. The dotted curve is an expanded view of the first 100 channels of the experimental data. This spectrum was decomposed into the Compton distribution of the 104 keV line (solid line), the tail of the Eu X-rays (dashed line), and the contribution of the 26 keV gamma ray (dot-dash curve) shown vertically expanded by a factor of 2. The shape of the Compton distribution was obtained by using a Cu absorber in front of the detector which eliminated the 26 keV and X-ray contributions to the spectrum. A spectrum with a thinner Cu absorber which completely absorbed the 26 keV transition but only partially absorbed the X-rays was next recorded and the X-ray tail shape was obtained by subtracting the thick absorber spectrum from the thin absorber one. Subtraction of the normalized Compton and X-ray tail contributions

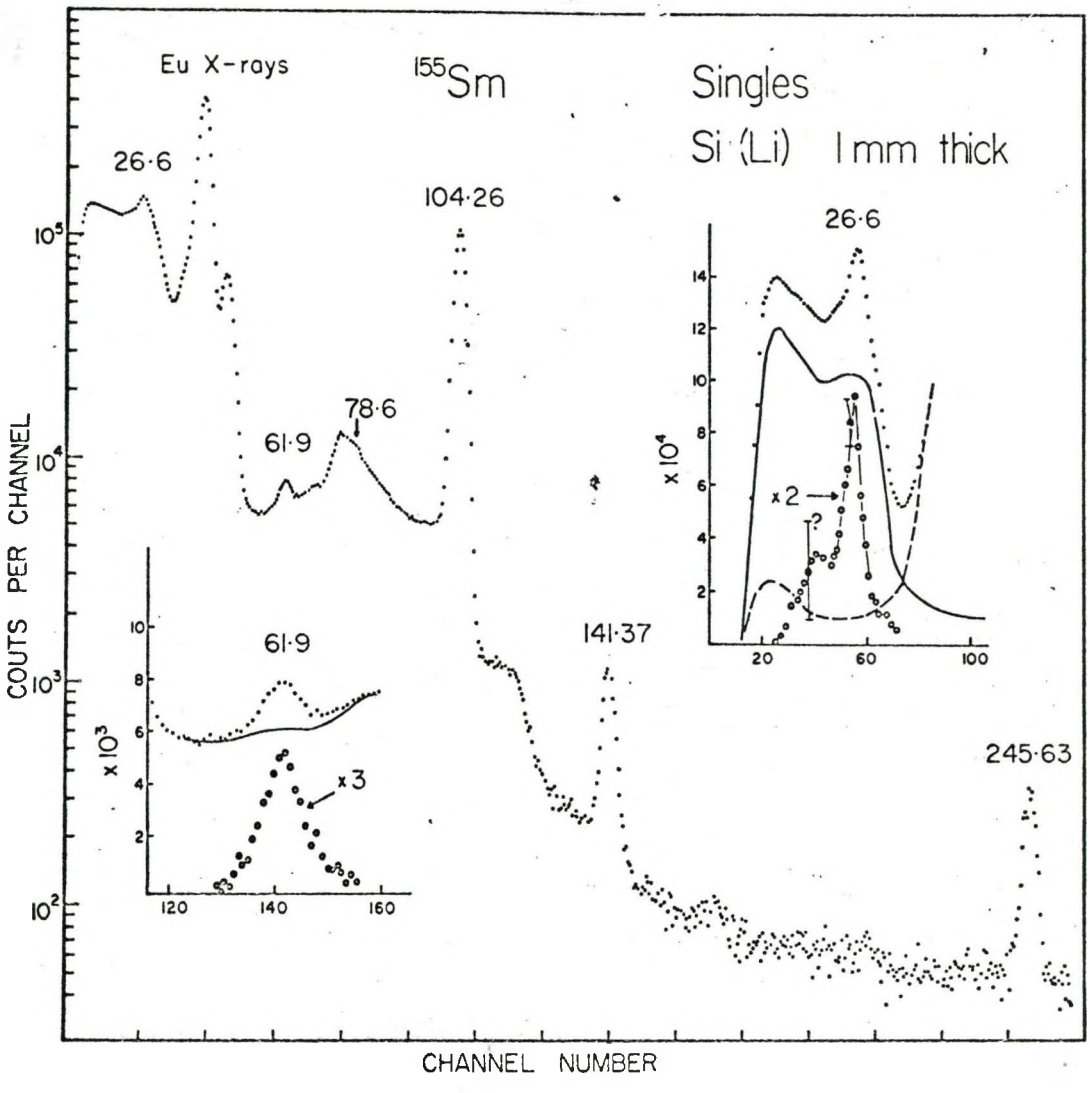

Figure 8 ^{155}Sm Low Energy Si(Li) Spectrum

from the total spectrum yielded the resultant 26 keV line shape. The detection efficiency of this detector was determined by comparison with a NaI detector of dimensions 2.5 cm x 0.3 cm which was covered with a thin Be window.

The energies and intensities of the 35 gamma rays observed in the singles spectra are listed in Table 1 along with the transitions observed in the coincidence measurements. Also listed are the gamma ray results of Funke et al (1966,1968) and Widemann et al (1968). Widemann et al, from singles gamma ray measurements, list a transition at 63.1 ± 0.5 keV of about 5% the intensity of the 61.55 keV gamma ray, as well as one at 80 ± 0.5 keV of about 10% the strength of the 78.6 keV transition which is near the backscattered peak of the strong 104 keV gamma ray. Since these authors do not present any data in support of these two transitions, and since they have not been seen in the present work, their reality is open to question. The results of Agin, Mandeville, and Potnis (1967) published during the present investigation do not add anything to the known data and will not be further discussed.

Wideman et al (1968) have also measured the conversion electron spectrum of ^{155}Sm. They observed 77 electron lines below 250 keV and have been able to associate an appreciable number of them with transitions in ^{155}Eu or in impurities. Identified transitions assigned by these workers to ^{155}Eu are: (10.0), 25.69, 61.55, (62.2), 78.65, (79.6),104.35, (105.9), (107), (114.5), (121.1), (129.2), 138.4, 141.37, (142.5), 167.1, 168.6, (205), 228.5, and 245.6 keV. The transitions in brackets

TABLE I

Energies, Intensities and Classifications of Transitions in ^{155}Eu

Present Work			Funke	Wide-mann	Classification
Energy	Photon Intensity per 100 Decays	Method Seen			
26.6 ±0.6	0.6±0.2	Si	26	25.7	104.3→ 78.5
				30.5	
				53.1	
Eu Xrays	17.1	Si			
61.8 ±0.3	0.4	Si,Ge,γγ	62	61.55	307.4→245.7
				63.1	
64.5 ±0.5	0.007	γγ			169.0→104.3
78.5 ±0.5	1.2±0.6	Si,Ge,γγ	79	78.65	78.5→ 0
				80	
84.1 ±0.5	0.0024	γγ			391.4→307.4
90.1 ±0.5	0.010	γγ			169.0→ 78.5
104.26±0.14	72.5	Si,Ge,γγ	105	104.35	104.3→ 0
138.6 ±0.25	0.064	Ge,	135	138.2	307.4→169.0
141.37±0.13	2.34	Si,Ge,γγ	141	141.35	245.7→104.3
167.5 ±0.3	0.048	Ge,γγ	168	167.1	307.5→ 78.5
169.1 ±0.3	0.050	Ge,γγ		168.7	169.0→ 0
178.3 ±0.5	0.002	γγ			1101.6→922.8
183.4 ±0.5	0.002	γγ			1106.7→922.8
195.7 ±0.4	0.009	Ge,γγ			1106.7→911.2
203.1 ±0.2	0.045	Ge,γγ	203	202.6	307.4→104.3

TABLE I (continued)

Energies, Intensities and Classifications of Transitions in ^{155}Eu

Present Work			Funke	Wide-	Classification
Energy	Photon Intensity per 100 Decays	Method Seen			
220.1 ±0.6	0.0022	γγ			1096.9→876.9
228.7 ±0.6	0.066	Ge,γγ	229	228.5	307.4→ 78.5
229 ±1	0.003	γγ			1106.7→876.9
245.68±0.13	3.95	Ge,γγ	246	245.6	245.7→ 0
			280		
287.1 ±0.4	0.0012	γγ			391.4→104.3
307.3 ±0.3	0.012	Ge,γγ	307	307.0	307.4→ 0
426.2 ±0.2	0.012	Ge,γγ	429	426.4	817.6→391.4
460.80±0.13	0.069	Ge,γγ	462	461.2	768.2→307.4
510.2 ±0.2	0.011	Ge,γγ	509	510.7	817.6→307.4
522.54±0.15	0.15	Ge,γγ	522	522.9	768.2→245.7
571.8 ±0.2	0.0176	Ge,γγ	570	572	817.6→245.7
603.8 ±0.2	0.0084	Ge,γγ	602	603.8	911.2→307.4
631.2 ±0.2	0.014	Ge,γγ	630	631.5	876.9→245.7
648.6 ±0.2	0.0076	Ge,γγ	647	649.0	817.6→169.0
664.00±0.16	0.061	Ge,γγ	663	664.4	768.4→104.3
665 ±1	0.006	γγ			911.2→245.7
677.2 ±0.3	0.0067	Ge,γγ	676	677.6	922.7→245.7
713.4 ±0.8	0.003	Ge,	710	713.7	817.6→104.3
				758	
768.4 ±0.4	0.0055	Ge	768	768.5	768.2→ 0
			818.1		818.6→ 0

TABLE I (continued)

Energies, Intensities and Classifications of Transitions in ^{155}Eu

Present Work			Funke	Widemann	Classification
Energy	Photon Intensity per 100 Decays	Method Seen			
830 ±20	0.001	γγ			911.2→ 78.5
			861.1		1106.7→245.7
880 ±10	0.003	γγ			876.9→ 0
910 ±20	0.001	γγ	911		911.2→ 0
920 ±20	0.001	γγ	923		922.8→ 0
932.9 ± 0.4	0.008	Ge,γγ	931	932.6	1101.6→169.0
997.9 ± 0.4	0.010	Ge,γγ	996	997.2	1101.6→104.3
1002.7 ± 9.3	0.012	Ge,γγ	1004	1002.3	1106.7→104.3
			1018		1263.0→245.7
1060 ±20	~0.001	γγ	1055		1301.4→245.7
			1096		1096.9→ 0
1130 ±20	0.002	γγ	1132		1301.4→169.0
1159.7 ± 0.3	0.0036	Ge,γγ	1158	1159.0	1263.0→104.3
				1174.5	
1197.7 ± 0.4	0.003	Ge,γγ	1197	1196.7	1301.4→104.3
1207.8 ± 1.0	0.0015	Ge		1207	
1223.0 ± 0.3	0.019	Ge,γγ	1223	1222.6	1301.4→ 78.5
1262.4 ± 0.5	0.0024	Ge	1262	1262	1263.0→ 0
1301.2 ± 0.2	0.067	Ge	1302	1301.3	1301.4→ 0

have not been observed in the present work, and in addition do not fit in the decay scheme to be proposed. Of these, the underlined ones have been placed by Widemann et al (1968) in their decay scheme and will be discussed later.

Several of the higher energy transitions reported by Funke et al (1968) were unobserved in the present singles studies because of the small active volume of the detector used. These have been of some importance in deduced the decay scheme proposed here, and will be further discussed in the section on coincidence experiments.

3.4 Gamma-Gamma Coincidence Results

The experimental and analysis techniques used in the two-parameter coincidence experiments have been already discussed. For the investigation of the ^{155}Sm decay two coincidence experiments were carried out. In the first no absorber was used in front of either the NaI or Ge(Li) counters while in the second a graded Pb+Cd absorber was used to reduce the number of 104 keV quanta reaching the scintillation detector. In both experiments the detectors used were a 1.5 cm^2 × 4 mm thick Ge(Li) detector and a 7.5 cm × 7.5 cm NaI counter. For the no-absorber experiment almost all the coincidence events were concentrated in the intense 104-141 keV cascade. No new results were found; however, a confirmation of the 62-245, 62-141-104, 228-78 and 203-104 keV cascades was obtained. No

further discussion of this experiment will be presented. A gain of ~ 0.8 keV per channel along the Ge(Li) axis and 4.6 keV per channel along the NaI axis was used in the second experiment along with a true-to-chance rate of 30 to 1 at a 100 nsec. resolving time. The projections of the coincidence matrix onto the NaI and Ge(Li) axes are shown in Figure 9 for this experiment. The enhancement of lines at 169, 196 and 220 keV relative to the singles spectra is easily noted.

The levels up to 307 keV have been well established and apart from additional weak transitions which the coincidence results to be discussed have added, no further discussion of these levels will be given.

Ge(Li) coincidence spectra in coincidence with the 141 and 245 keV transitions which depopulate the 245 keV level are shown in Figure 10. These two spectra should correspond apart from the 104 keV transition which is strongly in coincidence with the 141 keV transition but not the 245 keV. Except for the 169 keV line in the lower spectrum which is due to the 138.4 keV transition included in the 140 keV gate this appears in fact to be true. It should be noted that the upper spectrum of the diagram is a difference spectrum while the lower is not. The 104, 141 and 245 peaks seen in the 245 keV gated spectrum are due to improper background subtraction, chance events, and also partially to coincidences with the 220 and 228 keV photopeaks included in the gate. Compton contributions of

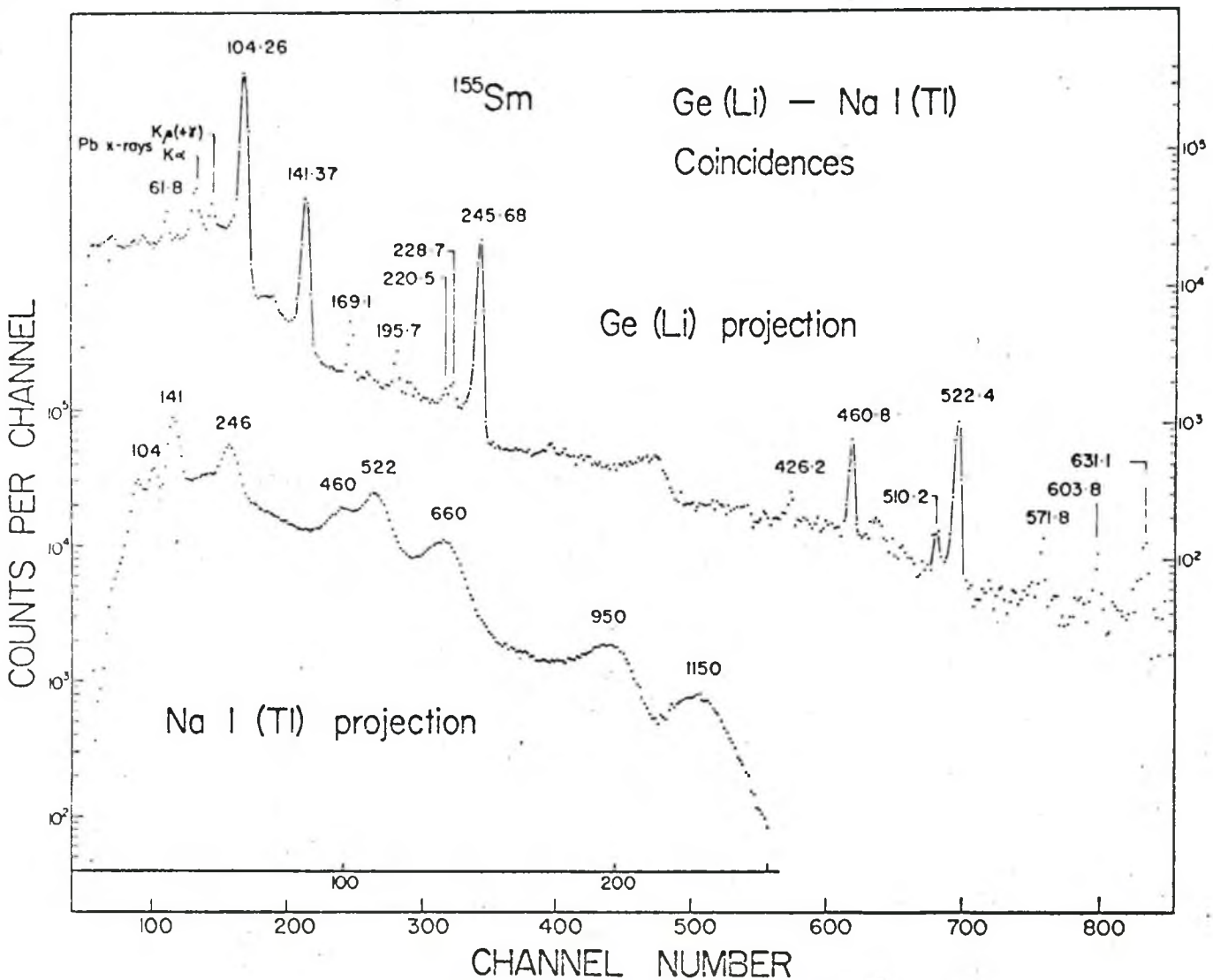

Figure 9 ^{155}Sm Coincidence Projections

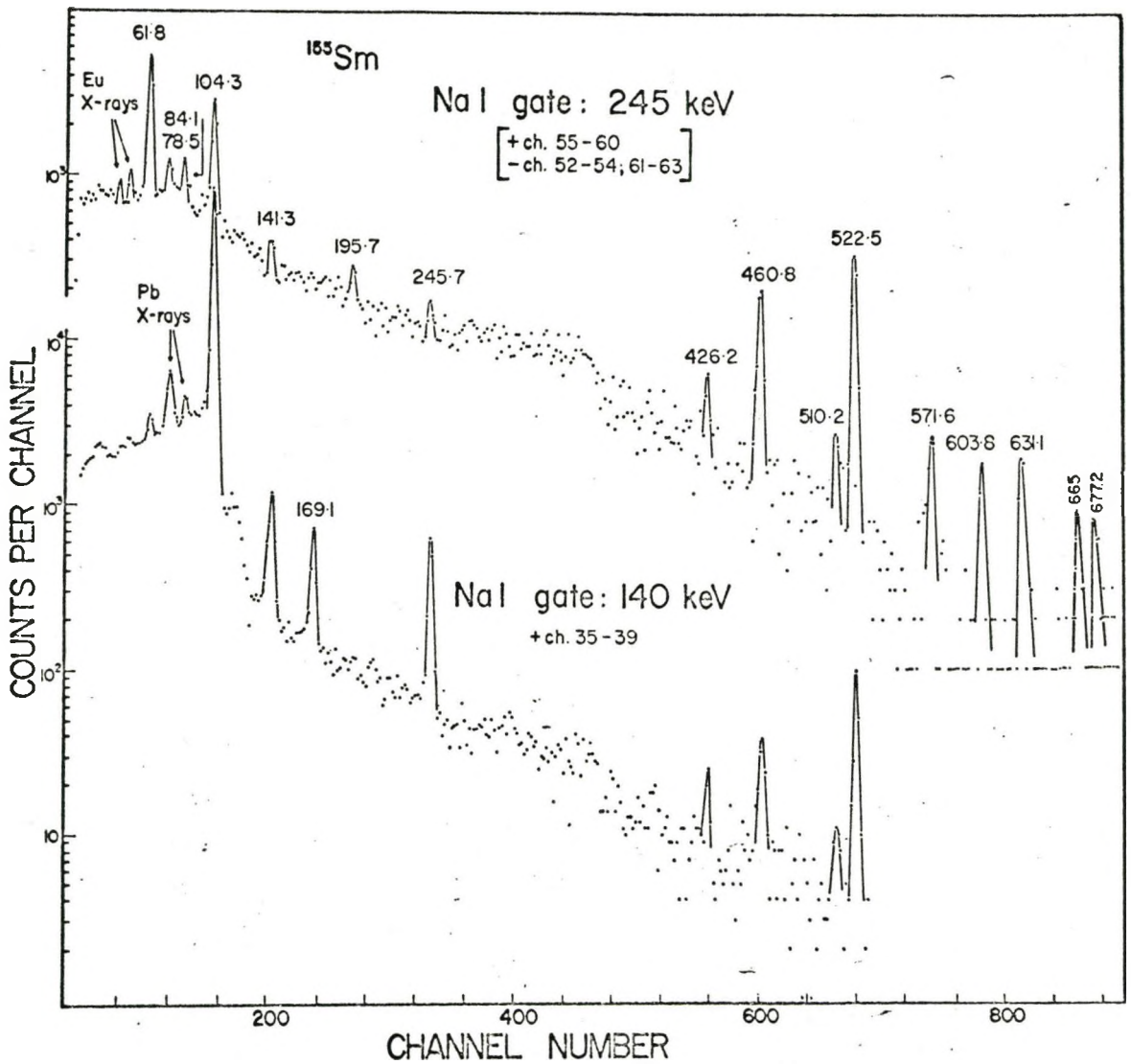

Figure 10 ^{155}Sm Ge(Li) Coincidence Spectra

higher energy events produce the 141, 245 and a portion of the 104 keV peaks in the lower spectrum.

The peak at 61.8 keV in Figure 10 arises from the 61-245 and 61-141 keV cascades which are the main decay routes of the 307 keV level. Peaks seen at 78 and 84 keV are largely, but not entirely, due to Pb X-rays. That they are in fact partly due to real transitions is evident since their relative heights do not remain constant in all spectra. The enhancement of the 84 keV peak in these spectra is due to the 84-62-245 keV cascade which arises in the decay of the 391 keV level. Further evidence in support of this level will be later presented. Energy sums and coincidence data together suggest that the 62, 522, 572, 631, 665 and 677 keV transitions feed the 245 keV level while the 84, 461, 510 and 603 keV gamma rays feed the 307 keV level which is strongly coupled to the 245 keV level by the 62 keV transition. The 196 keV peak will be shown to arise from a 195-603-62-245 keV cascade. It should finally be noted that the 665 keV transition observed here is not the strong 664.0 keV gamma ray seen in the singles spectra and which feeds the 104 keV level. It is in fact a second unresolved transition whose intensity can be deduced from the strengths of the 665 and 677 keV peaks to be 0.006%.

Figure 11 shows the Ge(Li) spectrum in coincidence with a NaI gate which includes the photopeaks of the 426 and 460 keV transitions. The insert below 100 keV is for a gate of reduced

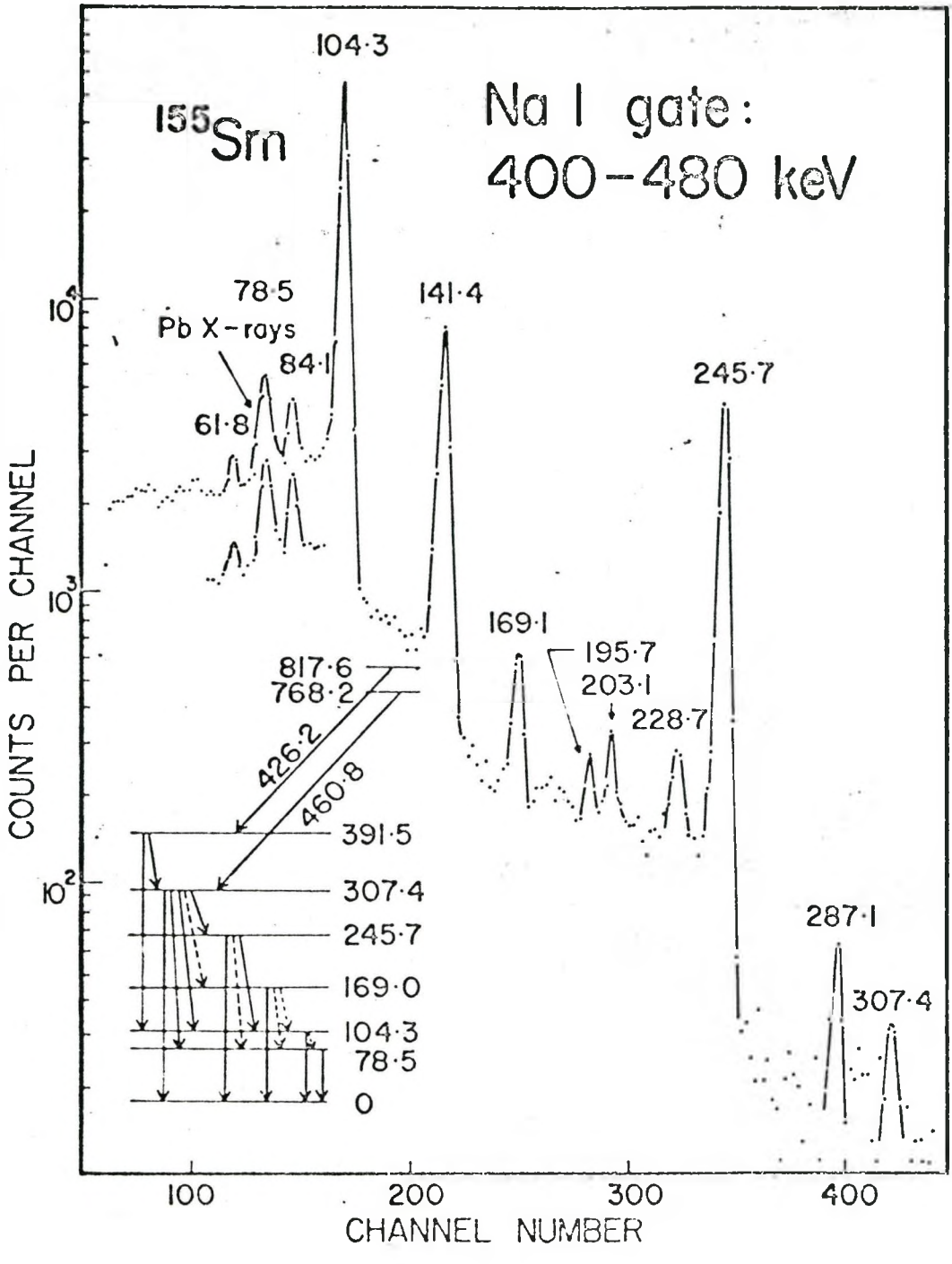

Figure 11 ^{155}Sm Coincidence Spectrum

energy (400-430 keV) and shows that the 84 keV peak is enhanced in this spectrum. This enhancement along with energy sums and the appearance of the 287.1 keV gamma ray in this gate have led to the establishment of the level at 391.5 keV. The 62, 203, 228 and 307 keV transitions all of which depopulate the 307 keV level are observed in the spectrum and show that the 460 keV transition feeds the 307 rather than the 245 keV level. No background has been subtracted from the above spectrum, and the 196 keV peak is due to the Compton distributions of the 603 and 665 keV transitions in this gate.

In Figure 12 are shown the Ge(Li) spectra in coincidence with three other NaI gates. Figure 12c shows further evidence for the previously discussed 169-138 keV cascade. The 140 keV regions of the coincidence matrix in coincidence with paired channels in the 150-190 keV NaI spectrum are shown. The enhancement of the weak 138.6 keV transition at 170 keV (channels 41+42) is quite drastic.

A broad NaI gate from 1160 to 1300 keV was used to obtain the spectrum shown in Figure 12a. The 78.5 keV gamma ray which is obscured by the 104 keV backscattered peak in the singles spectra and by Pb X-rays in most of the coincidence spectra is shown highly enhanced due to the 1223-78 keV cascade. The strong 104 keV peak is due mainly to coincidences with the 1159 and 1197 keV transitions which are included in this gate. It will be shown later (Figure 14c) that there exists a transi-

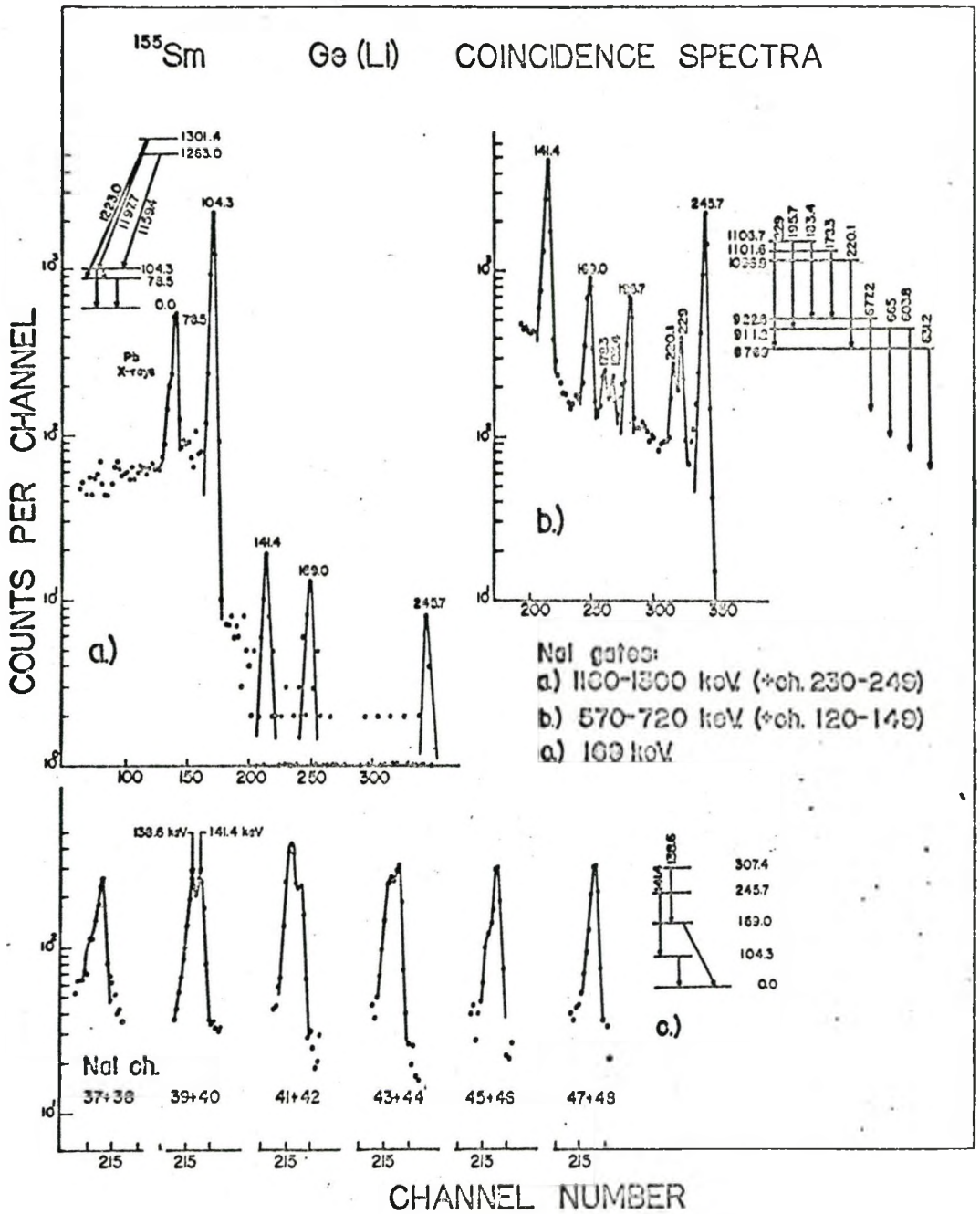

155
Figure 12 Sm Ge(Li) Coincidence Spectra

tion at 1130 keV which feeds the 169 keV level. The high energy tail of its photopeak present in the gate is sufficient to account for the 169 keV peak observed. From the true-to-chance ratio (30:1) and the singles spectrum, the chance contribution to the 141 and 245 keV peaks was estimated to be about one half; the remainder must be due to very weak gamma rays from levels above 1301 keV which feed the 245 keV level.

The Ge(Li) spectrum in coincidence with a NaI gate from 570 to 720 keV is seen in Figure 12b. This gate contains the following eight transitions; the 664.0 and 713.4 transitions which are in strong coincidence with the 104 keV gamma ray (not shown), the 571.8, 631.2, 665, and 677.2 keV transitions which populate the 245 keV level, the 603.8 keV gamma ray to the 307 keV level, and finally the 648.6 keV gamma ray which populates the 169 keV level. Further evidence for the 648.6 keV assignment is shown in Figure 14c which shows the NaI difference spectrum in coincidence with a 169 keV Ge(Li) gate. The 178.3, 183.4, 220.1 and 229 keV peaks seen in Figure 12b cannot be fitted into the well established low lying levels which are fed by the eight gamma rays in the gate; hence these must be high lying transitions which feed some of the levels in which the gating gamma rays originate. An analysis of this spectrum along with those in Figures 13a, 13b, 13c, 14a and 14b allows one to justify this claim and locate the high lying states involved.

It should first be remarked that the 229 keV transition seen in Figure 12b is not the transition from the 307 to the

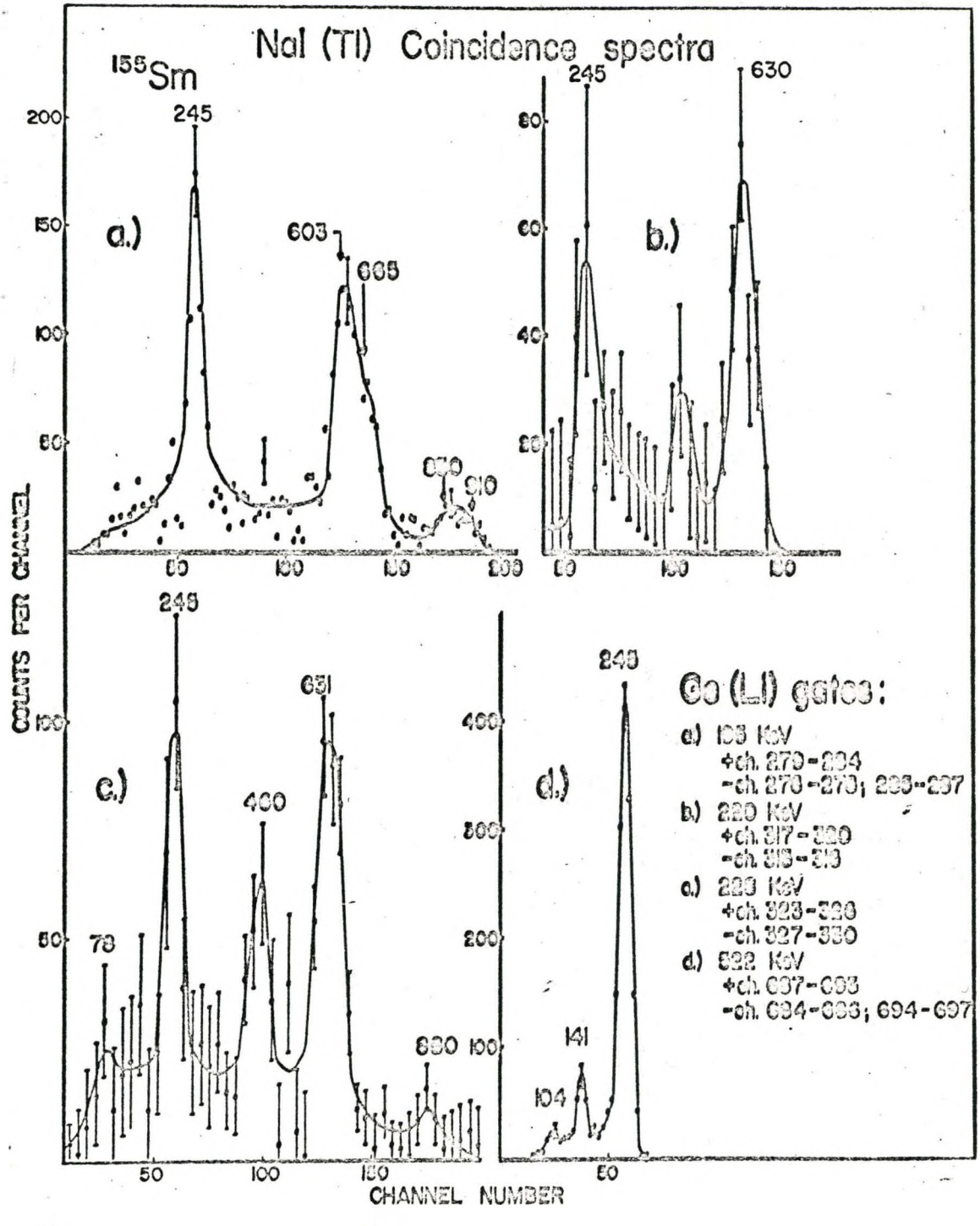

155
Figure 13 Sm NaI Coincidence Spectra

78 keV level already seen in Figure 11. In that spectrum the 228 keV transition is observed along with a 203 keV peak of comparable intensity which also depopulates the 307 keV level. The absence of this 203 keV peak in the present spectrum requires that there exist two unresolved gamma rays at this energy. An analysis of the coincidence peak areas indicates that the two components have respective intensities of 0.066 and 0.003% with the stronger component associated with the 307→78 keV assignment.

The weaker 228 and 220 keV transitions should be considered together in Figures 14a, 14b, 13b and 13c. NaI difference spectra in coincidence with Ge(Li) gates set on these peaks are seen in the latter two figures. These spectra both indicate coincidences with the 245 and 631 keV gamma rays. The 460 keV peak in Figure 13c is due to the previously assigned 228 keV component from the 307 keV level, and the similar but smaller peak in the 220 keV gated spectrum is due to a contribution of the 228 keV line to this gate. A peak at ~ 880 keV is also seen in Figure 13b. Its intensity was determined from its intensity relative to the 630 keV gamma ray to be 0.001%.

Figures 14a and 14b show the Ge(Li) spectra in coincidence with respective NaI gates of 830-880 and 880→940 keV. The 220 and 229 keV transitions are both seen clearly in the first spectrum but are substantially reduced in the second. This fact along with the results seen in Figures 12b, 13b and

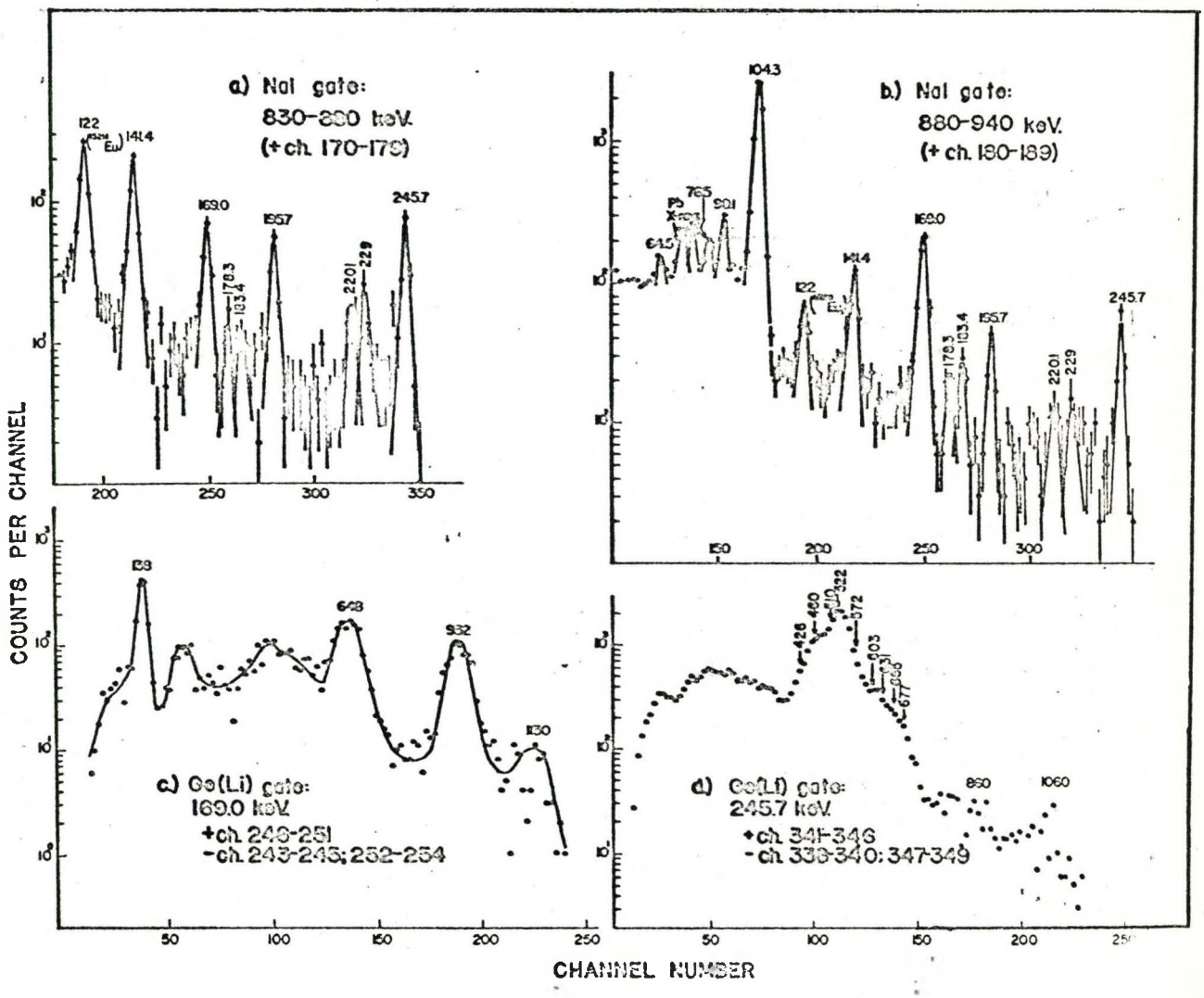

155

Figure 14 Sm Coincidence Spectra

13c and the energy sums have led to the introduction of new levels at 876.9 and 1096.9 keV. These levels account for the observed 220-631-245, 228-631-245, and 228-876 keV cascades. Funke et al (1968) report the existance of a weak 1096 keV transition which is assumed to be the ground state decay of the 1096.9 keV level proposed here. The 229 keV transition depopulates the 1106.7 keV level for which further evidence will be presented.

Coincidence probabilities are required to estimate the intensities of the 220 and weaker 228 keV transitions, which are not observed in the singles spectra. Using the data of Figure 14b, comparison of the intensities of the transitions depopulating the 876 keV state with the peak areas of the 220 and 228 keV gamma rays yields intensities for the latter transitions of 0.003 and 0.004%, respectively. The value of 0.004% for the 228 keV line agrees well with the estimate of 0.003% obtained from the 570-720 keV NaI gate.

The NaI difference spectrum in coincidence with the 195 keV transition is displayed in Figure 13a. This relatively weak transition is seen to be in coincidence with the 245 keV gamma ray as well as with unresolved doublets at 630 and 900 keV. Coincidences of the 195 keV transition with gamma rays in the 570-720 keV NaI window and with gamma rays in both the 830-880 and 880-940 keV gates (Figures 14a and 14b) are also observed. These data may be accounted for by assuming the existance of 195-911,

195-833, 195-665, 195-603, and 195-603-245 keV cascades, which define a new level at 911 keV and lend support to the previously introduced level at 1106 keV. Funke et al (1968) have observed a 911 keV transition in their singles spectra. This presumably is the transition seen in Figure 13a, and we shall adopt their Ge(Li) energy determination as correct. The 830 keV transition seen in Figure 13a is defined by the decay scheme to be 833 keV. Using the 603 keV line as an intensity standard and correcting for the detection efficiency results in intensity values of 0.004, ~ 0.001, and ~ 0.001% for the 665, 833 and 911 keV transitions, respectively.

Two weak peaks, namely the 178 and 183 keV, remain as yet unaccounted for in Figure 12b. These two transitions are observed also in Figures 14a and 14b where they are more prominent in the 880--940 than in the 830-880 keV gate. These data may be explained by the introduction of a level at 922.8 keV which is populated by these two transitions and is subsequently depopulated by transitions of energy 677 and 923 keV. A 923 keV transition has also been reported in the work of Funke et al (1968). The intensities of the 178 and 183 keV gamma rays can be obtained from Figure 12b by comparison with either the 220-229 keV doublet or the 195 keV peak. Using the value of 0.002% for each of these lines, thus obtained, the 923 keV intensity is estimated to be ~ 0.001%.

Figure 13d shows the difference spectrum in coincidence

with a 522 keV Ge(Li) gate. A strong coincidence peak is seen at 245 keV corresponding to the depopulation of the 768 keV level. The greatly reduced strength of the 104 and 141 keV transitions in this spectrum is due to the use of an absorber in front of the NaI detector. From the absence of counts beyond the 245 keV peak in this spectrum, an upper limit of 0.001% can be set on the intensity of gamma rays feeding the 768 keV level.

Most of the lines in Figure 14b have now been accounted for. Of those remaining, the 64.5, 90.1 and 169.0 keV are due to coincidences with the 932 keV gamma ray which feeds the 169 keV level, while the 122 keV is due to the strong 840-122 keV cascade in the 9.3 hr ^{152m}Eu impurity. This peak is much more prominent in the 830-880 keV gate of Figure 14a.

Figure 14c offers confirmation for several cascades which have been already discussed. This difference spectrum shows 169 keV coincidences with transitions at 138, 648, 932 and 1130 keV. The intensity of the 1130 keV obtained from this spectrum is ~ 0.002%. The peak at ~ 250 keV is due to improper background subtraction.

The complex of gamma rays in coincidence with the 245 keV gate is shown in Figure 14d. No attempt has been made to extract the individual peaks from this complex. The peak at 1060 keV arises from coincidences with a transition of of intensity $\sim$0.001% which proceeds from the 1301 to the 245 keV state.

3.5 Log $f_o t$ Values

Since no direct measurements have been made of the beta groups involved in the present decay, the log $f_o t$ values have been derived from the gamma ray intensity balance. The total decay energy of 1625 ± 15 keV as reported by Funke et al (1965A) has been used in arriving at the present values. Since none of the reported experiments have detected the beta group feeding the ground state, the intensity of this group has been arbitrarily taken as zero. The remaining log $f_o t$ values are, of course, relatively insensitive to the intensity of the ground state beta feed and would not have been significantly altered had a ground state feed as large as 10% been assumed.

Allowance for the effect of internal conversion has been made for all the low energy transitions; in those cases where the experimental conversion coefficients are unknown, theoretical values for pure multipoles have been employed. The 61.8 (M1) and 104 (E1) keV transitions are the only two cases where the internal conversion contributions have a significant effect on the intensity balance. For the 104 keV case the theoretical value of 0.22 for α_K together with the K/L ratio of 7.0 reported by Hatch et al (1968) have been used. This α_K is somewhat smallwr than the value of 0.27 ± 0.06 reported by Schmid and Burson (1959) but is supported by the present measurement of the total K X-ray intensity and the $\alpha_K = 0.22 \pm 0.02$ value reported recently by Widemann et al (1968). Table II presents the percentage beta feeds to each state in ^{155}Eu together with the corresponding log $f_o t$ values and possible final state interpretations.

TABLE II

Intensity of beta transitions and log $f_o t$ values for ^{155}Sm Decay

Level Energy		% Feed	log $f_o t$
0	5/2+[413]	(assumed 0)	
78.5	7/2,5/2+[413]	3.1 $\pm$3.5	>7.1
104.3	5/2-[532]	89 $\pm$8	5.6
169.0	7/2,5/2-[532]	0.02 $\pm$0.03	>8.8
245.7	3/2+[411]	3.98 $\pm$0.50	6.8
307.4	5/2,3/2+[411]	3.02 $\pm$0.50	6.8
391.4	7/2,3/2+[411]	(assumed 0)	9
768.2	3/2+[422]	0.29 $\pm$0.03	>7.1
817.6	5/2,3/2+[422]	0.29 $\pm$0.01	7.8
876.9		0.010$\pm$0.003	8.5
911.2		0.004$\pm$0.001	8.8
922.7		0.005$\pm$0.001	8.7
1096.9		0.003$\pm$0.001	8.3
1101.7		0.020$\pm$0.003	7.3
1160.7		0.030$\pm$0.004	7.2
1263.0	3/2+, 5/2$\pm$	0.008$\pm$0.002	7.3
1301.4	5/2$\pm$	0.10 $\pm$0.02	6.2
Total		99.8 $\pm$12.5	

3.6 The ^{155}Sm Decay Scheme

The energy, intensity, and coincidence measurements of the present work have been combined with the results of other workers to produce the decay scheme shown in Figure 15. Observed coincidences are indicated by dots on the transitions involved. The scheme involves 16 excited states and 52 classified transitions. The levels below 307 keV have been well established by other workers and the present work has added several new connecting gamma rays and has sharpened the energy determinations of these levels. The 169.0→104.3 assignment for the 63.1 $\pm$ 0.5 keV transition reported by Widemann et al (1968) must be rejected from energy considerations alone. A new level has been added at 391.4 keV. on the basis of both coincidence data and energy sums. Widemann et al postulate a level at 388 $\pm$ 1 keV to account for their transitions of 142.5 and 80 $\pm$ 0.5 keV. No evidence for lines at these energies has been observed in this study nor do the limits of error on energy assigned by these authors allow them to be located as transitions from the 391.4 keV level.

New transitions have been found involving the previously established 768 keV state. The levels at 817 and 911 keV are introduced here for the first time. No evidence has been seen for the 758 keV level which Widemann et al (1968) have reported. They claim that this level is depopulated by a 758 keV gamma ray, which is unobserved in the present work and gamma rays

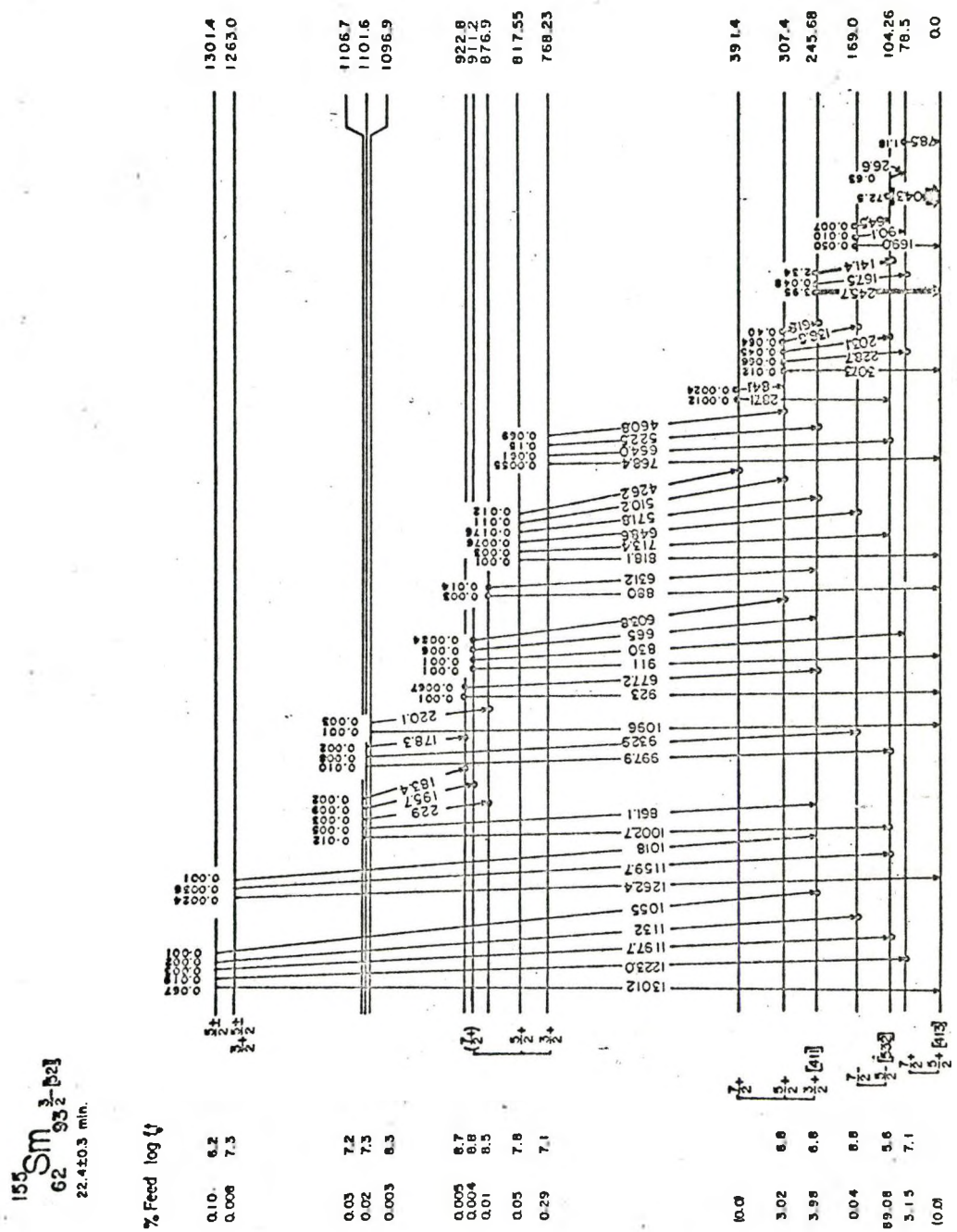

Figure 15 ^{155}Sm Decay Scheme

at 677 and 510 keV which our coincidence data clearly place in other places in the decay scheme. Our coincidence data has been used to place the 426 and 572 keV transitions from the 817 keV state to the 391 and 246 keV levels respectively, in contradiction to their assignment by Widemann et al (1968) as 1301→878 and 878→307 keV transitions.

Coincidence data and energy sums have been used to introduce levels at 876, 922, 1101, 1106, 1263 and 1301 keV. Each of these levels is located in the level scheme by at least three transitions. The weakly fed level at 1097 keV has been introduced on the basis of a 220-631 keV cascade and the weak 1096 keV transition that has been observed by Funke et al (1968).

Three new levels at 1002, 1174, and 1207 keV have been introduced by Widemann et al (1968) to account for three gamma rays at these energies. There is no real evidence from the present work for these levels; the 1002 keV gamma ray has been fitted elsewhere by coincidence and energy measurements, the 1207 keV could just as well be located elsewhere, and the 1174 keV has not been observed. These authors find support for the 1174 keV level in a transition at 129 keV, seen in their conversion data, which they assign as a 1301→1174 keV transition. No evidence for a 129 keV line is seen in the present work. Their levels at 1002 and 1207 keV are also supported by transitions at 100 and 94 keV respectively but they do not present

any evidence for the existence of these transitions in either the gamma ray or conversion electron spectra.

A detailed discussion of the excited levels and rotational bands in ^{155}Eu will be given in a later section together with a discussion of the ^{153}Eu levels also investigated in these studies.

CHAPTER IV

THE DECAY OF ^{153}Sm

4.1 Introduction

The population of levels in $^{153}_{63}$Eu following the decay of 47 hr $^{153}_{62}$Sm (β^-) and 242 day $^{153}_{64}$Gd (E.C.) has been the topic of a very large number of investigations. Sund and Wiedenbeck (1960) in 1960 presented a list of some 25 publications on these levels. Several additional investigations have been reported since that time, most notably by the ones by Suter et al (1962), Alexander (1964), Funke et al (1965), and Blichert-Toft et al (1966). Precise measurements have been made of the energies (Alexander (1964)) and conversion coefficients (Suter (1962)) of the transitions depopulating the five low-lying states below 175 keV, which are fed by both the ^{153}Sm and ^{153}Gd decays. No doubt exists as to the positions and nature of these levels.

Various problems exist, however, in the positions of levels and transitions above 200 keV which are populated by the beta decay of ^{153}Sm. The total beta feed intensity to these levels is less than 0.2%. In the most recently published work, Blichert-Toft et al (1966) used Ge(Li) detectors to discover a large number of new transitions. Among the new levels they have proposed are several which have been given an interesting

beta vibrational interpretation.

The present work was undertaken to firmly establish or to reject these new levels using the more accurate energy sums obtainable from higher resolution Ge(Li) detectors and the results of coincidence experiments. Also, in view of the data on the ^{155}Sm decay already presented and the (^{3}He,d) data to be presented, the accepted 1/2+[411] interpretation of the level doublet at 635 keV seemed doubtful and warranted further investigation.

4.2 Ge(Li) Singles Results

The Ge(Li) singles spectra were taken using four different Ge(Li) detectors; a planar 1.5 cm^2 x 4 mm Nuclear Diodes detector with a resolution of 2.0 keV at 400 keV, a thin window 0.5 cm^2 x 4 mm Nuclear Diodes detector with a resolution of 1.6 keV at 662 keV, a 25 cm^3 co-axial Nuclear Diodes detector with a 3.2 keV resolution at 1.33 MeV, and finally a 5 cm^3 R.C.A. detector at the Chalk River National Laboratory with a resolution of 1.6 keV at 450 keV.

The low energy gamma ray spectrum of ^{153}Sm taken with the thin window planar detector is shown in Figure 16. Peaks above the 103 keV transition (not shown) are about two orders of magnitude weaker in intensity. The lower curve of the diagram shows the region below 65 keV taken with a 1.5 g/cm^2 Cu absorber interposed between source and detector. Previously unreported peaks are seen at 23.0, 31.9, 55.9, and possibly at 59.3 and 93.11 keV. The shoulder just below the K_α peak can be seen from the lower

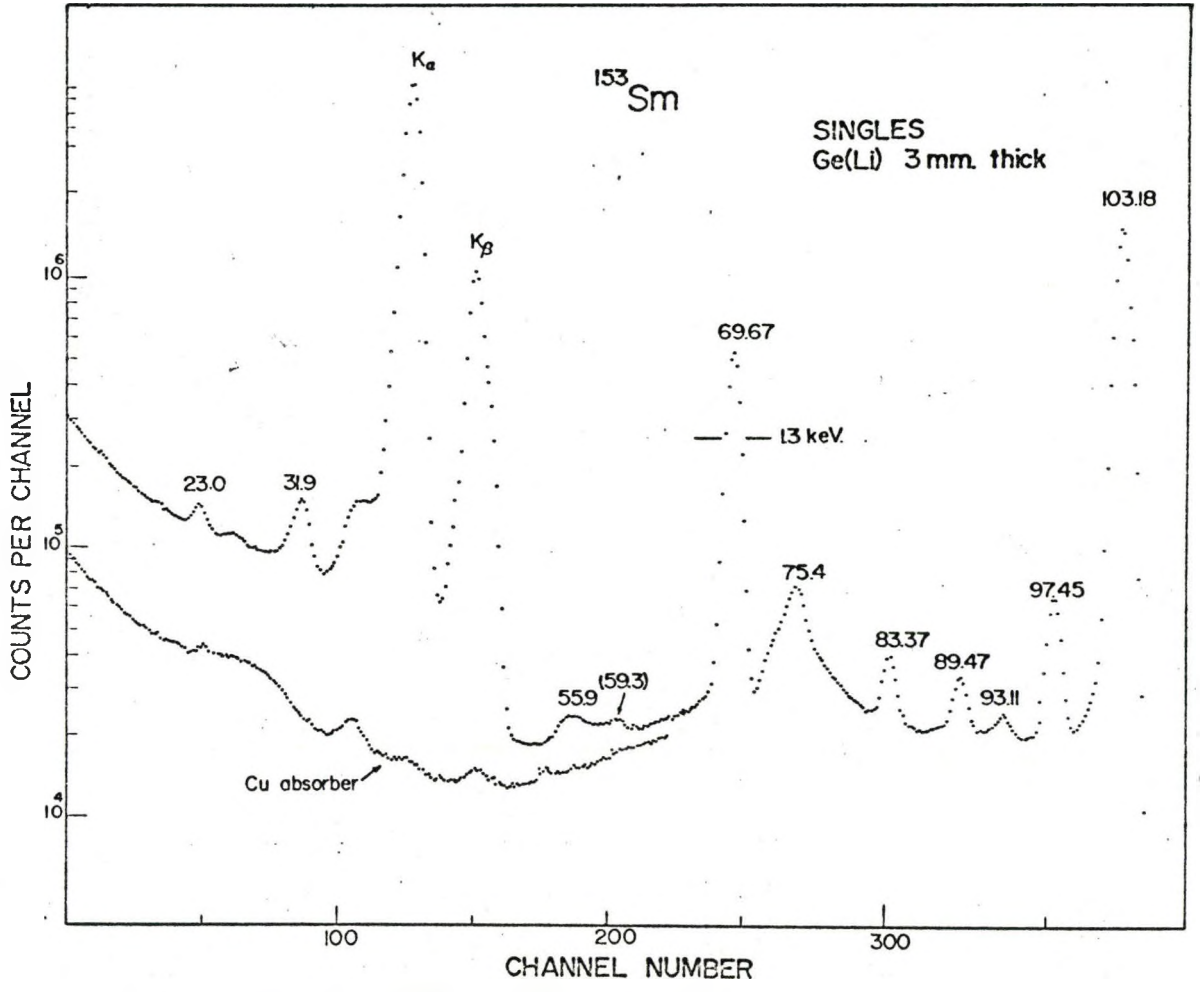

Figure 16 ^{153}Sm Low Energy Ge(Li) Spectrum

spectrum to be due to some type of scattering of quanta in the detector. The 93.1 keV peak remains in the spectrum when a Cu absorber is in place and is hence not a sum peak. To help determine whether the new low energy transitions are due to the depopulation of low-lying states, a spectrum of ^{153}Gd (which populates only the lowest five excited states of ^{153}Eu) was taken with the same detector. This spectrum is shown is Figure 17. The 31.9 keV peak is observed also in this spectrum while the 55.9 and 59.3 are not. A weak indication of the 23 keV transition is also seen. The large enhancement of the 97.5 keV peak in this spectrum relative to the ^{153}Sm spectrum makes the confirmation of the 93.1 keV peak somewhat difficult. However, a definite bump on the low-energy side of the 97.5 keV peak at $93.4^{+}_{-}0.3$ keV does exist. These data together indicate that the 93 keV transition is associated with the low-lying levels in ^{153}Eu. This transition does not however correspond to an energy difference between known states. The energies of the stronger low energy transitions have been taken from the literature (Alexander (1964)).

To investigate the higher energy portion of the gamma ray spectrum source strengths were increased to about 20 mCuries and Pb and Cd absorbers were placed in front of the detectors. Figure 18 shows a spectrum taken with the Chalk River detector, using a 5 mm Pb + 2 mm Cd absorber. A number of previously unresolved transitions are observed. The close doublet at about 597 keV is shown unfolded in the insert.

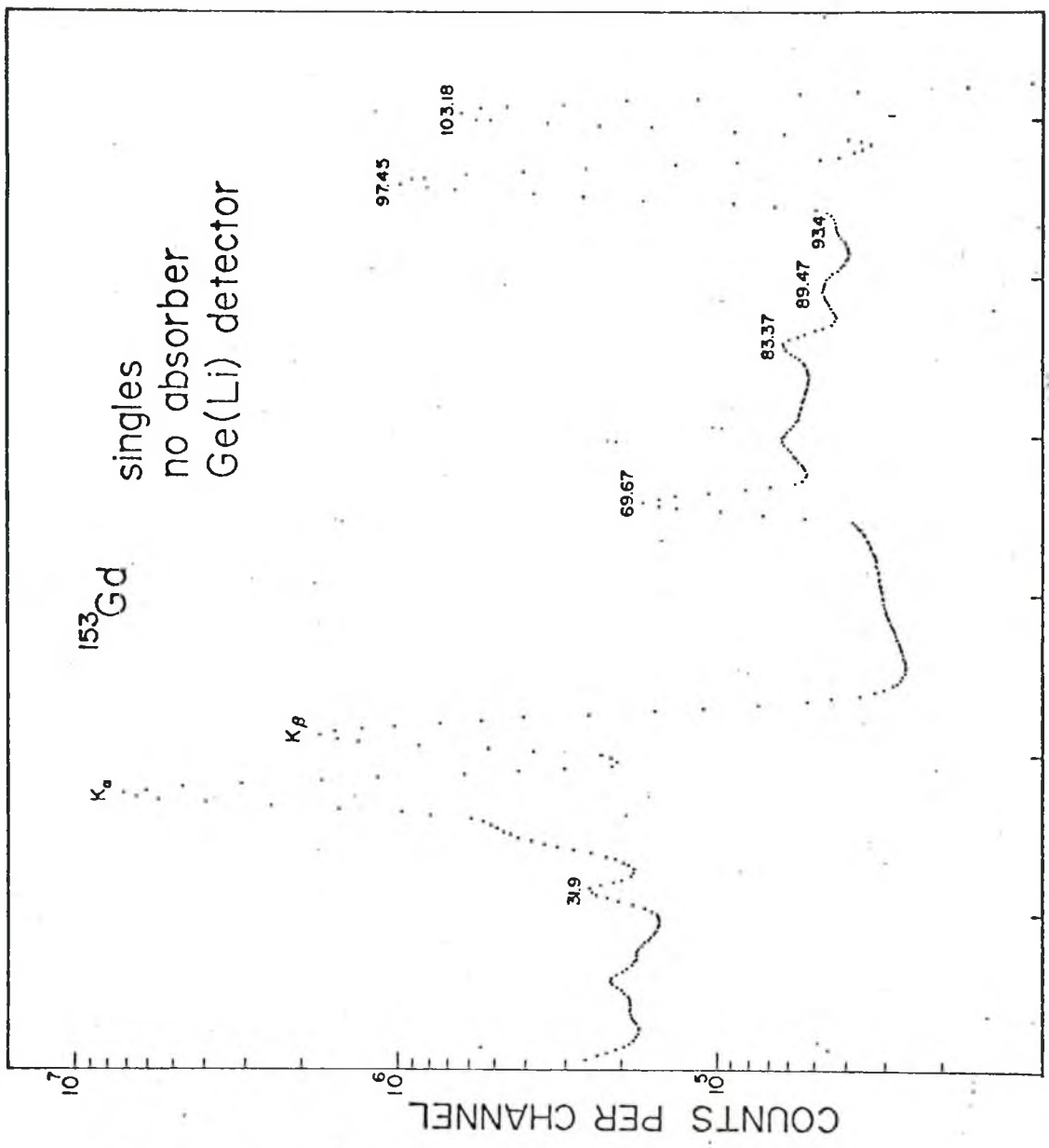

Figure 17 ^{153}Gd Low Energy Ge(Li) Spectrum

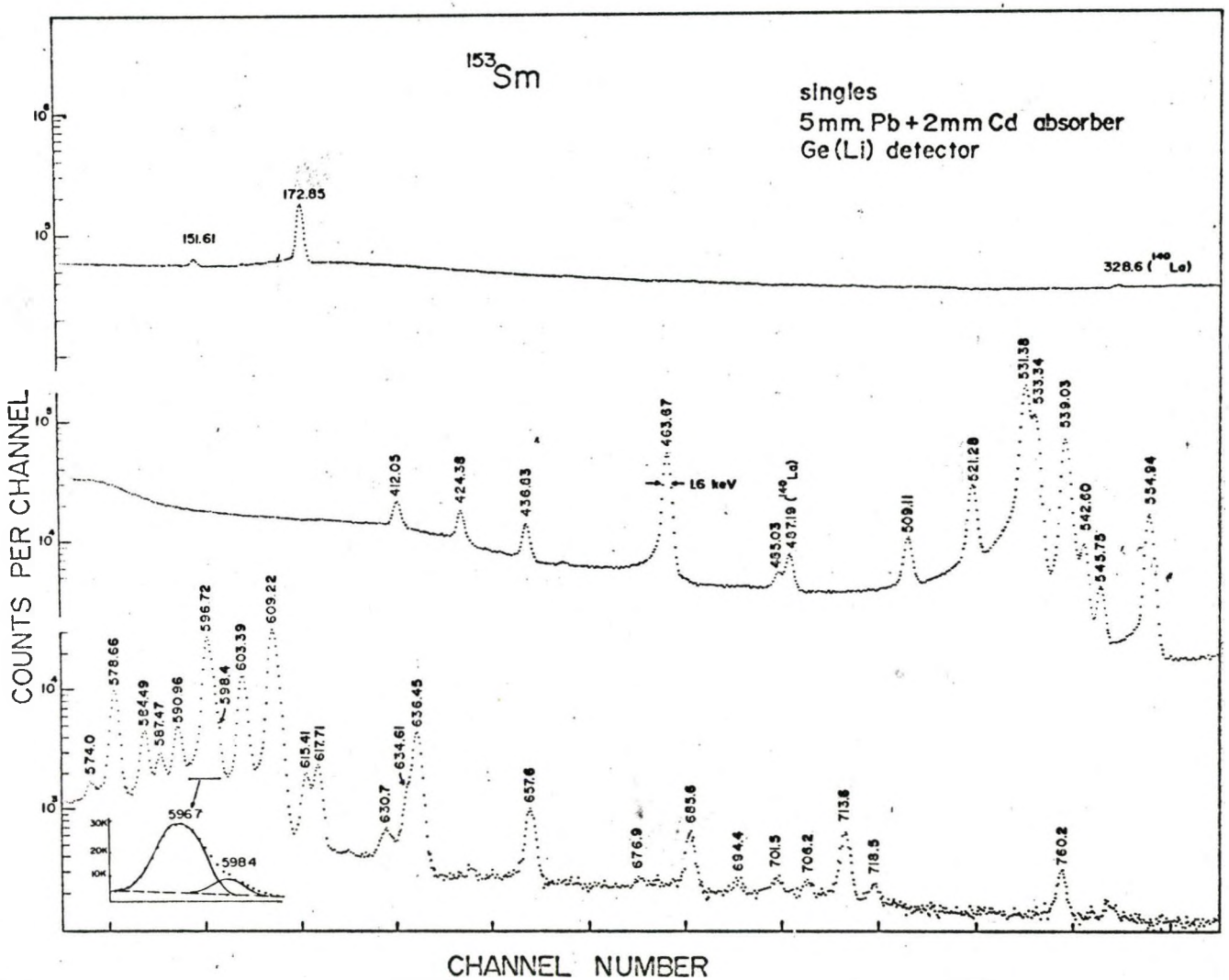

Figure 18 ^{153}Sm Spectrum with Absorber

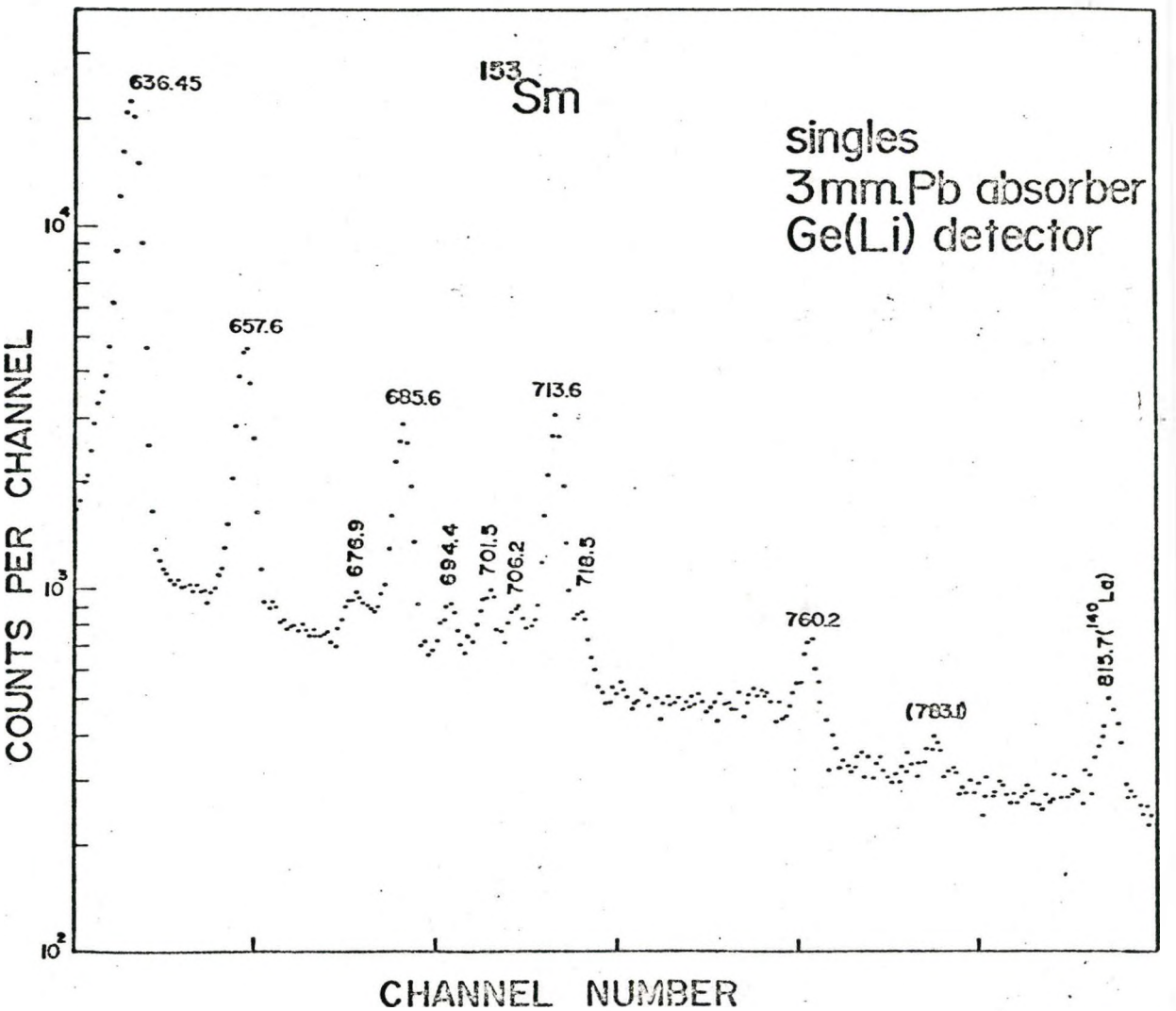

Figure 19 ^{153}Sm High Energy Spectrum

The upper portion of the ^{153}Sm gamma ray spectrum with improved statistics and taken on the 4 mm planar detector over a time period of six days is shown in Figure 19. Peaks attributed to the ^{153}Sm decay have been observed up to 760 keV.

The energies of the more prominent transitions were determined by taking spectra containing the transitions of ^{153}Sm along with those of several well known standards. Standards used were ^{203}Hg, ^{207}Bi, ^{137}Cs, ^{185}Os, and ^{54}Mn. The strong peaks were then used as internal standards for the remaining weak lines. Listed energies are the result of a weighted average of several runs all of which have had corrections for system non-linearity applied.

The intensities and energies of 49 transitions observed in the singles spectra are given in TableIII. The table also shows the classification of the transitions proposed in this work. Blichert-Toft's (1966) intensities, while not presented, agree well with the present measurements for the stronger well- resolved transitions. The classifications have been based on energy fits and the coincidence results to be discussed below.

4.3 Gamma-Gamma Coincidence Results

A two-parameter gamma-gamma coincidence experiment was performed in order to test the assignment of some of the higher energy transitions whose positions in the decay scheme had been assigned by other workers on the basis of energy sums alone. The present work shows that even with energy errors

TABLE III

Energies, Intensities and Classifications of Transitions in ^{153}Eu

Present Work		Blichert-Toft et al	Classification
Energy (keV)	Photons per 10^4 decays		
23.0 ±0.3**	10 **		
31.9 ±0.3 b)	30		
55.9 ±0.3	3.5		
(59.3 ±0.4) b)	1.0		
69.67 *	404	69.67	172.9→103.2
75.4	60	75.4	172.9→ 97.5
83.37 *	14		
89.47 *	13	83.37	83.4→ 0.0
93.11±0.15 b)	3.5	89.47	172.9→ 83.4
97.0 ±0.5 a)	0.5		269.9→151.6
97.45 *	71	97.45	97.5→ 0.0
103.18 *	2820	103.175	103.2→ 0.0
118.0 ±0.5 a)	0.01		269.9→151.6
151.61 *	1.15	151.5	151.6→ 0.0
166.7 ±0.5 a)	0.03		
172.85 *	8	172.847	172.9→ 0.0
412.05±0.20	0.23	412.1	681.9→269.9
424.38±0.20	0.23	424.3	694.2→269.9
436.83±0.20	0.18	437.3	706.6→269.9
463.67±0.15	1.55	463.6	636.5→172.9
	<0.008	481	
485.03±0.20	0.04	485	657.6→172.9

TABLE III (continued)

Energies, Intensities and Classifications of Transitions in ^{153}Sm

Present Work		Blichert-Toft et al	Classification
Energy (keV)	Photons per 10^4 Decays		
509.11±0.15	0.22	509.2	681.9→172.9
521.28±0.15	0.75	521.3	694.2→172.9
531.38±0.15	6.4	531.8	634.6→103.2
533.34±0.15	3.2		636.5→103.2
539.03±0.10	2.0	539.4	636.5→103.2
542.60±0.20	0.27		694.2→151.6
545.75±0.15	0.10		718.6→172.9
554.94±0.10	0.51	554.7	706.6→151.6
574.01±0.30	0.01		657.6→ 83.4
578.66±0.15	0.33	578.5	681.9→103.2
584.49±0.20	0.086	584.2	681.9→ 97.5
587.47±0.02	0.034	589.3	760.3→172.9
590.96±0.20	0.091		694.2→103.2
596.72±0.15	1.15	596.7	694.2→ 97.5
598.4 ±0.3	0.15		(701.4→103.2,681.9→83.4)
603.39±0.15	0.31	603.0	706.2→103.2
609.22±0.10	1.27	609.1	706.6→ 97.5
615.41±0.20	0.08	615.9	718.6→103.2
617.71±0.20	0.11		701.4→ 83.4
630.70±0.30	0.01		
634.61±0.30	0.03		634.5 0.0

TABLE III (continued)

Energies, Intensities and Classifications of Transitions in ^{153}Sm

Present Work		Blichert-Toft et al	Classification
Energy (keV)	Photons per 10^4 Decays		
636.45±0.25	0.19	636.2	636.5→ 0.0
657.55±0.25	0.04	657.7	657.6→ 0.0
676.9 ±0.5	0.001		760.3→ 83.4
685.6 ±0.3	0.023	683	
694.4 ±0.4	0.002		694.2→ 0.0
701.5 ±0.4	0.0025		701.4→ 0.0
706.2 ±0.4	0.006		706.6→ 0.0
713.6 ±0.3	0.019	713	
718.5 ±0.4	0.002		718.6→ 0.0
760.2 ±0.3	0.0025	760	760.3→ 0.0

* Energies accepted from Alexander (1964)

** Possible Indium X-rays from detector mount

a) Seen in coincidence only.

b) Possible X-ray escape peaks

of less than 0.15 keV, several important transitions cannot be placed uniquely in the scheme without the coincidence information.

The coincidence experiment was carried out using a 7.5 X 7.5 cm NaI detector together with a 25 cm^3 Nuclear Diodes Ge(Li) detector. A shaped anti-Compton shield was used between the detectors along with a graded 1.5 mm Pb + 0.8 mm Cd absorber in front of the NaI detector. In order to detect coincidences involving any of the low energy transitions, no absorber was used in the Ge(Li) direction.

The extremely weak intensities of all cascades in this decay, apart from the 69-103 keV cascade, required either high source activities with correspondingly increased chance rates, or very long count periods to achieve appreciable statistics. The compromise source strength chosen, which resulted in a true-to-chance ratio of 6 to 1 (at 100 nsec resolving time), required six days of counting to record 1.2×10^6 coincidence events. A gain of $\sim$ 3.5 keV per channel in the NaI and 0.6 keV per channel in the Ge(Li) directions of the 256 x 1024 channel coincidence matrix was used.

The projections of the coincidence matrix on both the NaI and Ge(Li) axes are shown in Figure 20. Two new transitions at 118.0 and 166.6 keV which were unobserved in the singles spectra are observed clearly along with a large enhancement of the 151.6 and 97.5 keV peaks. Lead X-rays due to gamma rays which

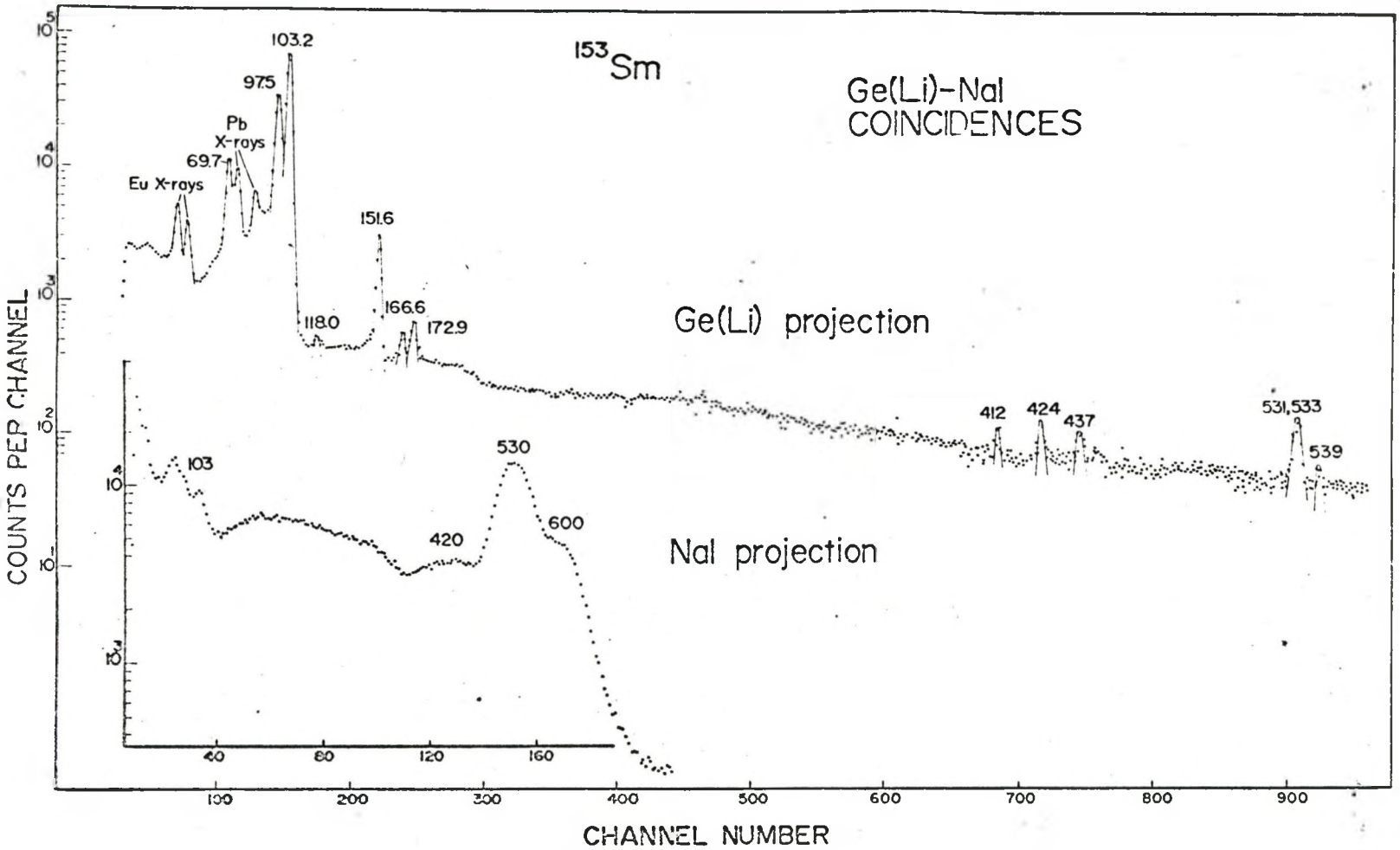

Figure 20 ^{153}Sm Coincidence Projections

are absorbed in the Compton shield and the graded absorber are unfortunately also present and prevent observation of the 83 and 75 keV transitions.

The Ge(Li) spectra in coincidence with various NaI gates are presented in Figure 21. The gating transitions are indicated in the accompanying partial decay schemes by a dot on the center of the transition arrow. In order to interpret these spectra they must be examined together with the NaI difference spectra in coincidence with Ge(Li) gates placed on the peaks seen in the projection spectrum (Figures 22 and 23).

Since the levels below 175 keV have been very well established by other workers, little effort has been spent here to confirm them. Figure 21a, which shows the Ge(Li) difference spectrum in coincidence with a 100-120 keV NaI gate containing the NaI photopeaks of the 97, 103 and 118 keV gamma rays, shows the only coincidence data to be presented specifically on this portion of the decay scheme. The strongly converted 69 keV gamma ray (α_K~5) and the Eu X-rays, both in coincidence with the 103 keV gamma ray in this gate are prominent features of the spectrum. The X-rays have been attenuated by an order of magnitude by the substantial dead layer of Ge on the Ge(Li) detector surface (~0.5 mm). The peak at 103 keV is almost entirely due to chance counts; also, there has been an improper subtraction of the large Compton background in this region. The errors in this background

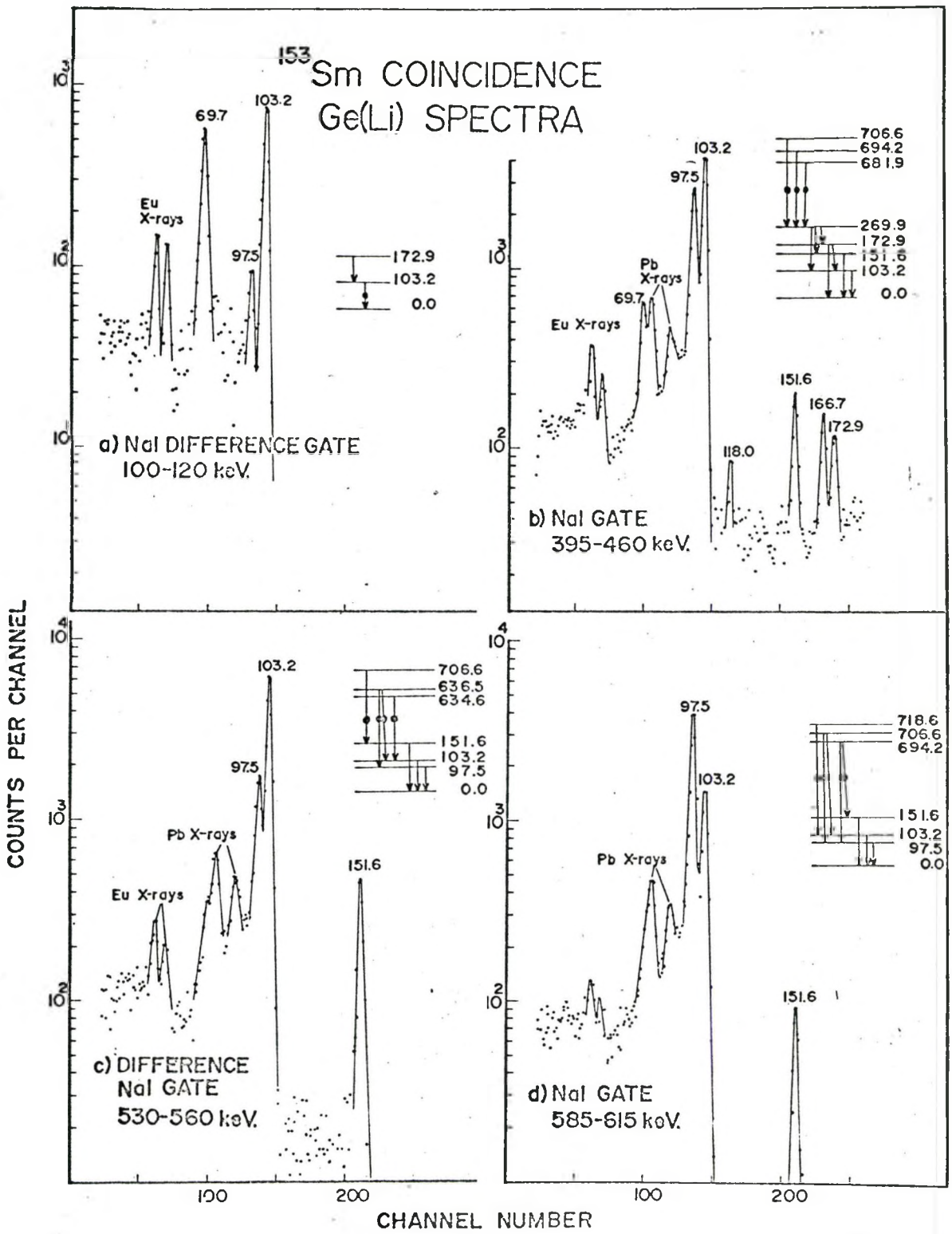

Figure 21 ^{153}Sm Ge(Li) Coincidence Spectra

subtraction are sufficient to account for almost all the intensity of the 97 keV peak seen.

Figure 21b together with 23b and 23c present evidence for a level at 269.9 keV. This level was first proposed by Funke et al (1965) who observed that the differences in energy between the gamma rays at 412, 424, and 437 keV corresponded to the differences in energy of the levels they proposed at 681, 694 and 706 keV. Their NaI-NaI coincidence data were consistent with gamma rays at 96.6 and 166.3 keV de-exciting the 269 keV level but no direct evidence for these gamma rays was found. Blichert-Toft et al (1966) classified these three lines in quite a different fashion; the 412 and 424 feeding the 172 keV level, and the 437 feeding the 151 keV level. This interpretation was also consistent with the low-resolution coincidence information of Funke et al (1965). The present experiments clearly support Funke's interpretation of the data and reject the assignments of Blichert-Toft.

Figure 21b shows the Ge(Li) spectrum in coincidence with a wide NaI gate set on the range 395-460 keV. Included in this gate are the photopeaks of the 412, 424, 437, and 464 keV transitions. The three peaks at 97, 118.0, and 166.6 keV have the energies appropriate to the 269→172, 269-151, and 269-103 keV transitions expected on the Funke proposal. Since a strong 97 keV gamma ray has already been located as the 97.45→0 transition, this suggestion requires the introduction of

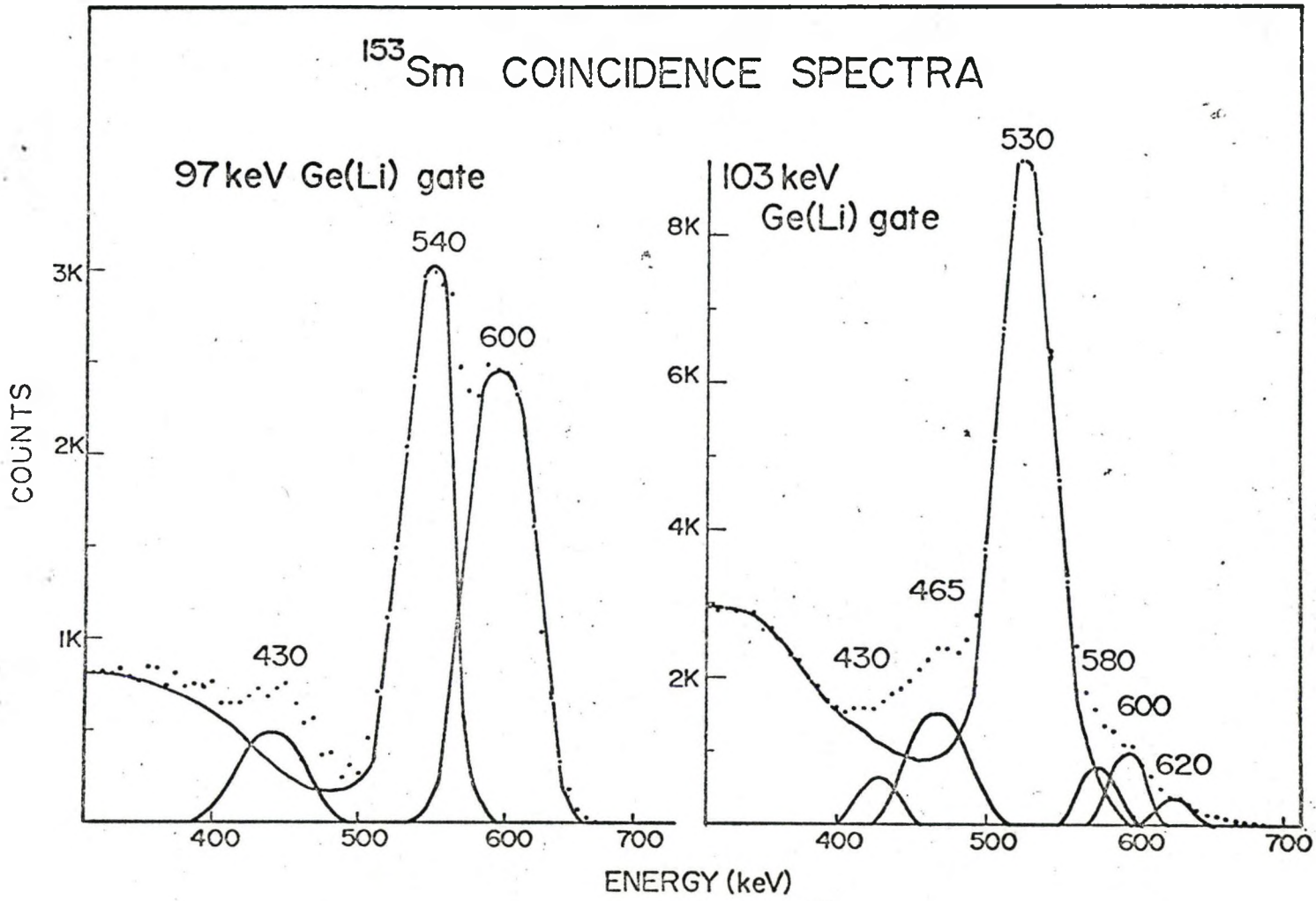

Figure 22 97 and 103 keV. Ge(Li) Gates

a hitherto unknown transition of this energy. It will be shown below that the new transition is responsible for ~ 90% of the observed peak in this spectrum. The Eu X-ray, 69, 103, and 172 keV peaks along with about one tenth of the 97 keV peak can be explained by coincidences with the relatively strong 463.8 keV transition which feeds the 172.9 keV level and which is partially included in this gate. The pattern of gamma rays de-exciting the 172 keV level would predict a ratio of 20 to 1 for the 103 to 97 keV peak heights. Since the observed ratio is ~ 2 to 1 most of the 97 keV peak is due to the 269-172 keV transition. The peak at 151 keV can be accounted for by coincidences with the 412, 424, and the 437 keV transitions via the 118.0 keV gamma ray which links the 269 and 151 keV levels, and is also partially due to an unsubtracted Compton contribution of the 555 keV transition which is in strong coincidence with the 151 keV transition.

The NaI difference spectra in coincidence with Ge(Li) gates on the 118, 166 and 151 keV peaks respectively, (Figures 23b, 23b, and 23e) provide a means of determining the intensities of these two new 118 and 166 keV transitions in addition to confirming the feeds to the 269 keV level. By normalizing to the 151-555 keV cascade shown in Figure 23e, (coincidence probability ~ 0.005) intensity values of 0.0001 and 0.0003% are obtained for the 118 and 166 keV transitions, respectively, from Figures 23b and 23c. It should be noted that this total de-

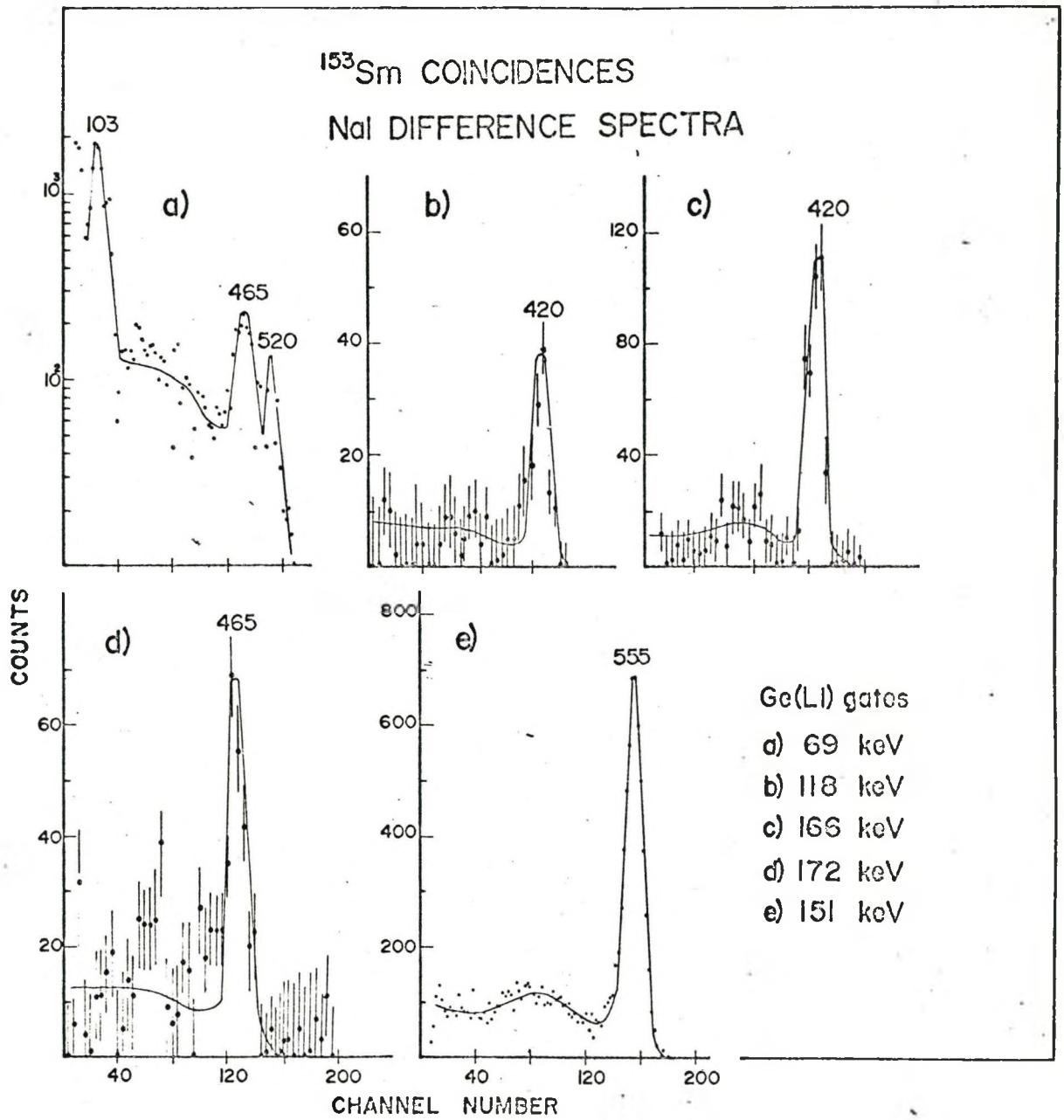

Figure 23 ^{153}Sm NaI Coincidence Spectra

exciting intensity for the 269 keV level is somewhat less than the proposed populating intensity of ∿ 0.006. No evidence is seen in the coincidence data for the 269 and 186 keV transitions from this level to the ground and 83.4 keV states, respectively. The large enhancement of the 97 keV peak in Figure 21b and the lack of these alternate means of de-excitation confirm that there exists a second unresolved transition at 97 keV from the 269 keV level to the 172 keV level.

Additional coincidence support for the second 97 keV gamma ray exists in Figure 22 which shows the higher energy portions of the NaI difference spectra in coincidence with gates on the 97 and 103 keV peaks. A broad peak at ∿ 430 keV is seen to exist in both these spectra. The peaks shown have been obtained by subtracting Compton contributions, using the line shape of the simple 555 keV spectrum shown in Figure 23e. These data can be explained by ∿430-97 and ∿430-97-69-103 keV cascades, and the intensity for the 97 keV transition of 0.005% obtained from these spectra accounts for most of the depopulation of the 269 keV level.

A transition of energy 172 keV (from the 269 keV level to the 97 keV level) may also be present. The analogous transition of energy 287 keV between the corresponding levels in ^{155}Eu has been observed. The Ge(Li) spectrum shown in Figure 21b indicates, however, that if such a transition exists, it must be substantially weaker than the 166 keV gamma ray, since a major

portion, if not all, of the 172 keV intensity has been accounted for by coincidences with the 464 keV radiation. An upper limit of 0.0001% is placed on this transition.

Figure 21c shows the Ge(Li) difference spectrum in coincidence with a 530-560 keV NaI gate. The stronger transitions included in this gate and indicated on the partial decay scheme are those at 531, 533, 539, and 555 keV. The 151 keV peak in this spectrum arises from the 555-151 keV cascade (see also Figure 23e) and firmly establishes the 706 keV level. These two spectra confirm the assignment made by Funke et al (1965) and reject the 658-103 assignment of Blichert-Toft et al (1966). A slight shoulder is indicated on the lower energy side of the K_{α} Pb X-ray peak. This may be the 68.2 keV transition between the 151 and the 83 keV levels postulated by Funke et al (1965); however, because of the low true-to-chance ratio in the present experiments, and the large background of the broad Pb X-ray peaks, this evidence is somewhat suspect. No evidence is seen here in support of the 54 keV transition between the 151 and 97 keV levels also postulated by these workers. The doublet of transitions at 531 and 533 keV shown in the partial decay scheme and observed prominently in the singles spectra accounts for the 103 keV peak, while the 539 keV transition from the 636 keV level produces the 97 keV peak. The NaI difference spectra of Figure 22 support these statements. The 636-97 keV assignment for the relatively strong 539 keV transi-

tion made by Funke et al (1965) is confirmed while the 712-172 keV assignment of Blichert-Toft et al (1966) must be rejected.

The Ge(Li) spectrum in coincidence with a 585-615 keV NaI gate is shown in Figure 21d. Among the more intense transitions included in this gate are those at 578, 597, 603, and 609 keV. The 151 keV peak in this spectrum is due to the high energy tail of the 555 keV peak in the gate. Its intensity relative to that in Figure 21c is reduced by a factor of about five. The very prominent 97 keV peak is accounted for by the 597-97 and 609-97 keV cascades. The broad peak at ~ 600 keV in the 97 keV gate of Figure 22 offers additional evidence for these assignments which agree with those of Funke et al (1965). Both these spectra force a rejection of the 712→103 and 597→0 keV assignments for the 609 and 597 keV transitions, respectively, which Blichert-Toft et al (1966) have proposed. A 760-151 keV assignment for the 609 keV transition, while possible by energy differences alone must likewise be rejected since there is no 609 keV peak in Figure 23e. The 103 keV peak in Figure 21d is due to several cascades; Figure 22 shows data in support of 578-103, 603-103, and 615-103 keV coincidences. Energy sums have been used along with the relative intensity pattern in singles spectra to obtain the decomposition of the unresolved peaks presented in this figure.

The relatively strong 464 keV transition has been partially discussed already in the explanation of Figure 21b. Figures 23a and 23d which show the NaI difference spectra in

coincidence with Ge(Li) gates on the 69 and 172 keV transitions confirm the 636→172 keV assignment already made. The coincidence probabilities of 0.008 and 0.0003 for the 464-69 and 464-172 keV cascades, respectively, derived from these two spectra agree with the observed singles intensity ratios for these gamma rays. The 69-103 keV cascade is again seen in Figure 23a together with a peak at ~ 520 keV. Several weak transitions in this energy range, namely the 485, 509 and 521 keV exist and have been assigned in the decay scheme proposed by the present work as feeding the 172 keV state. A large Pb X-ray background, however, has been subtracted from the original data to produce this difference spectrum. This background contains a large peak at ~ 530 keV due to the 530-103 keV cascade, and a small error in this subtraction could account for a large portion of this peak. While the peak at ~ 520 keV offers weak support for coincidences with the 69 keV gamma ray, the assignment of these weak gamma rays has been made mainly on the basis of the energy sums. The peak at 465 keV in the 103 keV gated spectrum of Figure 22 is due to the 464-69-103 keV cascade. A major portion of the 172 keV state decays via the 69 keV transition and the area of the 465 keV peak in this spectrum is consistent with this fact.

4.4 Log $f_o t$ Values

Careful direct measurements of the ^{153}Sm beta feeds to the low-lying states of ^{153}Eu have been made by various

workers and are listed by Suter et al (1962). These measurements show three intense beta groups to the ground, 103, and 172 keV states, and provide a direct measure of those log $f_o t$ values. A total beta decay energy of ∿805 keV has been measured by those workers for the decay of ^{153}Sm, which appears to have a ground state assignment of 3/2+[651], based on both the reaction data of Kenefick and Sheline (1965) and the deformation and quadropole moment measurements of Waddington (1967). This assignment for ^{153}Sm differs from the 3/2-[521] one used by Suter et al (1962) and Blichert-Toft et al (1966) in interpreting their results, but agrees with that of Funke et al (1965).

The percentage beta feeds to each state in ^{153}Eu along with the corresponding log $f_o t$ values and possible final state interpretation are given in Table IV. Values for the first five states have been taken from Suter et al (1962) while those for the remaining states have been deduced from the intensity balance of the presently proposed decay scheme.

4.5 The ^{153}Sm Decay Scheme

The energy, intensity, and gamma ray coincidence measurements of the present work have been combined with the low energy and beta decay measurements of other workers to produce the decay scheme shown in Figure 24. The scheme contains 15 excited levels which are depopulated by 43 transitions. Several additional transitions observed in the gamma ray spectra have been left unassigned.

TABLE IV

Intensity of beta transitions and log $f_o t$ values for ^{153}Sm Decay

Level Energy		% Feed	log $f_o t$
0	5/2+[413]	20.0*	7.3
83.4	7/2,5/2+[413]	<0.3*	>9.1
97.5	5/2-[532]	0.8*	8.6
103.2	3/2+[411]	46.0*	6.7
151.6	7/2,5/2-[532]	0.004	~10
172.9	5/2,3/2+[411]	33.0*	6.8
269.9	7/2,3/2+[411]	(Assumed 0)	
634.6		0.066	7.6
636.5	3/2+[422]	0.069	7.5
657.6		0.0009	9.2
681.9	5/2,3/2+[422]	0.0087	8.1
694.2		0.022	7.5
701.4		0.0026	8.3
706.6		0.023	7.4
718.6		0.0018	8.4
760.3		0.0004	7.6

*Values taken from Suter et al (1962)

The levels up to 200 keV agree with the scheme of Blichert-Toft et al (1966). No evidence exists in the present investigation for the transitions at 14, 20, 54, and 68 keV which are postulated in the decay scheme of Funke et al (1965) as transitions within these five levels. The additional low-lying level at 269.9 keV has already been discussed.

Coincidence and singles gamma ray data have been used to place levels at 634, 636, 681, 706, and 718 keV. A newly observed gamma ray at 634.6 keV, presumed to be a ground state transition, supports the existance of the 634 keV level. Levels at 760, 701, and 658 keV have been assigned purely on the basis of energy sums, with three de-exciting gamma rays being assigned to each.

The level at 658 keV which is de-excited by the 485, 574, and 658 keV transitions is the least secure of these levels. The 658 keV transition could alternately be assigned as a 760→103 keV transition. Likewise, the 485 keV gamma ray can be given a 636→151 keV interpretation. Evidence will be provided, however, to show that the 636 kev level requires a spin and parity assignment of 3/2+. The existance of an M2 3/2+→7/2- transition is then required to explain this placement. An appreciable competion between this transition and the E1 and M1 transitions from this state to the 97 and 103 keV levels, respectively, seems highly unlikely. A slight question of doubt can be placed also on the remaining transition assigned

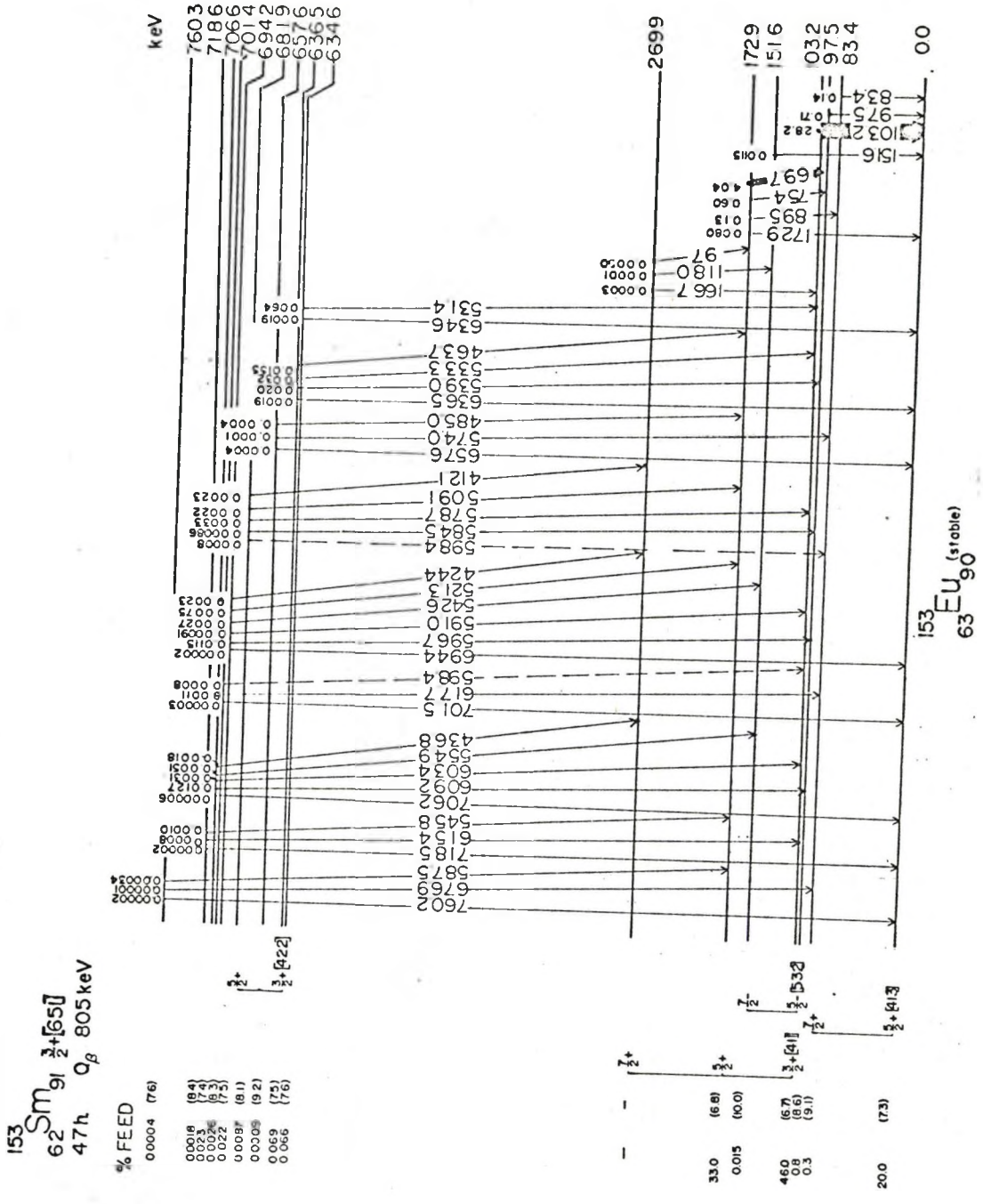

Figure 24 ^{153}Sm Decay Scheme

from this level, the 574 keV. Several transitions from the decay of ^{140}La have been observed as impurities, and a 1596.6 keV double escape peak interpretation could be given to this peak. The level at 658 keV has, despite these alternate assignments, been retained in the decay scheme.

A comment should also be made about the unplaced 685.6 keV transition. No coincidence data indicating a placement of it in the decay scheme has been observed, nor do energy sums indicate a probable assignment. Figure 19 shows a very weak indication of a peak at 783.1 keV which could be a ground state transition and would allow for a possible 685.6-97.4 keV cascade. The small beta decay energy available (~ 25 keV) and the very tentative identification of this high energy line make such an assignment somewhat premature.

The weak 598.4 keV transition which is not seen in the coincidence experiments fits equally well from energy considerations as either a 681.9→83.4 or 701.5→103.2 keV transition and has been indicated at both these locations in the decay scheme.

The interpretation of the levels of the present decay scheme will be discussed later, along with those of ^{155}Eu, in light of the (^{3}He,d) data to be presented next. No evidence has been seen in the present work for the interesting beta vibrational states proposed by Blichert-Toft et al (1966) nor for the levels at 589 and 597 keV.

CHAPTER V

THE (^{3}He,d) REACTIONS ON ^{152}Sm AND ^{154}Sm

5.1 Introduction

The data presented above on the beta decay of ^{153}Sm and ^{155}Sm to levels in ^{153}Eu and ^{155}Eu has led to the introduction of several new levels in these two odd-proton isotopes, in addition to raising questions as to the interpretation of some previously established states. For instance, the 1/2+[411] Nilsson state has been placed by various workers at 636 keV in ^{153}Eu and 765 keV in ^{155}Eu. The present beta decay studies indicate, however, that these two states are the base states of a 3/2+ rotational band. The reaction data presented in this chapter suggest that the bands are due either to a beta vibration or to the excitation of a hole state.

Levels in ^{153}Eu and ^{155}Eu can be excited either by a (^{3}He,d) stripping reaction on targets of ^{152}Sm and ^{154}Sm or by neutron activation of these same targets followed by beta decay (Fig. 4). Because of restrictions which are imposed by such factors as spin and parity change, Q value, ℓ value, and $C_{j\ell}$ coefficients (see Chapter I), the probability of populating a given level may be dramatically different in the two cases. The present experiments were primarily carried out to test or establish the interpretations of those states populated by

both processes. In addition, it was expected that new states which are populated only by the (^{3}He,d) reaction would be identified and would yield important information on the level structure of these nuclides.

5.2 Theoretical Calculations

It was earlier shown that for a single particle transfer reaction of the (^{3}He,d) type using an even-even target nucleus, the reaction cross-sections may be written

$$\frac{d\sigma}{d\Omega} = 2\, C^2_{j\ell}\, U^2 \phi_\ell$$

The ϕ_ℓ, or D.W.B.A., cross-sections have been calculated for the present studies by Satchler (1968) using the computer code JULIE. Figure 25 shows a plot of the calculations for the ^{150}Sm(^{3}He,d)^{151}Eu reaction using a lower cutoff radius of 4.1 f and a reaction Q value of -1.000 MeV. Similar results are obtained for Q = -0.500 and -2.000 MeV. These all show the same angular dependence but the absolute values of the cross-sections appear to decrease roughly exponentially with increasing Q. Figure 26 presents the $\phi_\ell(40°)$ dependence on Q for a ^{150}Sm target. Since the cross-section changes very slowly with mass, this family of curves can be used to obtain the absolute cross-sections of each of the levels populated in the reactions with ^{152}Sm and ^{154}Sm targets by using the listed (ground state) Q values of +0.41 and +1.19 MeV respectively. Differences of 15% in the magnitude of the reaction

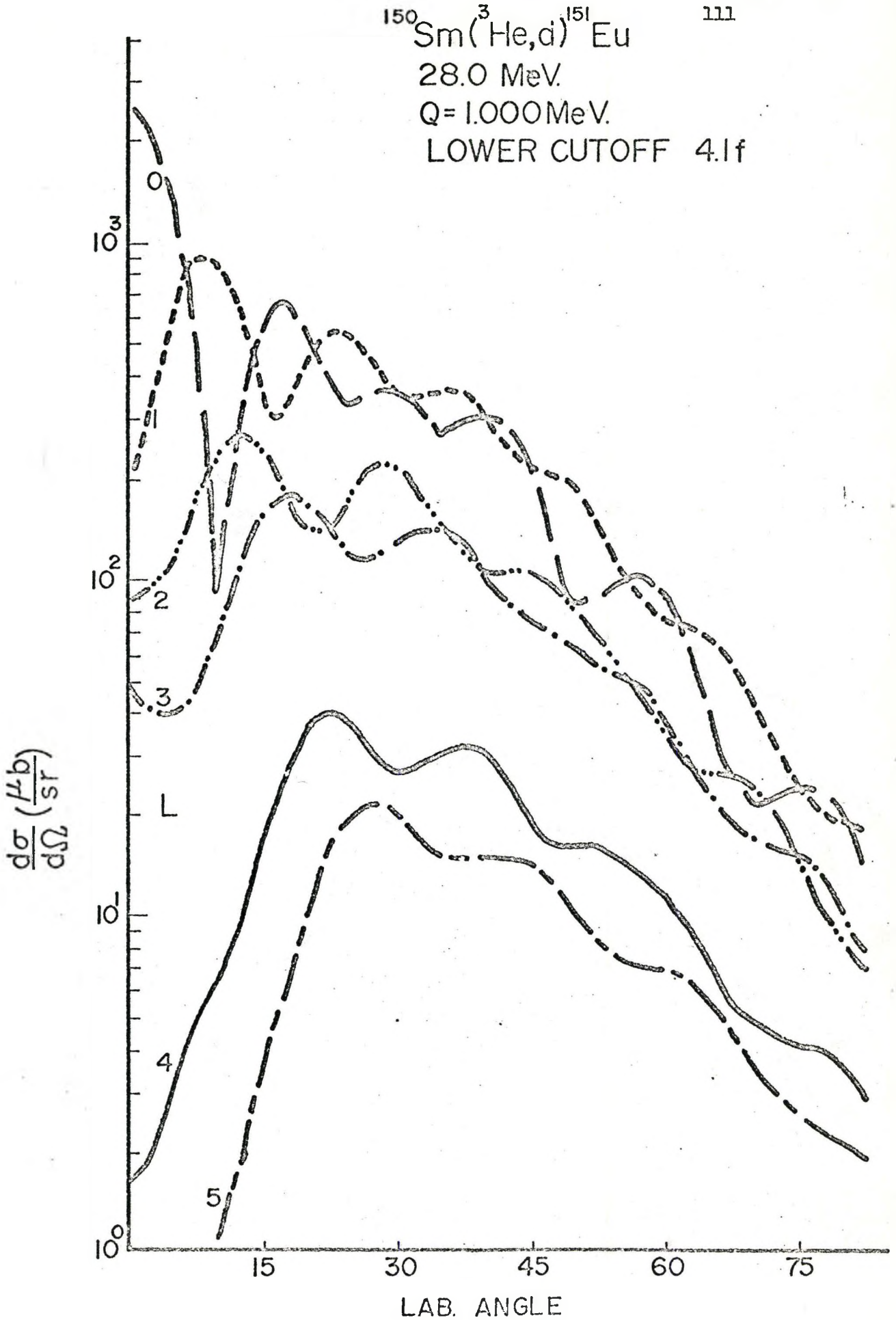
150Sm(3He,d)151Eu
28.0 MeV.
Q= 1.000MeV.
LOWER CUTOFF 4.1f
0
1
2
3
L
4
5
10^3
10^2
10^1
10^0
dσ/dΩ (μb/sr)
15
30
45
60
75
LAB. ANGLE

Figure 25

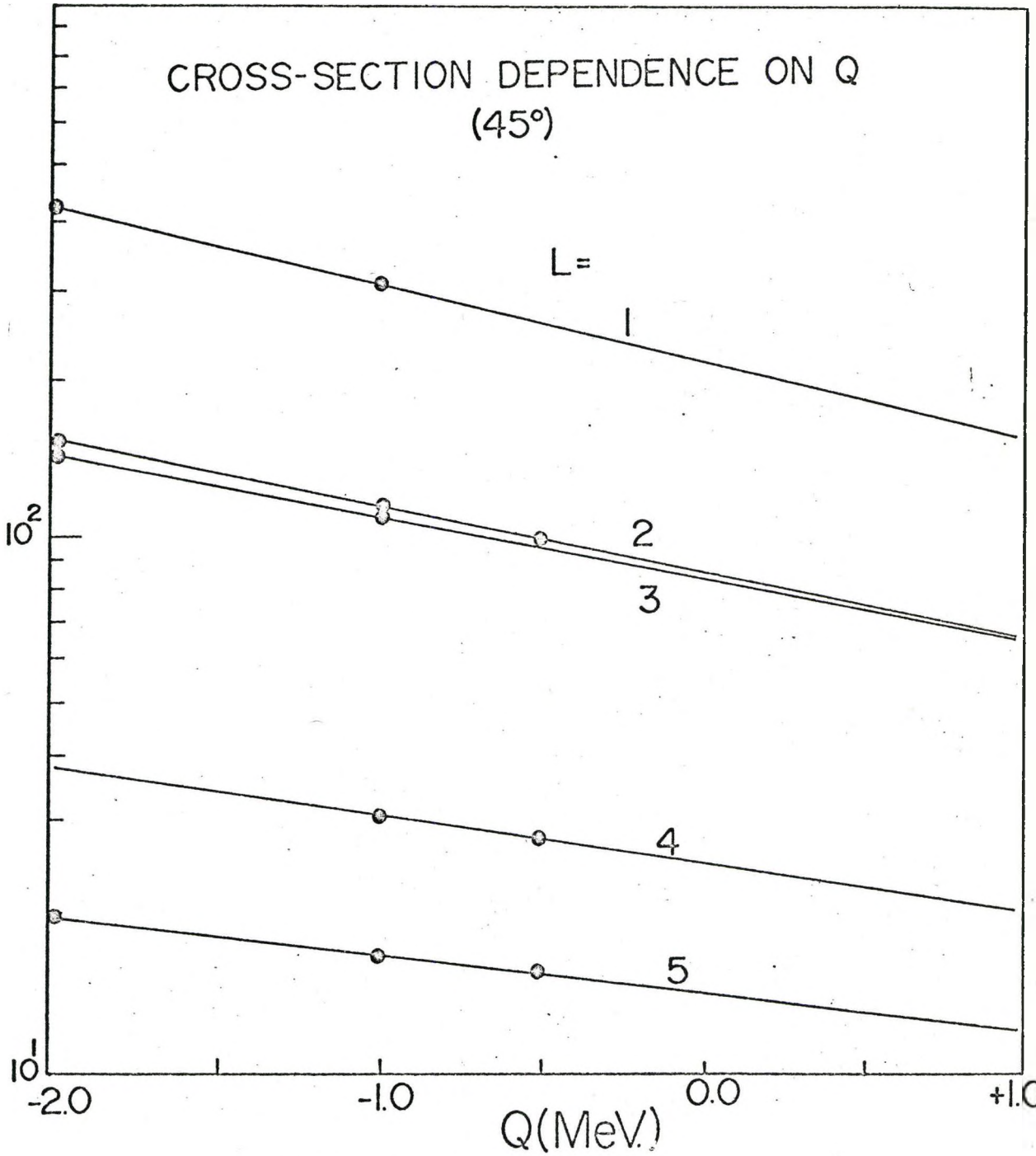

D.W.B.A. PARAMETERS

	V_0	W_0	r_0	r_c	a	V_s	W_s	R_G	b	τ_1
^{3}He	175	17.5	1.14	1.40	0.72	–	–	1.60	0.79	–
d	111	–	1.05	1.25	0.86	–	–	1.24	0.79	70.8

Figure 26

cross-sections but not in the shape of the angular distribution have been found in calculations using different choices of cut-off radii. A comparison of experimental values with the calculations using a lower cut-off of 4.1f will be presented in the discussion of the experimental results.

5.3 Experimental Procedure

The beam of 28 MeV ^{3}He ions was obtained for the present experiments from the MP tandem Van de Graaff accelerator at the University of Rochester. Outgoing reaction deuterons were magnetically analyzed and detected by means of photographic emulsions in the Enge split-pole particle spectrograph which has been already described. Angular distributions of the various deuteron groups were measured by making exposures at 8 and 9 angles for ^{152}Sm and ^{154}Sm respectively, over a range of 10° to 70°. A spectrograph angle of acceptance of 3.29 millisteradians was used. Thin strips of 0.3 g/cm^2 aluminum were used over the photographic plates to remove possible tritons from the spectra and also to degrade the deuteron energies in order to obtain more readily visible tracks in the emulsions. Isotopically enriched targets of ^{152}Sm (99.2%) and ^{154}Sm (99.3%) metal ~40-80 μg/cm^2 thick were prepared on 50 μg/cm^2 carbon backings using the La reduction technique. Beam currents of 1-2 μA were used and integrated charges of (5-10) × 10^3 μCoulombs for each exposure were measured by means of a Faraday cup and a charge integrator.

Normalization of the various exposures and conversion of peak intensities to absolute cross-sections was achieved by recording the 45° elastically scattered ^{3}He ions with a 2 mm thick NaI detector. Pulses from the detector, which subtended a solid angle of 0.69 millisteradians at the target, were analyzed by a 400 channel Victoreen analyzer and were also recorded by a scalar gated on the elastic peak. A typical spectrum showing the elastically scattered ions from both the target and the carbon backing is shown in Figure 27. Because the gate, as indicated in the spectrum, contained a considerable portion of the peak due to ions scattered from the carbon backing, and also because considerable variation existed in the ratio of metal to carbon thickness, the integrated peak area indicated in the figure was used for normalization rather than the scalar values.

For low energy ions, the Rutherford scattering formula correctly predicts the scattered cross sections for all angles. However, for 28 MeV ^{3}He particles, the impact parameter for large angle scattering (ie > 30°) is so small that non-elastic processes account for an appreciable number of the interactions. The ratio of elastic to classical Rutherford cross-sections for 28 MeV ^{3}He ions on W and Yb have been measured by Burke and Alford (1968). At 45° these measurements show elastic cross-sections of 0.90 σ_R and 0.72 σ_R respectively. From these measurements an extrapolated value of 0.60 σ_R corresponding to 700 mb/sr

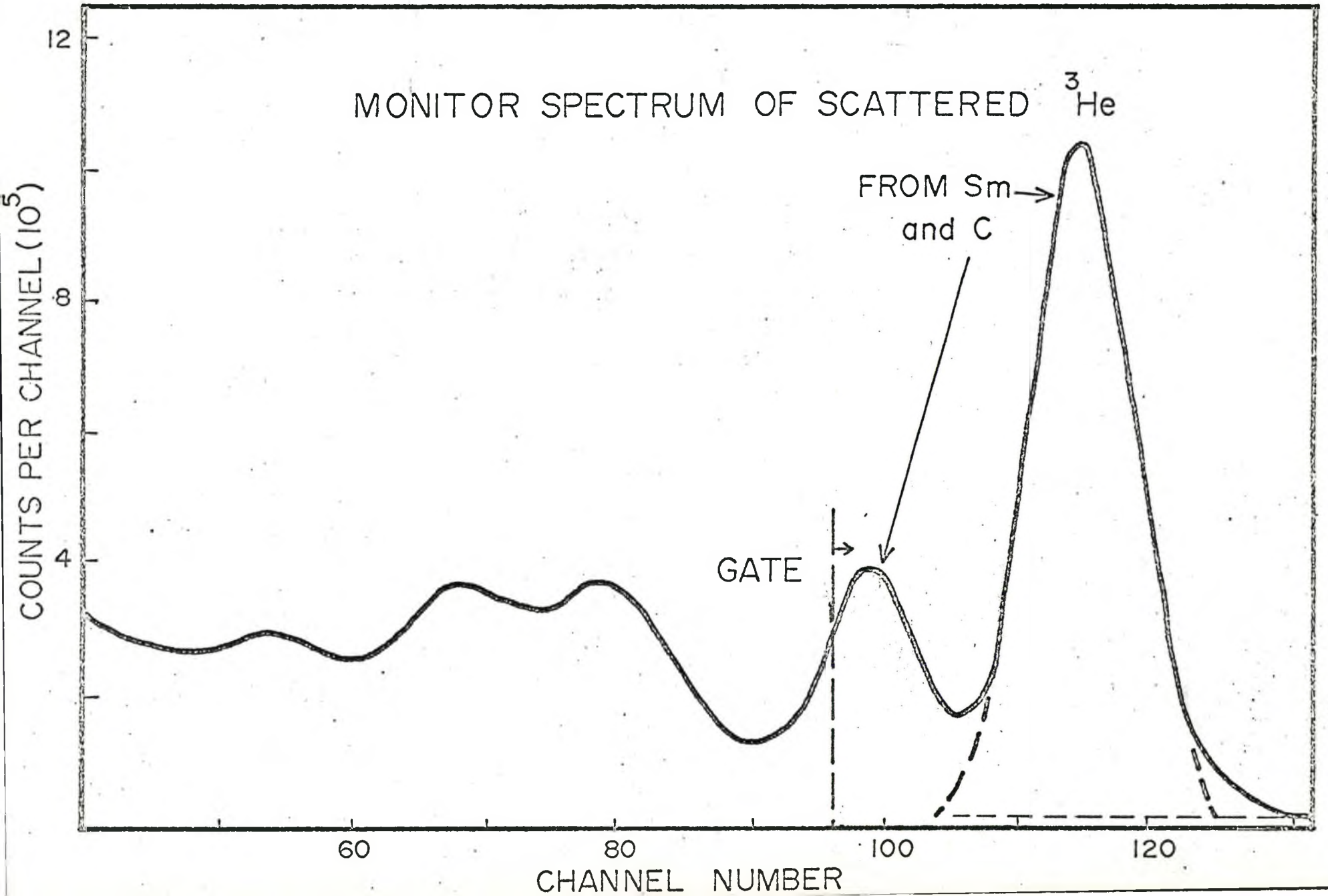
MONITOR SPECTRUM OF SCATTERED ^{3}He
FROM Sm and C
GATE
COUNTS PER CHANNEL (10^5)
CHANNEL NUMBER
12
8
4
60
80
100
120

Figure 27

at 45° was used to convert the relative deuteron peak intensities to absolute cross-sections.

5.4 Energy and Angular Distribution Results

The deuteron spectra from ^{152}Sm(θ=20°) and ^{154}Sm (θ=50°) targets shown in Figures 28 and 29 are typical. Several prominent peaks, notably the one at ~695 keV excitation energy in Figure 28 and the one at ~902 keV in Figure 29 are appreciably broader than adjacent peaks and exhibit a more distinct doublet nature at other angles.

The excitation energies and the reaction cross-sections deduced from such spectra for the population of the levels observed in ^{153}Eu and ^{155}Eu are listed in Tables V and VI together with the level assignments proposed by the present work. The listed energies are the result of a weighted mean of the energies determined for each exposure. Typical peak widths of 15-25 keV were obtained on the deuteron spectra and from the mean deviation of energies calculated from different exposures, it is estimated that the uncertainties in the excitation energies of the stronger peaks are ~ $\pm$ 3 keV. For weaker and incompletely resolved peaks this error should probably be increased by almost a factor of two. The strongly populated level at 172 keV in ^{153}Eu and the corresponding 307 keV level in ^{155}Eu were used to establish the excitation energy zero point, since variations of the order of 25 keV have been found to exist in the Q value obtained on different days of operation. The source

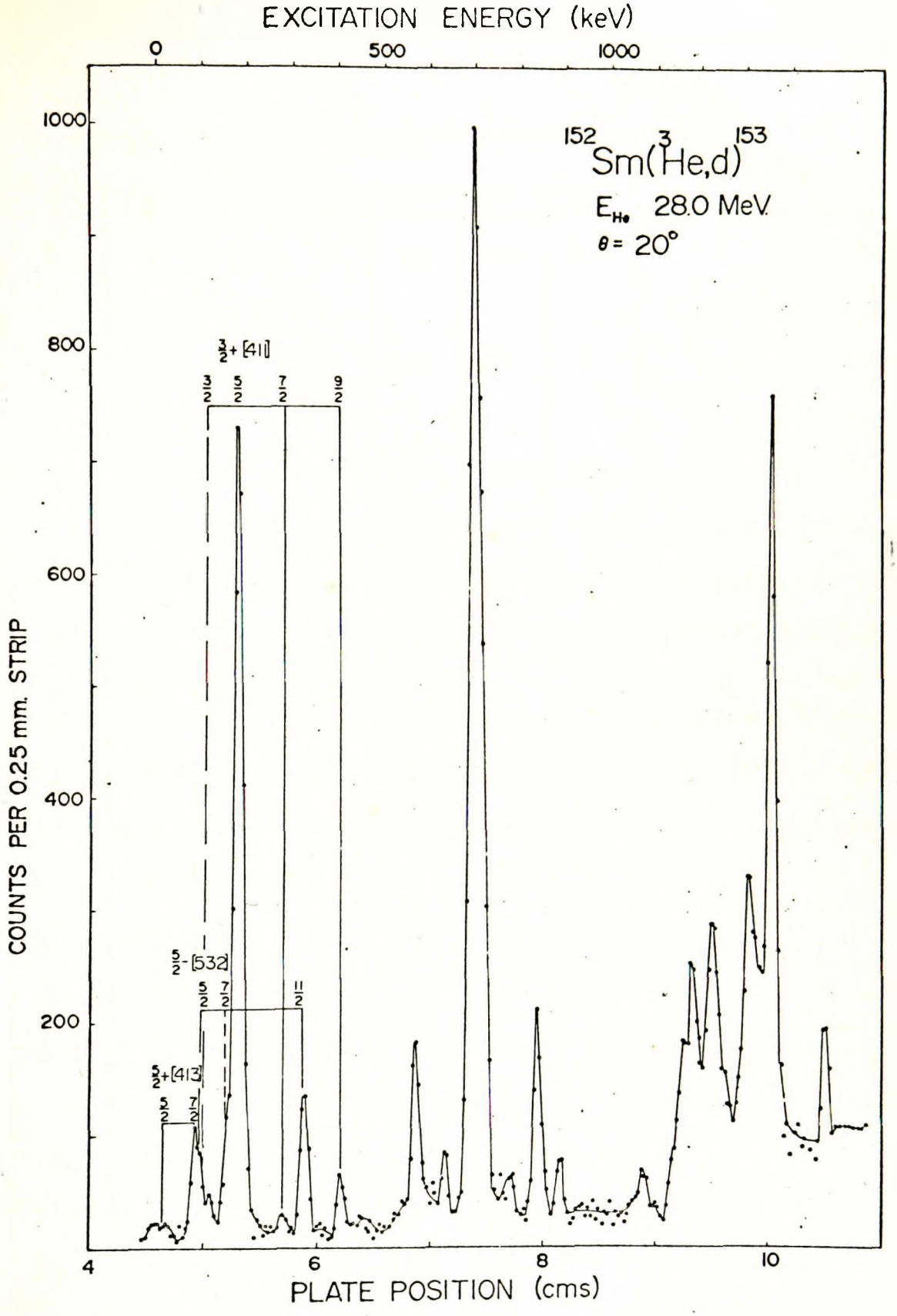

Figure 28 $^{152}Sm(^{3}He,d)^{153}Eu$ Deuteron Spectrum

TABLE V

Level Populated by the $^{152}Sm(^{3}He,d)^{153}Eu$ Reaction

Energy (keV)	Reaction Cross Sections (μb/sr)								Assignment
	10°	15°	20°	25°	30°	35°	40°	70°	
0	Un*	Un	5	1.5	2	Un	Un	Un	5/2+[413]
83									7/2,5/2+[413]
97	12	9.5	21	26	17	39	24	5	5/2-[532]
103									3/2+[411]
172	210	261	186	196	231	199	168	38	ℓ=2,5/2,3/2+[411]
263	Un	4.5	3	3.5	Un	Un	2	0.7	7/2,3/2+[411]
319	3	4	22	43	47	36	54	15	ℓ=5,11/2,5/2-[532]
394	5	3.5	7	9.5	8.5	2.5	10	5	9/2,3/2+[411]
563	5	8.7	28	35	21	28	26	11	ℓ=4 or 5,7/2+[404] or 11/2, 7/2-[523]
628	3.5	11	8.0	13	12	15	7.5	2.5	
695	395	437	308	328	398	359	297	64	ℓ=2 (Complex)
774	7	10	5.5	9.5	7.5	11	9	2	
832	55	51	36	33	57	42	35	9.5	ℓ=2
880	obsc**	75	9	11	15	6.5	15	7.5	
1063	obsc	obsc	9.5	11	9.5	12	7	5.5	
1130									
1164	119	obsc	77	39	83	62	54	13	
1170									
1214	62	60	79	78	78	59	61	12	ℓ=3
1294	74	47	76	64	58	51	35	4	ℓ=1
1341	59	117	132	114	150	121	116	19	ℓ=3
1461	40	34	21	25	33	35	30	5	ℓ=2

* Unobserved

** Obscured by C impurity peaks.

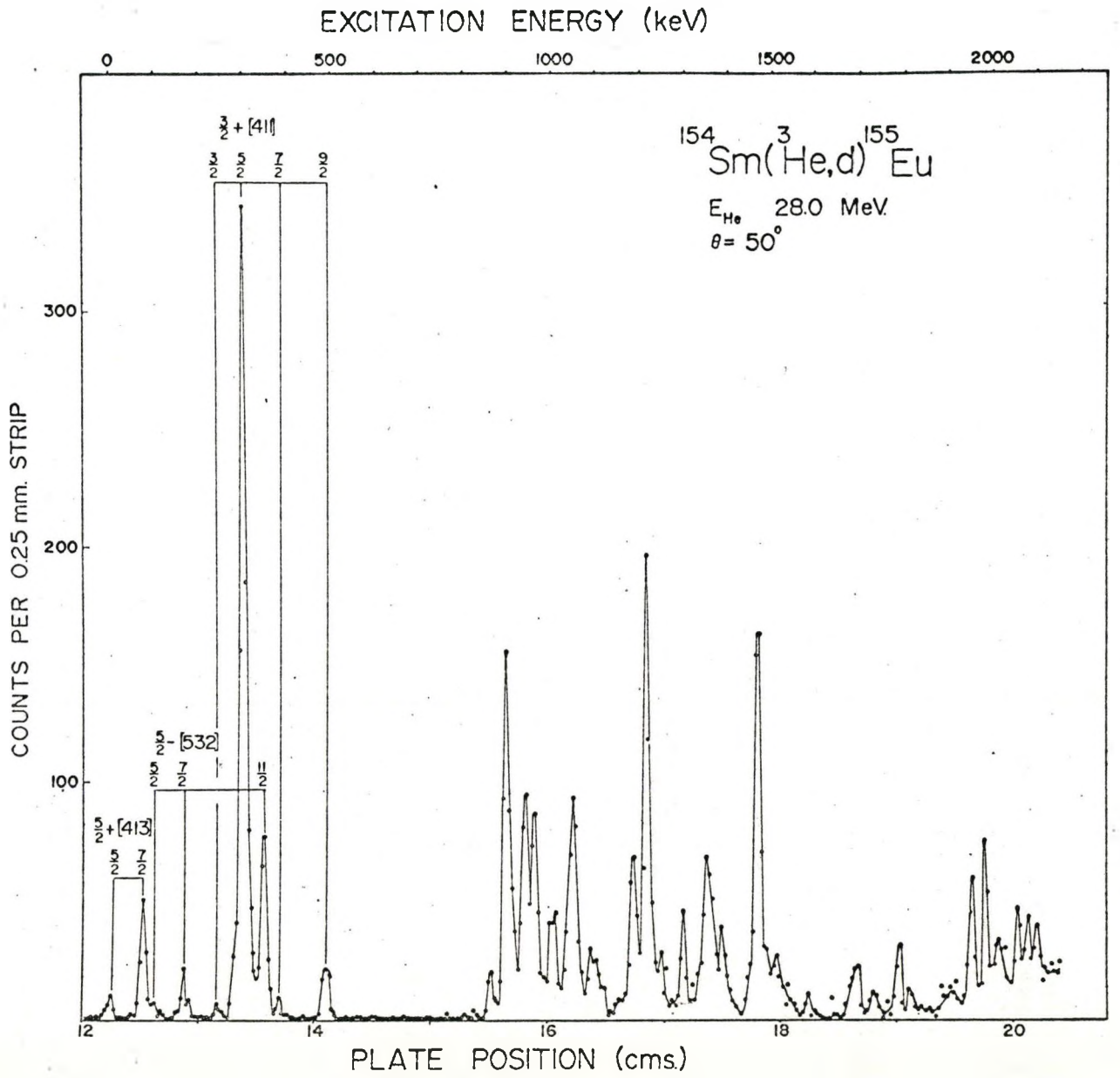

Figure 29 ^{154}Sm(^{3}He,d) ^{155}Eu Deuteron Spectrum

TABLE VI

Levels Populated by the $^{154}Sm(^{3}He,d)^{155}Eu$ Reaction

Energy (keV)	Reaction Cross Sections (μb/sr)									Assignment
	10°	15°	20°	25°	30°	40°	50°	60°	70°	
0	Un	~6	Un	Un	~4	~1.5	~0.5	~1	~0.2	5/2+[413]
78	Un	~6.5	~9	Un	~8	10	7	~2.5	~2.0	7/2,5/2+[413]
104	Un	3	4	Un	4	4	2.5	2.5	1.5	5/2-[532]
169	Obs	13	10	Un	8	6	4.5	1.5	2.0	7/2,5/2-[532]
246	Obs	15	4	Un	15	5	2.5	1.5	1	3/2+[411]
307	191	225	118	141	178	125	76	45	26	ℓ=2 5/2,3/2+[411]
356	5.5	4.3	19	32	28	27	21	12	7.4	ℓ=5 11/2,5/2-[532]
391	Un	Un	9	15	Un	7.5	3	2	1.5	7/2,3/2+[411]
498	2.2	6.0	5.1	10	9.8	5.6	5.4	7.0	4.1	ℓ=4 9/2,3/2+[411]
869	12	18	11	7.5	12	9.1	4.2	3.4	2.5	
905	101	129	76	92	84	66	44	23	14	ℓ=2 (Complex)
947	43	48	29	27	34	25	19	10	6.4	ℓ=2
968	5.5	10	30	46	33	35	22	12	6.4	ℓ=4 or 5 7/2+[404] or 1/2,7/2-[523]
1013	18	35	17	21	24	18	11	10	6	(Complex)
1054	48	61	38	48	48	45	30	16	13	ℓ=2 or 3
1096 1103	23	31	26	22	27	23	15	5.5	4	
1187	18	28	24	23	23	29	16	9.1	61	ℓ=3
1218	79	99	53	68	70	83	52	23	15	ℓ=2
1250	6	15	15	11	15	Un	5.5	5.5	Un	
1303	52	28	34	34	29	27	11	8.5	3.9	ℓ=1
1358	98	63	71	67	58	51	22	15	6	ℓ=1
1386	Un	Un	12	17	17	20	13	6	1	
1464	94	93	53	63	69	56	43	22	16	ℓ=2

of this variation is unknown, but it is presumably associated with the calibration of the beam analyzing magnet.

To test the reliability of the plate counting procedure several of the stronger peaks were recounted. The agreement between different determinations was found to be within ~ 3% for peak areas of (1-3) $\times 10^3$ deuteron tracks. The uncertainties introduced by statistics and background subtraction, particularly for the weaker peaks, appreciably increases the uncertainty in the estimated relative peak intensities. The exposure normalization procedure has already been discussed. It is estimated that the procedure used in determining the elastic peak areas for the different exposures is consistent to within ~ 5% and that the error in the areas of these peaks is also of about this size. As previously discussed, an extrapolated value of 0.60 has been estimated for the ratio of elastic scattered to classical Rutherford cross-sections. An error of not greater than 10% is estimated in this value. Allowing in addition for possible errors in both the spectrograph and monitor solid angles, it is estimated that the absolute reaction cross-section errors are ~ $\pm$ 25% for the stronger peaks, with a considerable increase in this value for incompletely resolved peaks or for weak peaks with $\frac{d\sigma}{d\Omega} \lesssim 20$ μb/sr. The relative cross-sections used in the angular distributions are expected, however, to be somewhat more accurate.

Angular distributions of the prominent peaks in the

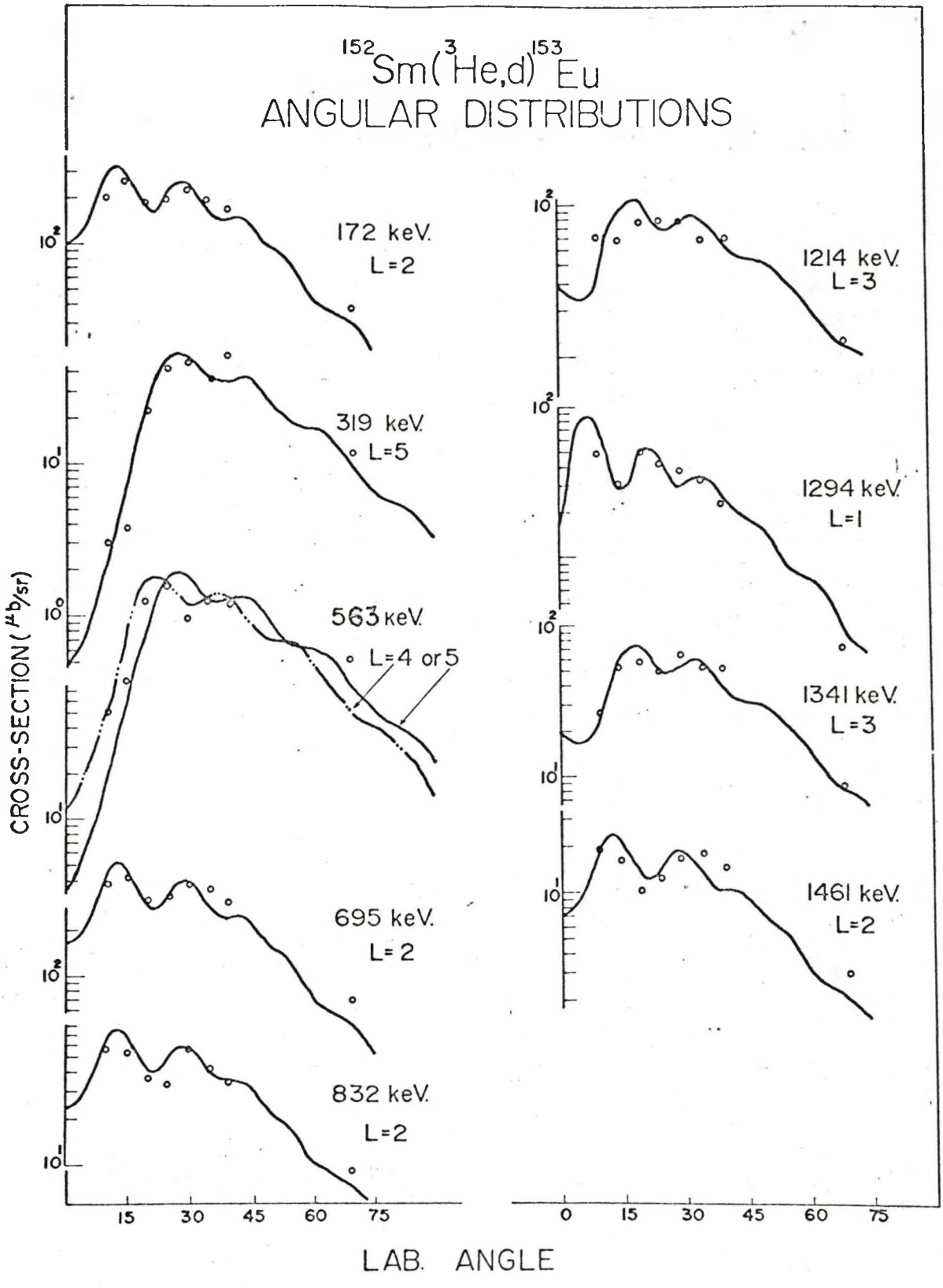

Figure 30 $^{152}Sm(^{3}He,d)^{153}Eu$ Angular Distributions

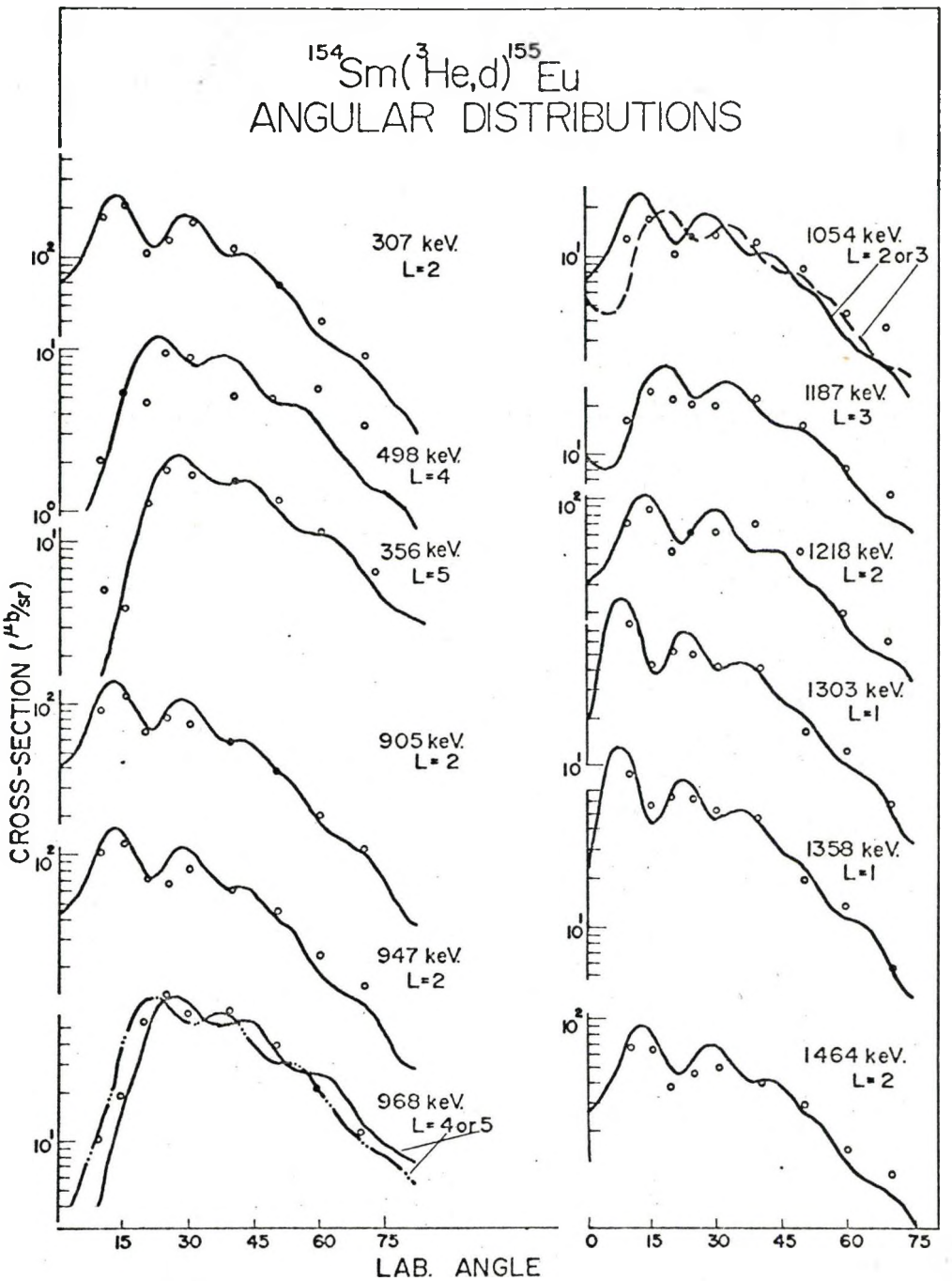

Figure 31 ^{154}Sm(^{3}He,d)^{155}Eu Angular Distributions

deuteron spectra are shown in Figures 30 and 31. The theoretical curves of Figure 25 have been used in these figures and the ℓ values "fitted" are indicated. No attempt has been made to numerically compute the best fit; the theoretical curves have been adjusted in vertical position to obtain the best visual fit. Previously mentioned doublets at 694 keV in ^{153}Eu and 902 keV in ^{155}Eu have been treated as single peaks and have been fitted as such. A considerable number of these distributions appear to fit unique calculated angular patterns. However, no proof exists that some of these do not in fact correspond to close doublets which, when considered together, appear as a good fit to one ℓ value. Though in general the quality of the fit is good, discrepancies of up to a factor of two do exist. These differences cannot be entirely attributed to experimental errors and must be due to inadequacies in the theory.

The reaction experiments were begun as an extension and confirmation of some of the results of the ^{155}Sm decay study. Conversely, the beta decay study of ^{153}Sm was begun as an extension of the ^{152}Sm(^{3}He,d)^{153}Eu reaction work. Both directions of attack have been of importance and the results presented in this section will be discussed in the next chapter together with those of the previous two chapters.

CHAPTER VI

DISCUSSION OF RESULTS

6.1 Introduction

The ground state spins of all the odd mass Eu isotopes from ^{147}Eu to ^{155}Eu appear to be 5/2 (Nuclear Data Sheets), with a positive parity being most probable in every case. Direct measurements have established the 5/2 assignment for ^{151}Eu and ^{153}Eu. The odd mass isotopes below ^{153}Eu are generally regarded as spherical, and a 5/2+ assignment is consistent with the explanation of the 63rd proton as being in a $d_{5/2}$ shell model state. For the case of deformed ^{153}Eu, the magnetic moment has also been measured and its value of 1.5 N.M. is consistent with a 5/2+[413] Nilsson state assignment. This assignment is also expected for ^{155}Eu and is in agreement with the angular correlation data of Sund et al (1960), and the log $f_o t$ values observed in the decay to ^{155}Gd (Nuclear Data Sheets).

Previously determined gamma ray branching ratios, multipolarities, log $f_o t$ values, and angular correlation patterns all combine to support an assignment of low-lying 5/2-[532] and 3/2+[411] intrinsic states in that order of excitation in both ^{153}Eu and ^{155}Eu. The present data, to be discussed in further detail below, leads to the same conclusions.

Figure 32

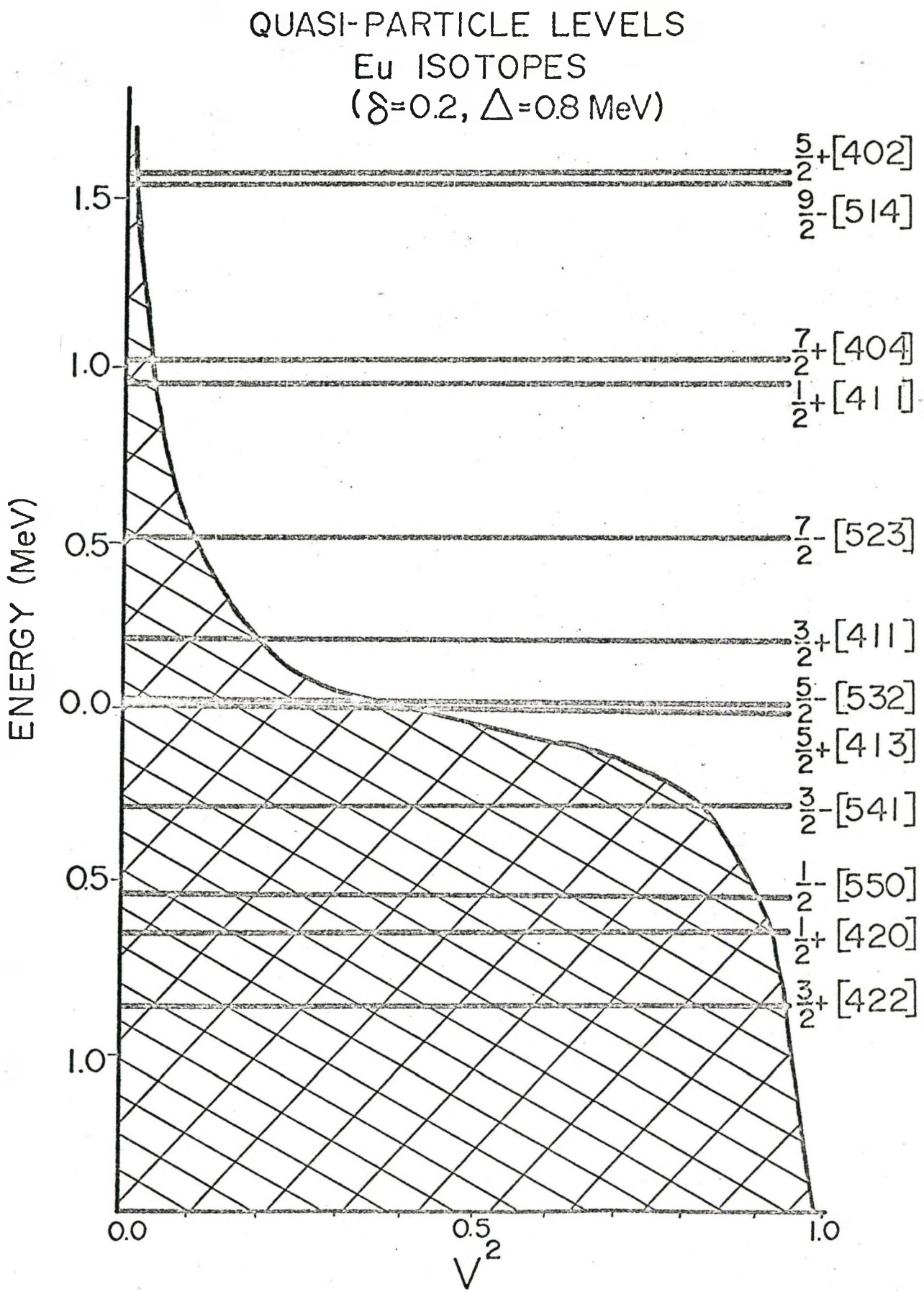
QUASI-PARTICLE LEVELS
Eu ISOTOPES
(δ=0.2, Δ=0.8 MeV)
ENERGY (MeV)
1.5
1.0
0.5
0.0
0.5
1.0
0.0
0.5
1.0
V²
5/2+[402]
9/2-[514]
7/2+[404]
1/2+[411]
7/2-[523]
3/2+[411]
5/2-[532]
5/2+[413]
3/2-[541]
1/2-[550]
1/2+[420]
3/2+[422]

Using the recent Nilsson model calculations of Chi (1967), the 63rd proton should be in the 5/2+[413] state for a deformation, δ, of ~ +0.2. At this deformation, the first two intrinsic states available in increasing energy are the 5/2-[532] and 3/2+[411] mentioned above. Most Nilsson model calculations, including those of Chi (1967), predict level energies on the basis of a potential with no pairing. The quasi-particle energies appropriate for a more realistic model with pairing can be obtained from these calculations using the equation

$$E_\nu = \sqrt{\Delta^2 + (\varepsilon_\nu - \lambda)^2}$$

which has been previously introduced and which in effect depresses the level spacings relative to the model with no pairing. In order to compare the experimentally determined level energies with those predicted by the Nilsson model plus pairing, one quasi-particle levels for an A~155 nucleus at δ = +0.2 were calculated using the above equation and the single particle energies of Chi (1967). The value of λ was chosen to correspond to the 5/2+[413] level energy and a Δ=0.8 MeV was used. This choice of Δ was made in view of the experimentally extracted value of 0.80 $\pm$ 0.15 MeV reported by Burke et al (1966) for Yb nuclei. Calculations carried out for Δ = 1.0 MeV were not significantly different. In addition to calculating the quasi-particle energies, it is possible to predict their population parameters, V^2. Figure 32 shows the results of these rather simple minded calculations together with the quasi-particle

TABLE VII

Theoretical Calculations of Soloviev et al (1966) for ^{155}Eu

Kπ	Energy (keV)	Structure
5/2+	0	5/2+[413] 96%
3/2+	60	3/2+[411] 92%, 1/2+[411]+Q_j(22) 7%
5/2-	160	5/2-[532] 98%
7/2-	540	7/2-[523] 98%
1/2+	600	1/2+[411] 67%, 3/2+[411]+Q_j(22) 19%; 5/2+[413]+Q_j(22) 14%
9/2+	700	9/2+[404] 84%; 9/2+[404]+Q_j(20) 14%
3/2-	1000	3/2-[541] 71%; 3/2-[541]+Q_j(20) 19%; 3/2+[411]+Q_j(30) 4%
5/2+	1100	5/2+[413]+Q_j(20) ~100%
5/2-	1150	5/2-[532]+Q_j(20) ~99%
5/2+	1200	5/2-[532]+Q_j(20) ~99%
3/2+	1250	3/2+[422] 74%; 1/2+[420]+Q_j(22) 10%, 3/2-[541]+Q_j(30) 7%

TABLE VIII

$C^2_{j\ell}$ Coefficients for $\delta = 0.2$

State	a	1/2	3/2	5/2	7/2	9/2	11/2
1/2+[411]	-0.8	0.071	0.500	0.227	0.172	0.027	
1/2-[541]	-2.9	0.061	0.063	0.270	0.029	0.520	0.055
3/2+[411]	-	-	0.034	0.758	0.123	0.081	
3/2+[422]	-	-	0.094	0.043	0.790	0.071	
5/2+[413]	-	-	-	0.027	0.930	0.042	
5/2-[532]	-	-	-	0.0016	0.074	0.020	0.902
7/2+[404]	-	-	-	-	0.99	0.01	
7/2-[523]	-	-	-	-	0.025	0.019	0.952

energy calculations. Five intrinsic states are predicted to lie below about 1 MeV of excitation energy.

Soloviev et al (1966) have also made some rather detailed calculations for the levels of ^{155}Eu. These calculations, which are somewhat more sophisticated than those of the simple model used above, take into account such factors as "blocking" and the quadropole interaction between various combinations of quasi-particle configurations. In addition to one quasi-particle states, they predict vibrational states as well as estimating the contributions of various configurations to a particular level. These calculations are reproduced in Table VII. The $C^2_{j\ell}$ coefficients of Chi (1967) for the odd proton states in this region are listed in Table VIII.

Several intrinsic states, or at least some members of the rotational bands built on them, have been observed in both the beta decay and (^{3}He,d) studies. The level schemes produced by the two population methods are compared in Figures 33(^{153}Eu) and 34 (^{155}Eu). A detailed discussion of these levels follows.

6.2 Low-Lying Rotational Bands

Three rotational bands below about 500 keV of energy are predicted to exist in both ^{153}Eu and ^{155}Eu by both the Nilsson model and the calculations of Soloviev (1966). These are built on the 5/2+[413], 5/2-[532], and 3/2+[411] states and

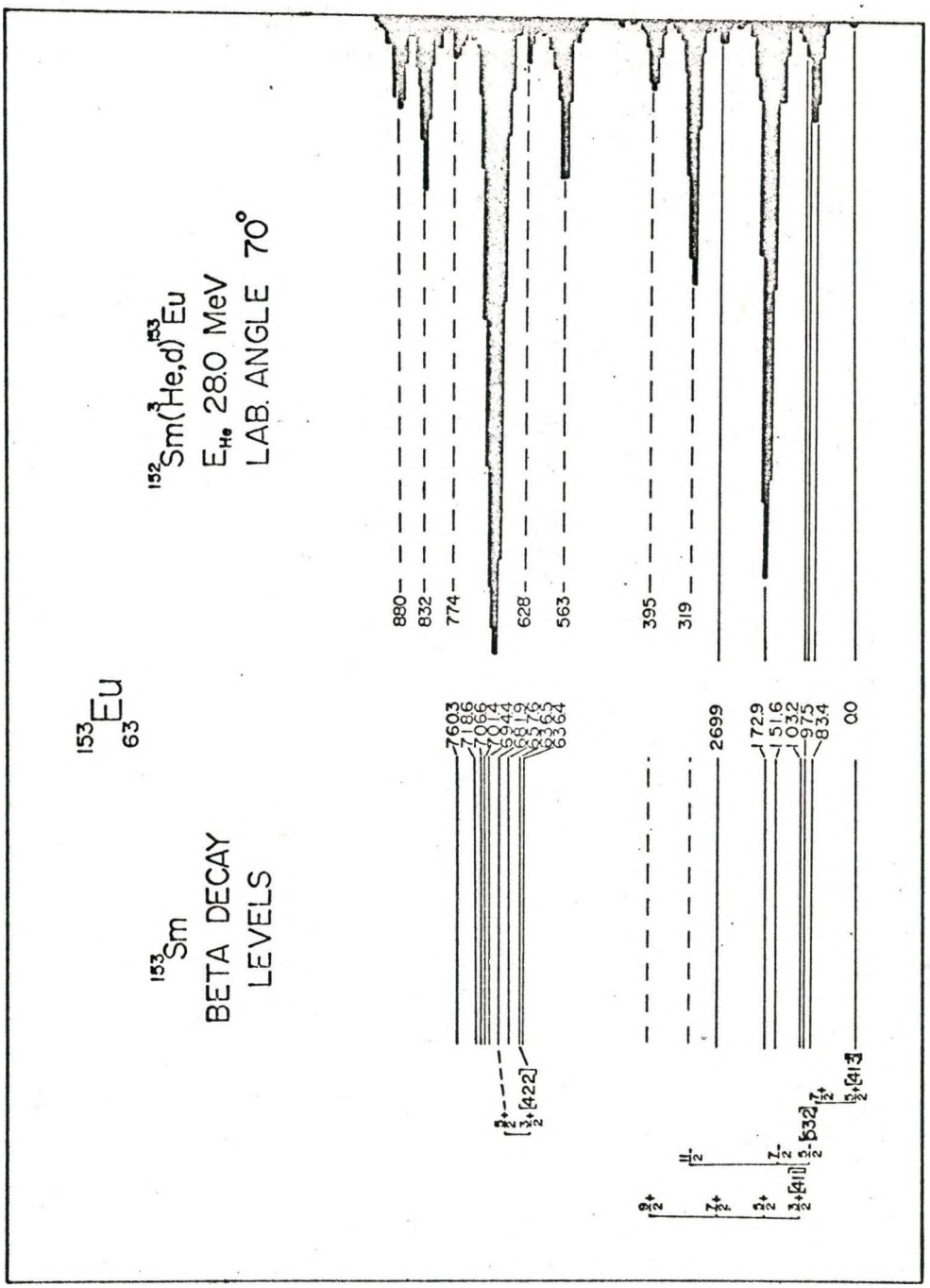

Figure 33 ^{153}Eu Comparative Level Schemes

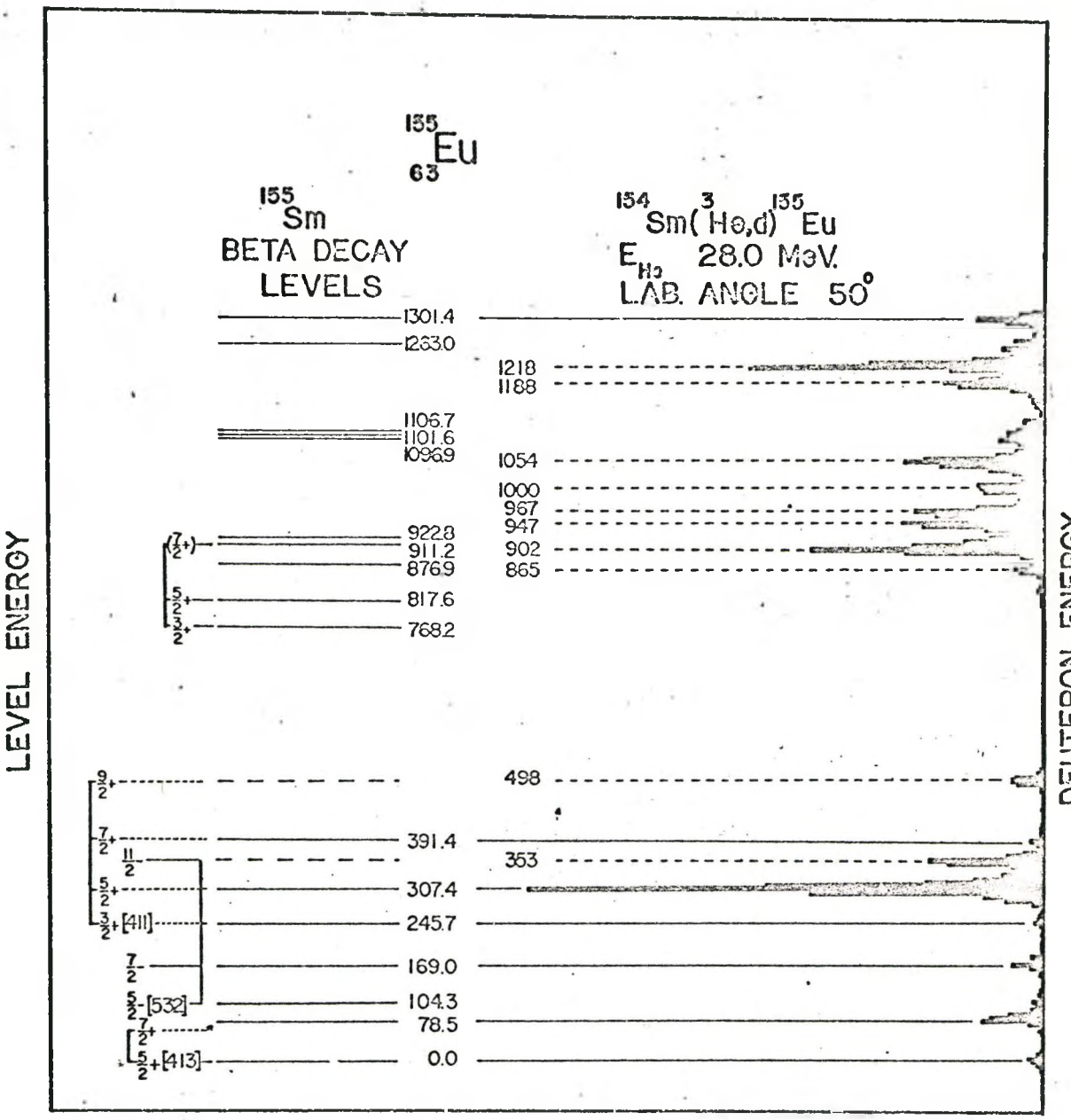

Figure 34 Eu Comparative Level Schemes

have been quite well established by previous workers. Additional confirmation of these bands in the form of new members located by either the beta decay or (^{3}He,d) studies and of the cross-sections observed in the stripping populations has been made by the present study. Each band will be discussed in turn.

6.2A The 5/2+[413] Orbital

The ground state rotational band in both ^{153}Eu and ^{155}Eu is built on the 5/2+[413] orbital. Only the 7/2 rotational members (at 83.4 keV in ^{153}Eu and 78.5 in ^{155}Eu) have been observed in the beta decay studies; beta feeds to higher rotational members from the spin 3/2 Sm isotopes are highly hindered. The 9/2+ member of this band has been reported from Coulomb excitation work at 191 keV in ^{153}Eu (Oleson and Elbek (1960)) but no data exists for the corresponding state in ^{155}Eu predicted at about 180 keV. Using the $C^2_{j\ell}$ coefficients listed in Table VIII and the DWBA calculations previously discussed, a differential cross-section of (3-5) μb/sr is predicted for the ground state which is populated by an ℓ=2 transfer. Weak evidence for a peak of this size at the proper energy has been seen in several exposures for both isotopes. Predicted cross-sections for the 7/2+(ℓ=4) and 9/2+(ℓ=4) levels respectively are ~ 20 μb/sr and ~ 0.5 μb/sr. [These estimates and those to follow are all for θ = 30°.] The 7/2+ level at 83 keV in ^{153}Eu is unresolved from the 97 and 103 keV levels, but would appear to have a cross-section of only ~ 10 μb/sr. A similar

estimate of size is made for the 78 keV level in ^{155}Eu which is unresolved from the 104 keV state. No reliable indication is seen for either of the 9/2+ states which would unfortunately lie near more strongly populated known levels.

6.2B The 5/2-[532] Orbital

The 5/2-[532] level is the next intrinsic state observed in ^{153}Eu and ^{155}Eu in agreement with the Nilsson calculations for δ=0.2, but in disagreement with the calculations of Soloviev et al (1967) who predict the 3/2+[411] below it. The 5/2 and 7/2 members of this band have been previously established at 97.5 and 151.6 keV in ^{153}Eu and 104.3 and 169.0 keV in ^{155}Eu. These levels appear at somewhat higher excitation than the value (~ 20 keV) predicted by the Nilsson calculation with pairing. No higher members of these bands are known from the beta decay studies. The 5/2-[532] state which at zero deformation corresponds to the $h_{11/2}$ shell model level can be seen from Table VIII to have a large $C^2_{j\ell}$ coefficient (0.902) for the 11/2 component, and the (^{3}He,d) reaction is then expected to populate this ℓ=5 state strongly. States at 319 keV in ^{153}Eu and 356 keV in ^{155}Eu are in fact seen at the positions predicted for the 11/2 members of this band on the basis of the first two levels. In addition these weak peaks are fortunately in a relatively clean part of the spectra and so it is possible to obtain good angular distribution patterns for them. These were presented in Figures 30 and 31 and are seen to fit the predicted

TABLE IX

5/2-[532] Band Populated by the (^{3}He,d) Reaction

Cross-Sections at 30° (μb/sr)				Relative $C^2_{j\ell}$ Values		
Spin	Predicted	^{153}Eu	^{155}Eu	Theory	^{153}Eu	^{155}Eu
5/2	~ 0.3	6	3.5	0.0016	0.03	0.02
7/2	10	not seen	8	0.074	-	0.04
9/2	0.4	Not	Seen	0.020	-	-
11/2	20	47	28	0.902	0.97	0.94

TABLE X

3/2+[411] Band Populated by the (^{3}He,d) Reaction

Cross-Sections at 30° (μb/sr)				Relative $C^2_{j\ell}$ Values		
Spin	Predicted	^{153}Eu	^{155}Eu	Theory	^{153}Eu	^{155}Eu
3/2	9	6	15	0.034	0.020	0.055
5/2	190	230	178	0.758	0.76	0.67
7/2	4	not	seen	0.123	-	-
9/2	2	8.5	10	0.081	0.22	0.25

ℓ=5 transfer pattern rather well. No evidence is seen in the deuteron spectra for the weak 9/2 members of this band which are expected at 244 keV in ^{153}Eu and 253 in ^{155}Eu. The latter could be obscured by the known 246 keV level. The experimentally observed reaction cross-sections and experimentally extracted $C^2_{j\ell}$ values (renormalized so that $\Sigma_j C^2_{j\ell} = 1$) are shown for both ^{153}Eu and ^{155}Eu in Table IX together with the predicted values. The angle θ= 30° has not been chosen because of best fit, but merely as a consistent reference angle. The experimental values are noted to be somewhat larger than the predicted ones, but the general pattern for the band is certainly in agreement with prediction.

6.2C <u>The 3/2+[411] Orbital</u>

The 3/2+[411] level at 103.2 keV in ^{153}Eu and 245.7 keV in ^{155}Eu is the third low-lying state predicted in these nuclei. The crude quasi-particle energy calculations shown in Figure 32 predict an energy of ~ 200 keV for this state. The first rotational members (spin 5/2) of the band, at 172.9 (^{153}Eu) and 307.4 keV (^{155}Eu), have been well established by previous investigations. The present beta decay studies have definitely identified the previously proposed level at 269.9 keV in ^{153}Eu as the 7/2+ member of the 3/2+[411] band and have led to the discovery of the corresponding level at 391.4 keV in ^{155}Eu. Calculations using the simple J(J+1) rule predict that the 9/2+ members of this band should lie at ~400 keV in ^{153}Eu and 500 keV

in ^{155}Eu. Distinct peaks are seen in the deuteron spectra at 395 (^{153}Eu) and 498 keV (^{155}Eu), and the fit to a predicted ℓ=4 angular distribution pattern is seen in Figure 31 for the latter. The 3/2+[411] state at zero deformation corresponds to a $d_{5/2}$ shell model state and so its Nilsson wave function is expected to have a large $d_{5/2}$ component. The $C^2_{j\ell}$ coefficients listed in Table VIII confirm this and so predict that a large peak corresponding to the level energy of the 5/2(ℓ=2) rotational member should exist in the deuteron spectra. This peak is in fact found to be one of the largest observed. The experimentally observed reaction cross-sections and normalized $C^2_{j\ell}$ values for both nuclei are listed in Table X together with the predicted values. These 30° values are typical of the values obtained at other angles.

At almost all angles, it appears that the strength of the 9/2 members (ℓ=4) is somewhat stronger than that expected from theory. The use of a smaller deformation parameter in the Nilsson calculations would only increase the discrepancy. Although it is possible that the cross-sections are high because the level is a doublet, the fact that the discrepancy occurs in both nuclei and that the fit to an ℓ=4 angular pattern is reasonably good would tend to indicate the excitation of the 9/2+ member of the band is accentuated. Again, as in the above two bands, while the experimental and predicted values do not exactly agree, the general agreement is quite good.

TABLE XI

Rotational Band Parameters

Band	Nuclide	$\frac{\hbar^2}{2I}$ (keV)	B(keV)	Energy above 3/2+[411] band
5/2+[413]	^{153}Eu	11.9		
	^{155}Eu	11.2		
5/2-[532]	^{153}Eu	9.2		
	^{155}Eu	9.3		
3/2+[411]	^{153}Eu	14.03	-0.007	
	^{155}Eu	12.64	-0.025	
3/2+[422]	^{153}Eu	~9		531
	^{155}Eu	6.17	0.294	522
	^{155}Tb	7.36	0.228	499

6.2D Summary of Low-Lying Bands

The band parameters for the three low-lying bands in ^{153}Eu and ^{155}Eu are summarized in Table XI together with those of the 3/2+[422] band to be discussed next.

6.3 The 1/2+[411] and 3/2+[422] Rotational Bands

A 1/2+[411] level is predicted to lie at about 900 keV of excitation in ^{153}Eu and ^{155}Eu by the calculations shown in Figure 32. Soloviev et al (1966)predict a state at ~ 600 keV whose major component of the wave function (67%) is the 1/2+[411]. This orbital has been observed in 9 isotopes and the decoupling parameter and moments of inertia determined in these cases are listed in Table XII. A decoupling parameter of -1.0 for a K=1/2 band places the 1/2 and 3/2 members at the same energy. The experimental data for this band thus indicate that these levels are near each other in energy. The model calculations and the apparent existence of two close lying low spin states in both ^{153}Eu (near 635 keV) and ^{155}Eu (near 760 keV) has made a 1/2+[411] assignment for these levels quite attractive. The present beta decay studies do confirm the existence of previously proposed levels at 634.6 and 636.4 keV in ^{153}Eu as well as the 768.2 keV level in ^{155}Eu. No evidence is seen for a second level in ^{155}Eu reported by previous workers near this energy. These reports appear to be the result of trying to fit the interpretation by forcing rather ambigious experimental data. The 1/2+[411] assignment for these levels must be rejected for

TABLE XII

1/2+[411] Band

Nuclide	a	$\frac{\hbar^2}{2I}$(keV)
^{159}Tb	-0.81	12.0
^{165}Ho	-0.46	12.3
^{167}Tm	-0.70	12.4
^{169}Tm	-0.78	12.5
^{171}Tm	-0.86	12.0
^{173}Yb	-0.74	12.8
^{171}Lu	(-0.71)	(13.2)
^{173}Lu	(-0.74)	12.8
^{177}Lu	(-0.78)	(13.0)

reasons outlined below.

The 1/2+[411] state, corresponding at zero deformation to a $d_{3/2}$ shell model level, has a large (0.500) j=3/2 component as well as an appreciable (0.071) j=1/2 component in its wave function. These two components, corresponding respectively to high cross-section ℓ=2 and ℓ=0 transfers, should give rise to large peaks in the deuteron spectra at the excitation energy of this predicted level doublet. Using even the reduced 67% fraction of the level strength predicted by Soloviev et al (1966) for this state, these peaks should be about one half as intense as the large ℓ=2 5/2,3/2+[411] peaks at 172 (^{153}Eu) and 307 keV (^{155}Eu). No deuterons are seen at all at 768 keV in the spectrum feeding levels in ^{155}Eu (see Figure 29) and while a small peak at about 628 keV excitation energy does exist in the ^{153}Eu spectrum (Figure 28) it is by no means large enough to account for the 1/2+[411] state.

A new interpretation is then needed for these levels and the following two are proposed as possibilities. The 636 and 681 keV levels in ^{153}Eu and the 768 and 817 keV levels in ^{155}Eu, the latter newly established, are all coupled to the 3/2+[411] band by strong transitions. Gamma branchings from these levels to the levels below 500 keV favour spin assignments of 3/2+ for the 636 and 768 keV, and 5/2+ for the 681 and 817 keV states. Soloviev et al (1966) predict a state at ~ 1250 keV whose major wave function component is due to a

3/2+[422] "hole" state. In addition they suggest that "a low-lying comparatively pure beta vibrational state may exist in this nucleus". Such a vibrational band could be based on the 3/2+[411] state which is seen in both nuclides. Both the "hole" and the""beta vibrational" interpretations are consistent with the absence of deuteron peaks at the above locations in the spectra.

The Alaga rules predict the ratios of reduced transition intensities from members of one rotational band to another. For pure transitions of the same multipolarity these ratios are dependent only on the initial and final K and I quantum numbers. The reduced ratios for the transitions depopulating the proposed 3/2+ band in both ^{153}Eu and ^{155}Eu are shown in Table XIII together with the predicted values for the various possible I and K combinations. The reduced ratios for both L=1 (dipole) and L=2 (quadropole) show a marked similarity for the 636 and 768 keV states as well as for the 682 and 817 keV. Assuming that the transitions are pure, the only consistent interpretations seem to be for predominantly dipole transitions and I,K values of 3/2,3/2 for the 636 and 768 keV, and 5/2,3/2 for the 682 and 817 keV states, respectively. E2 transition strengths for radiations from beta vibrational levels to levels of the associated base-state band are generally enhanced, and as the transitions appear to be more consistent with a dipole interpretation, the 3/2+[422] hole interpretation would appear to be favoured over the beta vibrational assignment. A similar $K\pi=3/2+$ band has been observed in ^{155}Tb by Blichert-Toft et al (1967). Their interpretation of the

TABLE XIII

Reduced Branching Ratios in ^{153}Eu and ^{155}Eu

Initial Level Energy (keV)	Transition Energy and Final State I_f K_f	L	L Branching Ratio: Reduced Exptal Ratio	I_i K_i 3/2 1/2	5/2 1/2	3/2 3/2	5/2 3/2	5/2 5/2	7/2 5/2
636 (^{153}Eu)	533→3/2 3/2	1	1.34	0.67	0.145	1.50	1.04	2.33	
	463→5/2 5/2	2	1.05	19.0	0.60	0.39	24.0	0.67	
768 (^{155}Eu)	522→3/2 3/2	1	1.60	0.67	0.145	1.50	1.04	2.33	
	460→5/2 3/2	2	1.16	19.0	0.60	0.39	24.0	0.67	
681 (^{153}Eu)	578→3/2 3/2	1	1.02		0.145		1.04	2.33	
	509→5/2 3/2	2	0.79		0.60		24.0	0.67	8.00
	509→5/2 3/2	1	0.50		0.96		0.52	6.00	1.40
	412→7/2 3/2	2	0.33		4.50		0.05	1.80	0.04
817 (^{155}Eu)	571→3/2 3/2	1	1.14		0.145		1.04	2.33	
	510→5/2 3/2	2	1.00		0.60		24.0	0.67	8.00
	510→5/2 3/2	1	0.53		0.96		0.52	6.00	1.40
	426→7/2 3/2	2	0.34		4.50		0.05	1.80	0.04
	713→5/2 5/2	1	0.25				0.41	2.44	0.54
	648→7/2 5/2	2	0.21		0.41		27.0	0.75	37.5

state is also 3/2+[422], and the band parameters found there agree well with those of the present study (see Table XI). The log $f_o t$ value (~8.8) for the beta feed to the 911 keV state in ^{155}Eu is not in disagreement with a 7/2+ assignment for this level as the third member of the band. The partial decay schemes of ^{153}Eu, ^{155}Eu, and ^{155}Tb pertinent to this band are compared in Figure 35.

The existence of two rather prominent doublet peaks in the deuteron spectra at ~ 905 keV (^{155}Eu) and ~ 695 keV (^{153}Eu) has already been commented on. Angular distributions appropriate to an ℓ=2 transfer have been fitted to these peaks (treated as single peaks) and are seen in Figures 30 and 31. As mentioned above, the 1/2+[411] band with a close level doublet for the 1/2 and 3/2 members is expected in this region. The $C^2_{j\ell}$ coefficients for the band favour the 3/2(ℓ=2, $C^2_{j\ell}$ = 0.500) member over the 1/2(ℓ=0, $C^2_{j\ell}$ = 0.071) and predict an appreciable population as well for the 5/2(ℓ=2, $C^2_{j\ell}$ = 0.227) member. Peaks assigned an ℓ=2 angular distribution pattern are seen in the ^{153}Eu spectra at 832 keV and in the ^{155}Eu at 1054 keV and could be considered as candidates for the spin 5/2 members. A visual resolution, at various angles, of the two doublet peaks places levels at ~ 692 and 704 keV (^{153}Eu) and 904 and 910 keV (^{155}Eu). An energy fit using the rotational formula results in band parameters for such an assignment of a = -0.76, $\frac{\hbar^2}{2I}$ = 14.9 keV in ^{153}Eu and a = -0.88, $\frac{\hbar^2}{2I}$ = 15.4 keV for ^{155}Eu. Both

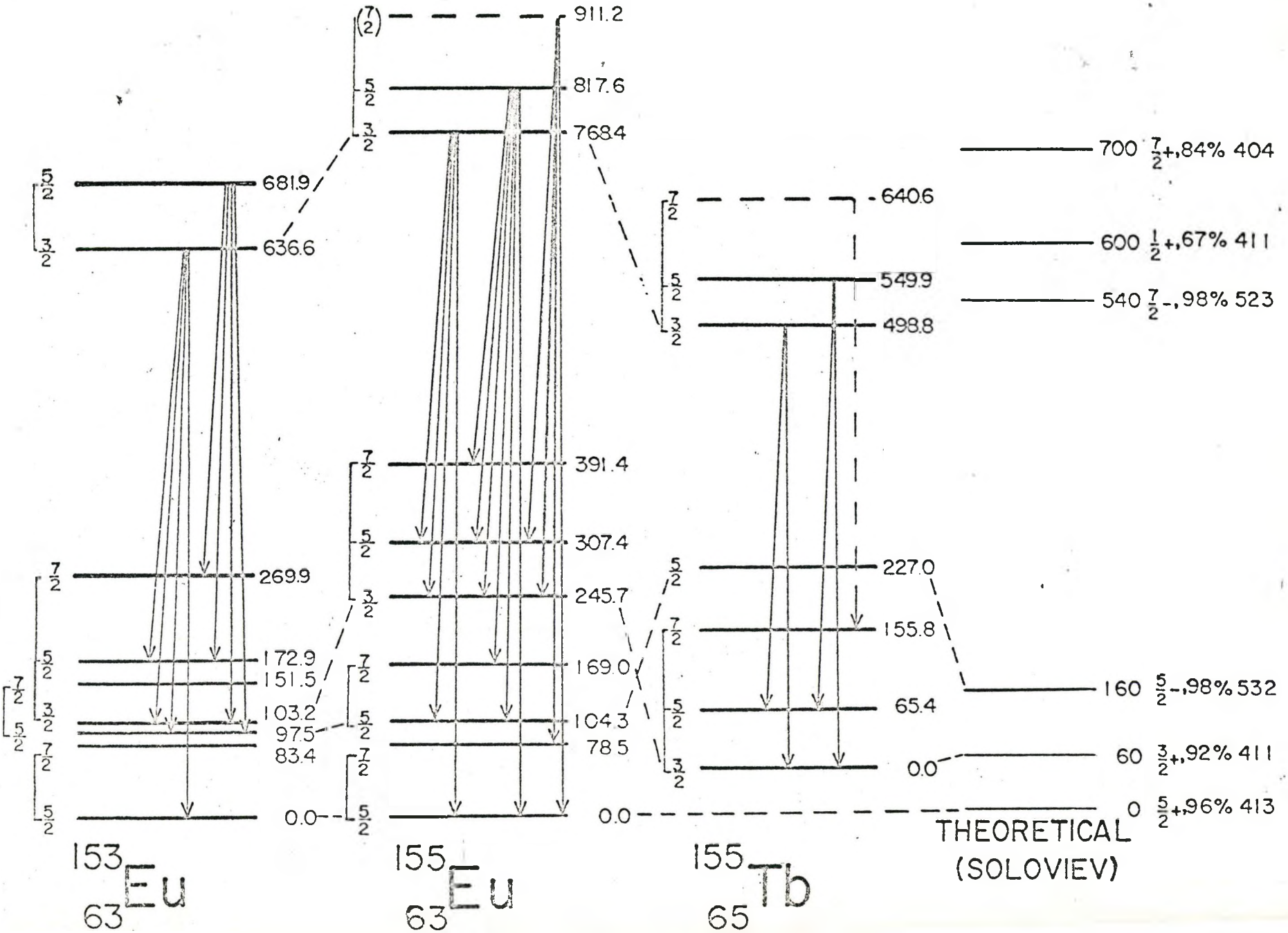
681.9
636.6
269.9
172.9
151.5
103.2
97.5
83.4
0.0
153 63 Eu
911.2
817.6
768.4
391.4
307.4
245.7
169.0
104.3
78.5
0.0
155 63 Eu
640.6
549.9
498.8
227.0
155.8
65.4
0.0
155 65 Tb
700 7/2+,84% 404
600 1/2+,67% 411
540 7/2-,98% 523
160 5/2-,98% 532
60 3/2+,92% 411
0 5/2+,96% 413
THEORETICAL
(SOLOVIEV)

Figure 35

the values obtained for the decoupling parameter are in good agreement with those found elsewhere (see Table XII); however, the $\frac{\hbar^2}{2I}$ parameter is about 2 keV larger than that found in other nuclei. This would correspond to a smaller than average moment of inertia which might be reasonable for nuclei near the edge of the deformed region.

The magnitudes of the experimentally observed cross-sections for these peaks should also be considered. Using the 67% 1/2+[411] contribution for the state predicted by Soloviev et al (1966) and combining the 1/2 and 3/2 members to form a doublet level, peaks corresponding to cross-sections (at 30°) of ~ 130 μb/sr for the 1/2,3/2 doublet and ~ 50 μb/sr for the 5/2 member are expected. Experimentally observed cross-sections are ~ 85 μb/sr and ~ 48 μb/sr for the ~ 905 and 1054 keV peaks in ^{155}Eu and ~ 395 μb/sr and 57 μb/sr for the ~ 695 and 832 keV levels in ^{153}Eu. It should be noted, at this point, that four states at 694, 701, 706, and 718 keV have been introduced in ^{153}Eu from the beta decay data. These states are all populated by a spin 3/2 parent nuclide and so are expected to be of low spin and may all contribute appreciably to the large peak at 695 keV. For this reason it is somewhat difficult to compare the experimental and predicted cross-sections for this peak. The 902 keV cross-section seen in the spectra is about 30% too small on the average, but good agreement with the predicted value for a 5/2 spin member is found for both the 1054 keV (^{155}Eu) and 832 keV (^{153}Eu) levels. A 1/2+[411] band assignment

for these two sets of levels would then appear to be quite attractive.

The beta decay schemes should also be examined in considering such an assignment. Using a first forbidden log $f_o t$ of ~7, a beta feed of ~0.1% to these levels in ^{155}Eu should result. No beta feed to levels at these energies has, however, been observed. Factors may, of course, exist which could increase the hindrance of this feed, but it is not obvious what they may be. For the case of ^{153}Eu a level at 694 keV does exist whose 0.02% beta feed would be in agreement with a log $f_o t$ of 7. In this case, however, the parent nucleus is in a 3/2+[651] state, and the transition is parity allowed. The $\Delta N=2$ change required, however, makes a log $f_o t$ value of ~ 7 not unreasonable. A weak 542 keV gamma ray has been placed from the 694 keV level to the spin 7/2-, 151 keV, level on the basis of energy fit alone, and if it does in fact correspond to that assignment, spins of 1/2+ or 3/2+ must be rejected as candidates for the 694 keV level. An alternate placement for this transition would make a 3/2+ assignment quite consistent with the remaining data.

No definite assignment or rejection of a 1/2+[411] interpretation for these states would seem justified on the basis of the present data and further investigation of these states is warranted.

6.4 The 7/2+[404] and 7/2-[523] States

Of the five low-lying particle states predicted in Figure 32 for these nuclides, the 7/2-[523] and 7/2+[404] remain to be discussed. Neither of these states are expected to be observed in the beta decay of the spin 3/2 ^{153}Sm and ^{155}Sm isotopes. The $C^2_{j\ell}$ coefficients listed in Table VIII show that the 7/2+[404] state has almost all its strength (0.99) concentrated in the 7/2 component of the wave function while the strength of the 7/2-[523] state is almost all in the 11/2 component (0.95). Predicted reaction cross-sections for peaks in the deuteron spectra corresponding to the 7/2,7/2+[404] (ℓ=4) are 40 μb/sr and for the 11/2,7/2-[523] level (ℓ=5) 28 μb/sr. Peaks corresponding to cross-sections of this size are seen at 563 keV in ^{153}Eu and at 967 keV in ^{155}Eu. The fits to either an ℓ=4 or ℓ=5 angular distribution appear equally good (see Figures 30 and 31). The experimental cross-sections observed are 22 μb/sr (^{155}Eu) and 21 μb/sr (^{153}Eu). The experimental values at most angles are generally midway between those predicted for the 7/2,7/2+[404] level and the 11/2,7/2-[523] level but tend to favour the latter. Studies of ^{165}Ho and the Lu isotopes (Nuclear Data Sheets) indicate that the 7/2-[523] state does, in agreement with model predictions, lie below the 7/2+[404] state and should hence be expected to appear first. Furthermore, a smaller than predicted cross-section is easier to account for than a larger one. However, no firm choice

TABLE XIV

L Assigned States and "S_{eff}" Values

Level Energy (keV)	L Value Assigned	S_{eff}
^{153}Eu 628	3 or 4	
1214	3	0.31
1294	1	0.07
1341	3	0.52
1461	2	0.14
^{155}Eu 947	2	0.10
1187	3	0.14
1218	2	0.31
1303	1	0.06
1358	1	0.10
1464	2	0.27

of one interpretation over the other seems justified, although it does appear that these two levels do in fact correspond to one of these Nilsson states. (Note: Using the 11/2-7/2 spacing of 210 keV in ^{165}Ho would place the 7/2-[523] state at ~ 350 keV in ^{153}Eu and at ~ 760 keV in ^{155}Eu if the 11/2-,7/2-[523] proposal is accepted).

6.5 Other Levels

A large number of unclassified levels in both ^{153}Eu and ^{155}Eu have been observed in both the beta decay and (^{3}He,d) studies. Angular distributions have been obtained for a number of these and ℓ values have been assigned which define the parity of the states and reduce the possible spins to $\ell \pm 1/2$. The theoretical cross-section expression may be re-written

$$\frac{d\sigma}{d\Omega} = 2\phi_{\ell} \, S_{eff}$$

where S_{eff} is used to denote a spectroscopic factor which depends on the product of $C^2_{j\ell}$, U^2 and the fractional wave function components predicted by Soloviev et al (1966). A large value of S_{eff} implies a large $C^2_{j\ell}$ value. Table XIV lists those states for which ℓ values have been assigned from angular determinations together with the S_{eff} values deduced from the differential cross-sections. Of these, the 1341 (ℓ=3) state in ^{153}Eu has the largest value. According to Chi (1967) the 5/2 member (ℓ=3, $C^2_{j\ell}$ = 0.27) of the $\frac{1}{2}$-[541] band is expected to fall very near the 1/2 member (ℓ=1, $C^2_{j\ell}$ = 0.061) because of the large decoupling para-

$^{153}_{63}$Eu LEVELS

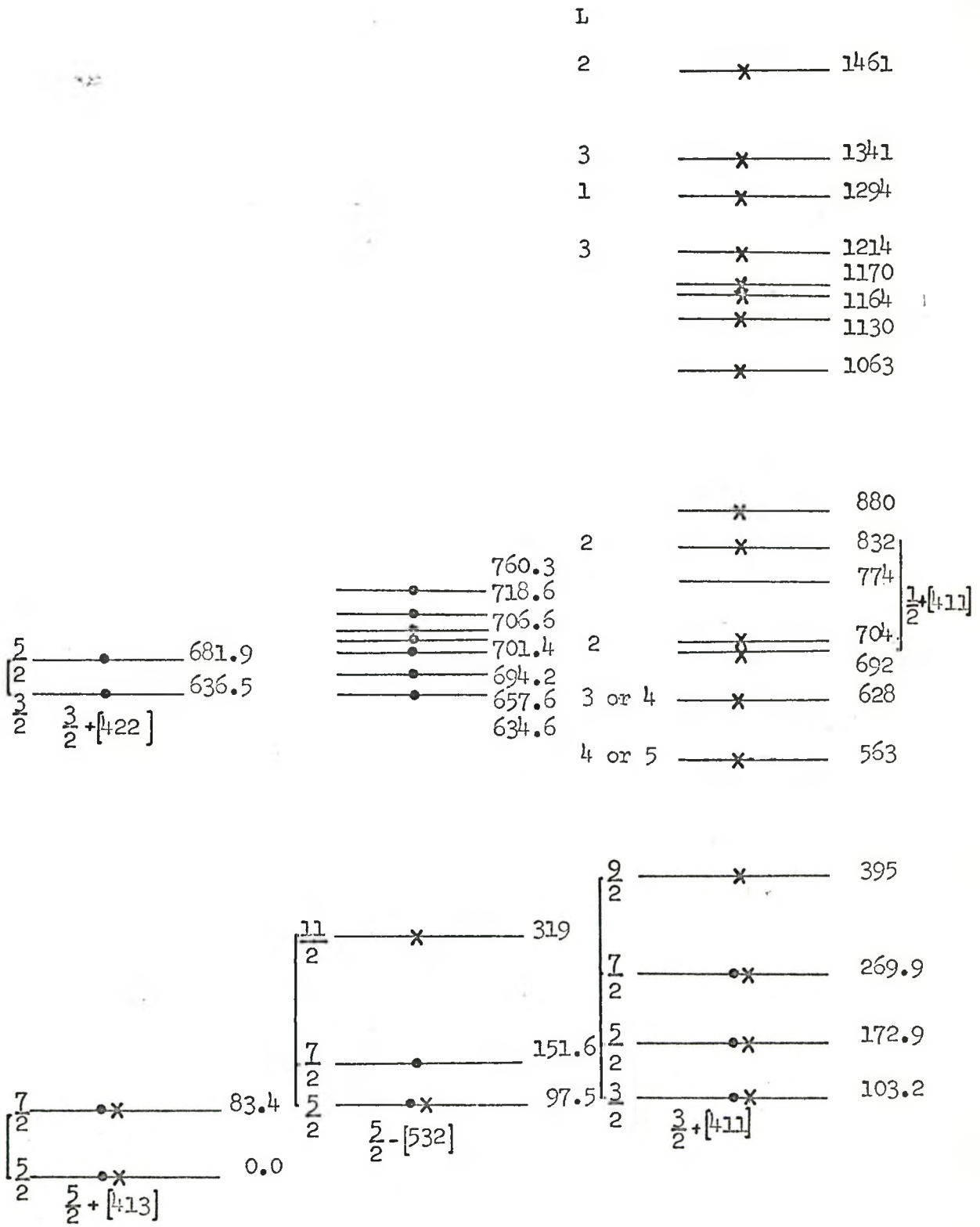

Figure 35

$^{155}_{63}$Eu LEVELS

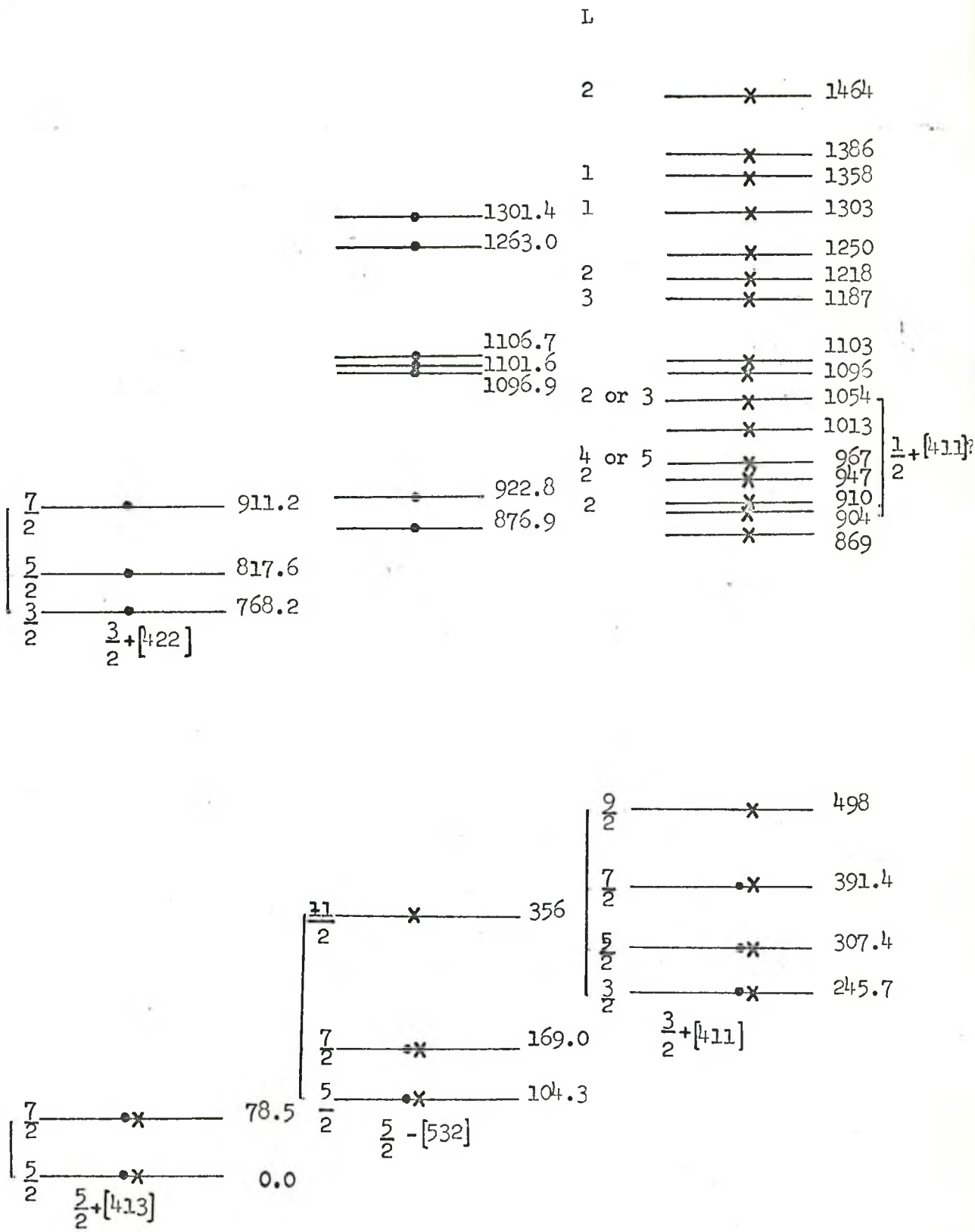

Figure 37

meter (a=+2.9). The 1341 keV.state could be a conceivable candidate for this level. However, the lack of suitable candidates for the 3/2 and 9/2 members of this band make such a consideration highly speculative. The 1303 keV level in ^{155}Eu assigned as ℓ=1 (hence spin 1/2-, or 3/2-) cannot be the same as the 1301 keV state of spin 5/2 found in the beta decay process. The presence of several strong ℓ=1 peaks in the high energy region is noteworthy since no 1/2- or 3/2 Nilsson states have been identified in this region.

6.6 Conclusions

The results of the present study on the levels in ^{153}Eu and ^{155}Eu are summarized in Figures 36 and 37. Approximately 30 excited states in ^{153}Eu and 35 in ^{155}Eu have been identified. The use of the word approximately is prompted by the fact that certain states apparently observed by both the beta decay and (^{3}He,d) reactions may in fact be different; or some others identified separately may be the same. On the figures states seen by the (^{3}He,d) reaction are indicated by crosses and those seen in beta decay by dots. Singles and coincidence gamma ray experiments have placed 52 transitions in ^{155}Eu and 44 in ^{153}Eu which depopulate these levels. Four rotational bands,some with newly introduced members, have been located in both nuclei, and several previously established levels have been given new interpretations.

REFERENCES

Agin, G.P., Mandeville, C.E., and Potnis, V.R. Nucl. Phys. A105 (1967) 698.

Alexander, P. Phys. Rev. 134 (1964) B499.

Alexander, P., Boehm, F., and Knkeleit, E. Phys. Rev. 133 (1964) B284

Bardeen, J., Cooper, L.N., and Schrieffer, R. Phys. Rev. 108 (1957) 1175.

Belyaev, S.T., K. Danske Vidensk. Selsk. Mat-Fys 31 No. 11 (1959).

Bes, D.R. and Cho, Y.C. Nucl. Phys. 86 (1966) 581.

Blichert-Toft, P.H., Funk,E.G., and Mihelich, J.W.
Nucl. Phys. 79 (1966) 12
Nucl. Phys. A100 (1967) 369.

Bohr, A. and Mottelson, B.R. K. Danske Vidensk. Selsk. Mat-Fys 27 No. 16 (1953).

Bohr, A., Mottelson, B.R., and Pines, D. Phys. Rev. 110 (1958) 936.

Burke, D.G. et al. K. Danske Vidensk. Selsk. Mat-Fys. 35 No. 2 (1966).

Burke, D.G. and Alford, W.P. (1968) Private Communication.

Butler, S.T. Proc. Roy. Soc. A208 (1951) 559.

Camp, D.C. UCRL Report 50156 (1967).

Chi, B.E. State Univ. of New York (Albany) Publication (1967).

Chinaglia, B. and Malvano, R. Nucl. Inst. and Meth. 45 (1966) 125.

Dzhelepov, B.S. et al. J. Nucl. Phys. (U.S.S.R.) 3 (1966) 785.

Enge, H.A. Rev. Sci. Inst. 29 (1958) 885.

Nucl. Inst. and Meth. 26 (1964) 83.

Fano, U. Phys. Rev. 72 (1947) 26.

Freck, D.V. and Wakefield, J. Nature 193 (1962) 669.

French, J.B. and MacFarlane, M.H. Rev. Mod. Phys. 32 (1960) 567.

Funke L. et al Nucl. Phys. 74 (1965) 145

Nucl. Phys. 70 (1965A) 335

Nucl. Phys. 88 (1966) 641

Unpublished Results (1968).

Hatch, E.N. et al. Bull. Am. Phys. Soc. 13 (1968) Paper HE3.

Haxel, O., Jensen, J.H.D., and Suess, H.E. Phys. Rev. 75 (1949) 1766.

Heath, R.L. AEC Report lDO-16408 (1957).

Kenefick, R.A. and Sheline, R.K. Phys. Rev. 139 (1965) B1479.

Kracik, B. Czech. J. Phys. B13 (1963) 79.

Marshalek, E.R. and Rasmussen, J.O. Nucl. Phys. 43 (1963) 438.

Mayer, M.G. Phys. Rev. 74 (1948) 235.

Newton, T.D. Can J. Phys. 38 (1960) 700.

Nilsson, S.G. K. Danske Vidensk Selsk Mat-Fys. 29 No. 16 (1955).

Nuclear Data Sheets (1963).

Oleson, M.C. and Elbek, B. Nucl. Phys. 15 (1960) 134.

Sakai, M. Nucl. Phys. A104 (1967) 301.

Satchler, G.R. Ann. Phys. 3 (1958) 275

Private Communication (1968).

Schmid, L.C. and Burson, S.B. Phys. Rev. 115 (1959) 447.

Siegbahn, K. $\alpha\cdot\beta\cdot\gamma\cdot$ Ray Spectroscopy, North-Holland Publishing Company, Amsterdam (1966).

Spencer, J.E. and Enge, H.E. Nucl. Inst. and Meth. 49 (1967) 181.

Soloviev, V.G., Vogel, P. and Jungklassen, G. Dubna Report E4-3051 (1966).

Soloviev, V.G. Soviet Journal of Nuclear Physics, Vol. 3, No. 6 730 (1967).

Sund, R.E., Arns, R.G., and Wiedenbeck, M.L. Phys. Rev. 118 (1960) 776.

Suter, T. et al. Nucl. Phys. 29 (1962) 33.

Tavendale, A.J. and Ewan, G.T. Nucl. OInst. and Meth. 25 (1963) 185.

Waddington, J.C. Ph.D. Thesis, McMaster University (1967).

Westgaard, L. and Bjørnholm,S. Nucl. Inst. and Meth. 42 (1966) 77.

Widemann, F. and Sebille, C. Nucl. Phys. A117 (1968) 129.